

OIL SHALE PROCESS WATER EVAPORATION

V.R. Hasfurther, T. Reeves
and R. McQuisten

Final Report 1990
WWRC-90-08

Final Report

to the

U.S. Department of Energy
Morgantown Energy Technology Center
Contract No. DE-AC21-84LC11049

V.R. Hasfurther
T. Reeves
Department of Civil Engineering
University of Wyoming
Laramie, Wyoming

R. McQuisten
Project Manager
U.S. Department of Energy
Laramie Project Office
Laramie, Wyoming

May 1990

ABSTRACT

OIL SHALE PROCESS WATER EVAPORATION

DOE Contract No. DE-AC21-84LC11049

The primary objectives of this research program were to study chemical, microclimatological, and interactive effects on the evaporation of low-quality oil shale process wastewaters to develop more applicable evaporation models and evaporation design criteria for the disposal of oil shale process waters and to analyze the processes associated with the release of potentially toxic emissions from these low-quality effluents. The research program incorporated field and laboratory studies analyzing microclimatic and chemical effects on the evaporation of oil shale process wastewaters.

Field studies at Laramie, Wyoming were designed to continuously monitor microclimatological conditions and the evaporation from three low-quality effluents using Class A evaporation pans. Fresh water evaporation was monitored as a control. Process waters were routinely monitored for concentrations of organic and inorganic constituents. Laboratory studies were designed to isolate and describe significant climatic, chemical, and interactive effects on evaporation rates. Results from the above studies were utilized to develop a regression model to predict evaporation from these low quality effluents. This model was then compared to commonly utilized models to estimate evaporation. A stochastic model was developed using a first order markov process to generate 1000 20-year climatological records. Mass balance techniques were then used to evaluate the new data sets for evaporation processes and determine critical design parameters for evaporation disposal ponds. Laboratory studies were conducted to determine significant effects on the Henry's Law Constant for eight organic compounds in two process waters. Henry's Law Constant is a necessary component to estimate or model the emission of organics from these low quality effluents.

Results of the research program indicate that oil shale process water evaporation is not significantly changed by oil shale water chemical composition or concentration from that of fresh water. However, the regression model developed specifically contains five climatic and six chemical variables which were significant in affecting the overall oil shale process water evaporation rate. Key impoundment design parameters were found to be the pond depth and the total allowable input of process water. Even using conservative estimates for a full scale oil shale operation, extremely large areas (1,000+ acres) will be required of industry for disposal of oil shale process waters by evaporation. The emissions research indicated that Henry's Law Constant values are extremely dependent upon temperature and the specific chemical composition of the oil shale process water and in order for the emission rates of a given compound to be accurately estimated for an oil shale process water, the Henry's Law Constant must be determined for each specific water and at expected disposal water temperatures of the process water.

ACKNOWLEDGMENTS

This project was sponsored through the Department of Energy's Laramie Project Office of the Morgantown Energy Technology Center under DOE Contract DE-AC21-84LC11049 with Richard McQuisten as the Contracting Officer's Technical Representative.

Five graduate students (Mitch Hall, Phillip Koontz, Sheree Eyre, Angela Vassar and Don Richard), two research associates (Matthew Haass and Sead El Gazawi), an electronic technician (Tim Kaser), and several undergraduate students at the University of Wyoming were greatly appreciated for their help in collection and analysis of data produced for this project.

Special thanks is also given to the City of Laramie, Wyoming for providing the field site and to the Civil Engineering Department at the University of Wyoming for the needed laboratory and shop space.

UNITS

A mixture of English and Metric units are used throughout this report. Instrumentation used resulted in measurements and data being in both unit systems. It was difficult in several instances to convert from one system to the other and still have the numbers be meaningful in terms of significant figures and measured values. It also allowed for better understanding of results in many situations for the authors and hopefully for the reader.

DATA

The actual data (original data and certain synthesized forms of the original data used in analysis) are not contained as a part of this report. This data can be obtained from the principal investigators, either on magnetic tape or floppy diskettes, by contacting the investigators through the Department of Civil Engineering, P.O. Box 3295, University Station, University of Wyoming, Laramie, Wyoming 82071.

TABLE OF CONTENTS

	<u>Page</u>
EXECUTIVE SUMMARY	1
INTRODUCTION AND PURPOSE	1
PROJECT DESCRIPTION	2
RESULTS/ACCOMPLISHMENTS	3
CONCLUSIONS AND RECOMMENDATIONS	7
INTRODUCTION	9
RETORTING PROCESSES	9
PROCESS WATERS PRODUCED	10
EVAPORATION DISPOSAL PROBLEMS	11
PURPOSE AND OBJECTIVES OF STUDY	12
EVAPORATION AND EMISSIONS	15
EVAPORATION TECHNOLOGY	15
EMISSIONS FROM EVAPORATING WATERS	23
EXPERIMENTAL FIELD SITE	28
LOCATION	28
FIELD LAYOUT	28
INSTRUMENTATION	30
MEASUREMENTS AND DATA HANDLING	35
EFFECTS OF CLIMATOLOGICAL PARAMETERS ON EVAPORATION	
RATE OF PROCESS WATERS	37
LITERATURE REVIEW	37
CLIMATOLOGICAL PARAMETERS AFFECTING EVAPORATION RATE	37
EFFECTS OF CHEMICAL COMPOSITION OF PROCESS WATERS ON	
EVAPORATION RATES	50
LABORATORY EVAPORATION STUDIES	50
EXPERIMENTAL DESIGN	50

TABLE OF CONTENTS

	<u>Page</u>
METHODOLOGY	50
FIELD EVAPORATION STUDIES	51
COMPARISON OF LABORATORY AND FIELD STUDIES - CONCLUSIONS	70
EVAPORATION MODELS FOR ASSESSMENT/DEVELOPMENT AND DESIGN OF OIL SHALE PROCESS WATER DISPOSAL	72
SELECTION AND ASSESSMENT OF EXISTING EVAPORATION MODELS	72
MATHEMATICAL/STATISTICAL MODELS	80
DIURNAL VARIATION OF EVAPORATION	84
CHEMICAL COMPOSITION AND RATE OF EMISSIONS FROM OIL SHALE PROCESS WATERS	102
CHEMICAL COMPOSITION OF EMISSIONS	102
CONCENTRATION (RATE) OF SELECTED EMISSIONS BEING RELEASED	105
FEASIBILITY OF USING EVAPORATION FOR THE DISPOSAL OF OIL SHALE PROCESS WATERS	119
SELECTION OF EVAPORATION MODEL	119
GUIDELINES FOR EVAPORATION POND DESIGN	119
DISCUSSION AND CONCLUSIONS	130
DISCUSSION OF RESULTS	130
CONCLUSIONS AND RECOMMENDATIONS	133
GLOSSARY	136
PROJECT PUBLICATIONS	143
REFERENCES	144
APPENDIX A: MINI-EVAPORATION PAN	149

LIST OF TABLES

<u>Table</u>	<u>Page</u>
1. Listing of Project Tasks by Objective	14
2. Water Quality Characteristics of Oil Shale Process Waters	27
3. Descriptive Statistics for Mean Daily Evaporation	41
4. Descriptive Statistics for Process Water Evaporation Rates	41
5. Climatological Variables Significantly Affecting Process Water Evaporation Rate Results From All Possible Subsets Regression Analysis (fresh water)	42
6. Climatological Variables Significantly Affecting Process Water Evaporation Rate Results From All Possible Subsets Regression Analysis (Rio Blanco)	42
7. Climatological Variables Significantly Affecting Process Water Evaporation Rate Results From All Possible Subsets Regression Analysis (Paraho)	43
8. Climatological Variables Significantly Affecting Process Water Evaporation Rate Results From All Possible Subsets Regression Analysis (Geokinetics)	43
9. Laboratory Evaporation Rates At 20°C And 80 Percent Relative Humidity With No Wind	45
10. Laboratory Evaporation Rates At 35°C And 80 Percent Relative Humidity With No Wind	45
11. Laboratory Evaporation Rates At 20°C And 80 Percent Relative Humidity With Wind	46
12. Laboratory Evaporation Rates At 35°C And 80 Percent Relative Humidity With Wind	46
13. Laboratory Evaporation Rates At 5°C And 80 Percent Relative Humidity With No Wind	47
14. Laboratory Evaporation Rates at 5°C And 80 Percent Relative Humidity With Wind	47
15. Laboratory Evaporation Analysis of Variance Interactions	48
16. Analysis of Variance for Orthogonal Component of Temperature and Relative Humidity With No Wind	49

LIST OF TABLES

<u>Table</u>		<u>Page</u>
17.	Analysis of Variance for Orthogonal Components of Temperature and Relative Humidity	49
18.	Laboratory Chemical Concentration Effects on Evaporation Rate at the Lowest or Level One Chemical Concentration	52
19.	Laboratory Chemical Concentration Effects on Evaporation Rate at Level Two Chemical Concentration	53
20.	Laboratory Chemical Concentration Effects on Evaporation Rate at a Medium Level (Level Three) Chemical Concentration	54
21.	Laboratory Chemical Concentration Effects on Evaporation Rate at Level Four Chemical Concentration	55
22.	Laboratory Chemical Concentration Effects on Evaporation Rate at the Highest Level or Level Five Chemical Concentration	56
23.	Regression Analysis of Evaporation Rates Versus Chemical Composition	58
24.	Descriptive Statistics for Chemical Concentrations of Oil Shale Waters. Time Period: Julian Day 183-312 of 1985	60
25.	Range of Chemical Composition of the Oil Shale Process Waters During 1986	62
26.	EPA Priority Pollutants Found In Oil Shale Process Waters	63
27.	WATEQ Computer Printout of Inorganic Constituents on Geokinetics Oil Shale Process Water	64
28.	Categories of Water Quality Data	69
29.	Parameters Required to Predict Evaporation for Established Models	72
30.	Coefficients of Correlation for the Ten Models	75
31.	R^2 , and R^2 Adjusted Coefficients for the Ten Models	75
32.	Evaporation Estimates by Method Compared to Pan Evaporation for Each of the Four Pans	76

LIST OF TABLES

<u>Table</u>	<u>Page</u>
33. Parameters Required to Estimate Evaporation in in Regression Models	81
34. Correlation Coefficients, R^2 , and R^2 Adjusted Values for Regression Models	83
35. Usable 33 Days of Hourly Evaporation Data	85
36. Hourly Evaporation Initial and Corrected Values for the Three Oil Shale Process Waters	86
37. Comparison of Measured and Estimated Evaporation	92
38. Ratios of Measured Evaporation vs. Kohler-Nordenson-Fox Estimates	93
39. Results of MERV calibration of the Kohler-Nordenson-Fox Equation	95
40. Ratios of Measured Evaporation vs. Calibrated KNF Estimates	96
41. Results of Regressions of Evaporation vs. Climatological Data for 33 days	97
42. Results of Regressions of Evaporation vs. Climatological Data for 4 days	99
43. Compounds Found in Paraho and Geokinetics Process Waters	104
44. Organic Compounds Studied	106
45. Aqueous Standard Mixtures	107
46. Volumes of Each Mixture Added to EPICS Bottles	110
47. Comparison of the Percent Coefficient of Variation with Different Liquid Volume Ratios for the Modified EPICS Method	112
48. Measured Henry's Law Constant Values	114
49. Henry's Law Constant Values	115
50. Temperature Coefficients	116
51. Analysis of Variance Results for Each Temperature	116

LIST OF FIGURES

<u>Figure</u>	<u>Page</u>
1. Oil Shale Evaporation Field Site	29
2. Diagram of Class A Pan and Holding Reservoir Arrangement	32
3. Detail of Stilling Basin and Level Sensing Probes	33
4. Total Measured Evaporation for Fresh Water and the Three Process Waters for the 1987 Field Season	40
5. Average Evaporation Rate for Each Chemical Concentration Level	57
6. Major Ion Distribution August 8, 1985 (Julian Day 220)	65
7. Major Ion Distribution September 6, 1985 (Julian Day 249)	66
8. Chemical Constituent Concentration with Time During 1985 for the Paraho Process Water	67
9. pH Concentration with Time During 1985	68
10. Daily Evaporation Pan #4 Geokinetics	78
11. Total Evaporation Estimated During 1987 for the Four Established Models	79
12. Evaporation Data, August 18, 1987 (day 230)	88
13. Overall Averages of Evaporation Data, June 24-September 16, 1987 (days 175-259)	89
14. Variation in Pond Depth: Set #1	125
15. Variation in Pond Depth: Set #2	126
16. Variation in Pond Depth: Set #3	127

EXECUTIVE SUMMARY

INTRODUCTION AND PURPOSE

Containment of oil shale process waters in open ponds has and continues to pose both control technology and environmental problems for industry. Design and construction of an economical evaporation pond depends on such items as excavation costs related to size, land costs, the concentration of chemical constituents in the water and the amount and/or rate of evaporation. Studies of fresh water evaporation have been carried on for several decades. Fairly sophisticated evaporation equations or models have been developed from these studies but in general have not addressed process waters laden with organic compounds. Associated environmental concerns may include watershed contamination, air quality, and sludge waste disposal.

Past research has indicated that, depending on the retort process to be used, the ratio of process waters to produced oil by above ground and modified in situ retorts will generally be between 0.2 and 2.3 barrels per barrel of oil. The oil shale process waters produced by retorting are generally heavily contaminated with high levels of organic and inorganic constituents. Disposal of these process waters constitutes difficult environmental and economic problems. In the western United States, one disposal method considered by industry is evaporation ponds or similar impoundments. Therefore, given the rates at which oil shale process waters could be produced on an industrial scale, accurate estimates of evaporation and emissions from these waters is critical for the planning and design of evaporation ponds.

Two primary purposes arise for this research program: (1) to study chemical, microclimatological, and interactive effects on the evaporation of low-quality oil shale process waters, and to develop more applicable evaporation models and evaporation design criteria for the disposal of oil shale process waters and (2) to analyze the processes associated with the release of potentially toxic emissions from these low-quality effluents. The research program incorporated both field and laboratory studies analyzing climatic and chemical effects on the evaporation of oil shale process waters.

The major objectives accomplished by this project were:

1. Determination of the effects of climatological parameters on the evaporation rate of the process waters.
2. Determination of the effects of chemical composition of the process waters on evaporation rates.
3. Development of a model applicable to the design of oil shale process water control by evaporation.
4. Determination of the chemical composition of emissions from process waters.
5. Assessment of the feasibility of using evaporation as a viable alternative for disposal of oil shale process waters.

PROJECT DESCRIPTION

Three oil shale process waters were used in a combined field and laboratory study effort. Two waters were from modified in situ retorting methods, and one from a surface retorting method. The field studies were designed to continuously monitor microclimatological conditions and evaporation from the three oil shale process waters using Class A evaporation pans. Freshwater evaporation was monitored as a control. The process waters were routinely monitored for concentrations of organic and inorganic constituents. These data were used to identify significant effects acting on the evaporation of these waters under confounded field conditions. Laboratory studies were designed to isolate and describe significant climatic, chemical, and interactive effects on evaporation rates under controlled conditions. Results from the above studies were used for two main purposes: (1) to determine significant effects on the evaporation rate of these waters, and (2) to develop a statistical model to be used for prediction of evaporation. The developed model was then compared to commonly used models for accuracy in estimating evaporation from these waters. A stochastic model was developed using a first order markov process to generate 1000, 20-year sets of climatic data for Laramie, Wyoming, the location of the field site for this study. The Kohler, Nordenson and Fox (KNF) mass balance model was then used to estimate evaporation for the 1000 sets of 20-year climate and determine critical design parameters for evaporation disposal ponds. Analysis of evaporation data was also conducted on a diurnal basis and modeled.

In conjunction with this research, laboratory studies were conducted to evaluate the processes associated with the release of toxic emissions during evaporation of these process waters. In these chemically complex waters, this is a very confounded problem. It was beyond the scope of this project to completely define the emission process and interacting processes of even the major organic species. Laboratory studies were designed, however, to study significant effects on the Henry's Law Constant (HLC) of eight major organic compounds in two of the oil shale process waters and in distilled water. HLC is a required component in most models used to estimate the emission rate or flux of a given compound from a liquid to a gaseous phase. HLC for a given compound is highly dependent on temperature, and moderately dependent on the ionic strength of the solution. Therefore, HLC values for a given chemical species in solution may change with the water temperature, the concentration of the compound, the total ionic strength of the water, and with interacting environmental variables. The purpose of this portion of the study was to measure HLC for selected major organic compounds in the process waters and to identify significant effects which may be caused by temperature and confounding compounds (i.e. matrix effects) on the measured HLC values.

For much of this study, Class A evaporation pans were used because they are the standard measurement for evaporation. Many studies have related evaporation from Class A pans to the evaporation of reservoirs and impoundments. A major drawback of this pan is its large size (4 ft. dia. x 10 in. deep). This size of evaporator was not practical for the laboratory studies designed for this program. A side-study, therefore, was conducted to design a mini pan for evaporation which could show good correlation to the measurements of a standard Class A evaporation pan. This was accomplished and the results are reported in an Appendix to this report.

RESULTS/ACCOMPLISHMENTS:

FIELD STUDIES

Data obtained from the field studies were primarily used for three purposes: (1) to determine and describe significant climatological and chemical effects as measured in a large scale field uncontrolled scenario, (2) to produce a statistical (empirical) model to predict evaporation from these waters, and (3) to provide a large database of evaporation and climatic data to be used in comparing and evaluating historically used models to the field developed model.

Field data obtained in 1985 was used to determine significant effects on the evaporation of process waters and to develop a model. A statistical analysis combining polynomial regression and significance testing was first used to screen each measured chemical and climatological parameter on an individual basis for effects on evaporation. These data were used to provide an indication of the statistical significance that each independent variable may have in a complex interactive model, and to indicate if polynomial (e.g., quadratic, cubic etc.) effects may exist for that variable. All possible subsets regression, using Mallows C_p and Adjusted R^2 criteria for model selection, was used to identify significant variables affecting evaporation, and to determine the best linear model.

Results of these analyses show that five climatological parameters and six chemical parameters were found to have significant effects on process water evaporation in a combined model. The climatological parameters are ambient air temperature, water temperature, wind speed (measured at the water surface), radiation intensity, and barometric pressure. The chemical parameters are alkalinity, chloride concentration, sulfate concentration, total dissolved solids (TDS), total organic carbon (TOC), and pH. All the parameters listed above were significant at the $\alpha = 0.05$ level, the climatic parameters, however, generally showed significance at higher levels of probability than the chemical parameters. The linear model produced from these analyses for all waters combined (fresh water and the three process waters) is given below:

$$\begin{aligned} E = & 0.01718 (T_a) + 0.00015 (T_a^2) + 0.00213 (T_s) + 0.00617 (T_b) + \\ & 0.01092 (W_g) + 0.00036 (R_s - 0.15074 (P) - 8.5426 \times 10^{-6} (ALK) + \\ & 1.7286 \times 10^{-4} (Cl) + 1.5014 \times 10^{-5} (SO_4) - 2.2181 \times 10^{-6} (TDS) + \\ & 1.9938 \times 10^{-5} (TOC) + 0.1428 (pH) + 2.20 \end{aligned} \quad (A)$$

where:

E - Evaporation rate (cm/hr)
T_a - Ambient temperature (°C)
T_s - Water temperature @ surface (°C)
T_b - Water temperature @ base (°C)
W_g - Wind speed at water surface (mph)
R_s - Radiation intensity (watt/m²)
P - Barometric pressure (in Hg)
ALK - Total alkalinity (ppm)
Cl - Chloride (ppm)
SO₄ - Sulfate (ppm)
TDS - Total dissolved solids (ppm)
TOC - Total organic carbon (ppm)
pH - pH (standard units)

A strict level of tolerance between independent parameters was used in the multiple regression analyses so that statistically redundant independent parameters would be excluded from the model. Multicollinearity, however, may still exist between some of the parameters. High multicollinearity can cause inaccuracies in the coefficients of the parameters involved. It is suspected that in the development of these regression models some multicollinearity exists between the chemical parameters and that inaccuracies exist in the coefficients. This hypothesis is based on data showing high correlations between the parameters.

LABORATORY STUDIES

Two laboratory studies were conducted to determine and identify significant effects on oil shale process water evaporation under controlled conditions. One study concentrated on climatological effects and interactions under conditions where chemical parameters could be held constant and climatological parameters could be controlled and replicated. The other study concentrated on effects caused by increasing chemical concentrations under conditions where climatic conditions were held constant. The purpose of these studies was to support the data and model development from the field studies. Both laboratory efforts utilized environmental chambers.

Results from the laboratory chemical study indicated that no significant effects caused by the increasing concentrations of chemical constituents could be demonstrated on process water evaporation rates. The range of concentrations studied were based on two times the range of TDS and TOC concentrations observed in the field study over one field season. These data indicate that in large scale evaporation, increasing chemical concentrations (at the levels studied) will not affect evaporation rates.

The laboratory climatic study was a four factor ANOVA design analyzing ambient air temperature at three levels, relative humidity at two levels, and wind speed at two levels for fresh and process water. ANOVA results indicate significant effects due to temperature, relative humidity, and wind at the $\alpha = 0.05$ level. No significant difference could be found between process waters and fresh water at even the $\alpha = 0.30$ level. Significant interactions ($\alpha = 0.05$) were found between temperature and relative humidity, temperature and wind speed, and relative humidity and wind speed. No three way interactions were significant.

MODEL COMPARISON STUDIES

Ten established evaporation models and the developed statistical evaporation model (Equation A) were compared for accuracy in predicting the daily evaporation from the process waters and from fresh water. Comparison and analyses performed were based on 160 days of evaporation data measured in 1985 and 1986. Regression analysis was used and determinations were made based on correlation coefficients and coefficient of determinations between the measured daily values and estimated daily values.

Results indicated that three established models and the developed statistical model (Equation A) showed good correlation with measured daily values. The three established models were the Kohler-Nordenson-Fox (KNF), the Priestly-Taylor (PT), and the Penman Combination Equation (PML). The developed statistical model showed the best correlations with measured daily values. The major difference in the developed model and the established models are the inclusion of chemical parameters. If these chemical parameters cannot be measured, estimates of evaporation on a daily basis from oil shale process waters can be obtained by use of one of the three established models after calibration for that location.

An unexpected conclusion was made from these data. All three established models identified, and the developed model (Equation A) used solar intensity as a factor or variable in estimating evaporation. The other seven models tested which simplified this parameter through the use of coefficients, or simply eliminated this parameter, were not as effective as the four identified models in estimating process water evaporation. It was concluded, therefore, that solar radiant flux is an important factor when estimating evaporation from process waters.

An evaluation of the KNF equation on a diurnal (hourly) basis was also performed for a 33-day period. The estimates using the sum of hourly KNF estimates were higher than the measured values by 10 to 15 percent. Therefore, the KNF equation was calibrated for diurnal variations. The results of the calibration were nearly as good as developed regression models for diurnal variations of evaporation versus climatological and chemical data. Use of the KNF equation is preferred to these models since empirical formulas are generally considered to be more transferable to other locations than are regression models.

DETERMINATION OF CRITICAL IMPOUNDMENT DESIGN PARAMETERS

Because chemical data cannot be projected for future oil shale process waters, the KNF equation was used to estimate evaporation on 1000 sets of 20-year climatological data produced by stochastic modeling. Results indicated that a conservatively designed pond would be able to safely contain a water depth of 64₃ inches (not including freeboard), while accommodating an inflow of 0.55 ft³/ft². The inflow volume of process water was then estimated using published data. These data indicate that between 0.22 and 2.3 barrels of process water could be produced per barrel of oil, depending on the exact process utilized. For a theoretical 50,000 barrel/day operation, these numbers translate to 11,000-115,000 barrels of processed water produced per day, or 518 to 5410 acre-feet/yr. Using the developed inflow figure of 0.55 ft³/ft², the pond size required for this theoretical operation would be between 940 and 9840 acres.

These results demonstrate the importance of making accurate evaporation estimates for these waters and the scope of the disposal problem. Obviously, similar modeling efforts will have to be repeated in the future. However, two major conclusions can be made from this analysis. Evaporation pond design will have to maintain fairly shallow depths (64 inches) in order to optimize free water evaporation, and that extremely large areas (1,000-10,000 acres) will have to be used if this management technique (evaporation ponds) is employed. These data further conclude, or suggest, that the volume of these waters that could potentially be produced may be an important factor in determining the retorting process used for production (i.e., the production of process water may have to be minimized) or that the utilization of evaporation ponds as a means of process water disposal in the western United States is highly questionable.

EMISSIONS RESEARCH

Henry's Law constants were measured for eight major organic compounds across three temperatures for two oil shale process waters and in distilled water in which the compound was inoculated. The process waters used were from the Geokinetics, Incorporated and Paraho Corporation processes. The eight compounds studied were chosen because of several factors, including the results of GC/MS analysis of the process waters (EPA 624; EPA 625), the range of previously measured HLC values, and their environmental importance. The compounds studied were: 1-hexene, n-hexane (n-hexane or one of its isomers), benzene, toluene, 2-pentanone, 2-hexanone, cyclohexanone, and 2,6 dimethylphenol. Temperatures analyzed were 10°C, 25°C and 40°C.

Analysis of variance results of the entire experimental model indicated that the type of waters, the water temperature, the compound, and a temperature-compound interaction all had significant effects on the HLC values. Further, ANOVA tests analyzed the significance of the water composition at each temperature. These results indicate that the water type and water-compound interactions always produced significant effects on the HLC at each temperature analyzed. In general, these results show that a strong matrix effect exists on the HLC that is dependent on the specific chemical characteristics of the individual water.

Regression analyses were used to further describe the temperature effects on the compounds. Analysis of the regression coefficients also showed that the temperature effect on HLC values are significantly different between process waters and distilled water. The observed differences between the slopes (regression coefficients) for each water and each compound show that the waters affect the HLC of each compound differently. This is further evidence of a very strong matrix effect.

The major results from this emissions research show that HLC values are extremely dependent upon temperature and the specific chemical composition of the process water. Evaluation of the literature has shown the importance of accurately measuring HLC for prediction of emission rates of different compounds in water. Mackay and Shiu (1981) concluded that the standard error in measuring HLC values should not exceed 10 percent when estimating emissions for environmental purposes. The major conclusion drawn from these data, therefore, is that in order for the emission rates of a given compound to be accurately estimated, the HLC must be known for each specific water and at each expected water temperature. The example presented on two of the eight compounds for which the HLC values were obtained indicate that emissions from oil shale process waters could be significant.

CONCLUSIONS AND RECOMMENDATIONS

Major conclusions of this study are:

1. When considered as a complete model, five climatological parameters and six chemical parameters produce significant effects on process water evaporation. Climatological parameters are: ambient temperature, water temperature, wind speed (measured at the water surface), radiation intensity, and barometric pressure. The chemical parameters are alkalinity, chloride concentration, sulfate concentration, total dissolved solids (TDS), total organic carbon (TOC), and pH; however, these results may be strongly effected by multicollinearity.
2. Under controlled climatic conditions, process water evaporation on a large scale was not significantly changed with increasing chemical concentrations over the range of concentrations studied.
3. Under controlled chemical conditions, process water evaporation was significantly affected by ambient temperature, relative humidity, wind speed, a temperature-wind speed interaction, and a relative humidity-wind speed interaction. No significant differences existed between process water and fresh tap water under the conditions studied.
4. Solar radiant flux is a critical parameter in selecting an evaporation model to estimate oil shale process water evaporation.
5. The statistical model (Equation A) developed for this study showed the best results in estimating oil shale process water evaporation; however, three existing established (KNF, Priestly-Taylor and Penman combination) models were also relatively accurate.

6. The calibrated Kohler-Nordenson-Fox evaporation equation for hourly data is at least as good as developed regression models for evaluating diurnal evaporation rate.
7. Key impoundment design parameters were found to be the pond depth and the total allowable input. Even under conservative estimates, extremely large areas (1,000+ acres) will have to be used for disposal of oil shale process waters by evaporation.
8. In order to accurately estimate emission rates from oil shale process waters for a given compound, the Henry's Law constant must be known for each specific water and at each expected water temperature.

Recommendations for future studies should include:

1. Comparison of the established and developed models of this study need to be analyzed on a broad range of evaporation data from different locations in the western United States.
2. Refinement in the stochastic procedures utilized to size evaporation pond impoundments and the statistical distribution to be used (normal or some other distribution).
3. More compounds found from the gas emission analyses studied in this report, including inorganics, should be measured for HLC and other constants such as partial pressure so that accurate estimates of emission rates from evaporation ponds can be made. This report only indicated that emissions from evaporation ponds could be significant and as such could be an environmentally important consideration for the oil shale industry.
4. Emission rates from oil shale process waters should be estimated and measured to determine if dissolved solid and matrix effects can be modeled.

OIL SHALE PROCESS WATER EVAPORATION

INTRODUCTION

It is reasonably certain that because of the importance of energy to the world as we know it today, when it becomes necessary to develop oil shale, this development could be very hasty to say the least (Welles, 1970; Russell, 1980).

It is this future haste that prompts the research of today. The huge hydrocarbon deposits of former Lake Uinta alone are staggering. In the present Piceance Creek Basin of Colorado alone, an estimated 720 billion barrels of crude oil are trapped in the rocks (Russell, 1980; Nat. Aca. of Sci., 1980). The entire Green River Formation is estimated to contain 2000 billion barrels of crude oil (Russell, 1980). To release this wealth on a mass scale, however, will require large investments, as well as place an enormous load on the environment in the way of land deformation, solid waste formation, air pollution, and a substantial demand for water (EPA, 1977).

RETORTING PROCESSES

Modern retorting proposes to process huge volumes of oil shale on a daily basis. The size of processing makes mining a much more significant consideration both from the standpoint of economics and efficiency than for coal, tar sands, uranium and similar possible energy resources (Nat. Aca. of Sci., 1980).

Today, two popular methods of retorting oil shale are common. The first is conventional above ground methods, the other is in-situ processing.

The theory behind above ground retorting methods is basically the same today as was used in the boom era of the 1920's. Modern processing, however, would take advantage of advanced strip mining technology (or possibly conventional underground room and pillar mining) to remove the vast quantities of oil shale that would be required. The shale would then be retorted in huge continuous retorts. In these devices, shale is fed into the retort and is moved through the retort mechanically, while hot gases are forced upward through the retort. The flow of hot gases (either internally or externally heated) drives the Kerogen from the rock and breaks it down into a high viscosity substance called shale oil (Keith, 1982).

In the late 1920's, oil shalers developed a new method of extracting oil from oil shale while it was still in the ground. This new method was much cheaper than mining, crushing, and burning the shale above ground, and was called in-situ retorting (Russell, 1980). Although in-situ retorting was cheaper than mining it still could not compete in the oil market as more and more crude oil deposits were being found.

The two most common methods of in-situ retorting today are called true and modified. In a true in-situ retort the ground is typically broken up with explosives to create cracks and voids, then the zone is ignited with an external source. The shale burns horizontally through the expanded zone, and as the combustion face moves across the zone the oil volatilizes then condenses ahead of the combustion face where it can be pumped to the surface. A modified in-situ retort, on the other hand, employs a minimum amount of conventional mining to create a cavern within the retort zone. When the rest of the zone is detonated, the cavern provides room for expansion, creating a shale which will burn more efficiently. A typical modified in-situ retort also differs from a true in-situ burn as the combustion face proceeds from top to bottom and the oil is removed from the bottom of the retort zone (Keith, 1982).

All of the methods of retorting oil shale work quite well, but the end results can be considerably different. Clearly, a shale which has been conventionally mined and crushed will burn much better and will have the highest possible yield. Above-ground retorting can recover greater than 95 percent of the potential oil in the rock. In-situ methods, by comparison, will have lower recovery efficiencies in the neighborhood of 55 to 70 percent (Welles, 1984). As the amount of mining and preparation decreases so does the removal efficiency. This decrease in efficiency, however, is offset by decreases in operational costs associated with mining, hauling, and crushing of the shale.

Today, above-ground retorting is the favored method because of its efficiency as a result of more control over the process (Welles, 1984). The other methods, however, are still being developed for areas where above-ground operations may not be economical.

PROCESS WATERS PRODUCED

It is estimated that a full scale oil shale retorting plant in the Piceance Creek Basin will be capable of producing 50,000 barrels of oil in a single day. To accomplish this, however, a plant of this capacity would have to mine almost 75,000 tons of oil shale in a single day either by conventional underground methods or in enormous open pit mines (which would also require the relocation of thousands of cubic yards of overburden). In addition, estimates of water needs range from as little as one to two barrels of water per barrel of oil, to as much as ten barrels of water for every barrel of shale oil produced, depending on the method (Keith, 1982; Nat. Aca. of Sci., 1980; McKell, 1984). Once used in the processing of shale oil, this water may have very undesirable characteristics.

The term oil shale retort water or process water is itself an all encompassing definition. For this report it will refer to water that is created as a product of combustion during the actual retorting operation. Wastewaters from oil shale retorting, however, also include waters used during the mining, crushing, and power generation phases of the oil shale processing operation (Nowacki, 1981). Retort water may also

include water in the form of steam during the separation of the oil from the rock. Another major source of wastewater is the groundwater itself. Any groundwater present during an in-situ retort will become polluted during the combustion phase of the operation and will be considered a retort water. Additionally, any groundwater that flows into an in-situ retort zone after combustion may become contaminated with residual organics as well as inorganics still in the zone. Although this is not technically a retort water, its characteristics may be similar. Even water pumped during mine dewatering for an above-ground retorting operation, although not considered as a retort water, may be polluted enough to be considered wastewater.

Depending on the retort process used for oil shale, the ratio of product water to oil products produced is generally assumed to be between 0.22 to 2.3 (Nowacki, 1981). In-situ retort processes may produce higher amounts of wastewater depending on the amount of ground water intrusion into the retort. In general, these effluents are heavily contaminated with high levels of organic and inorganic constituents. Disposal of these wastewaters constitutes difficult problems both environmentally and economically. Two methods currently being considered to dispose of these waters are: 1) codisposal with processed shale solid waste in embankments, and 2) disposal using evaporation ponds or impoundments. Other choices available are chemical, physical, and biological treatment which presently do not seem economically feasible at an industrial scale.

Codisposal of the process waters with the oil shale solid waste would be the desired method by most industries. This will be feasible only if the hydrologic conditions producing leachate from these solid waste embankments is found to be at environmentally safe levels. At the present time, codisposal of oil shale process water with the solid waste presents confounded hydrologic, geochemical, and geotechnical problems which have not been solved.

EVAPORATION DISPOSAL PROBLEMS

An EPA Oil Shale Research Group has indicated that a mature oil shale industry could produce one million barrels of oil per day. At this rate of production, between two hundred thousand and two million barrels of wastewater effluent would be produced each day, potentially over three hundred million barrels per year. Procedures utilizing disposal by evaporating the effluent will require precise data on evaporation rates to properly size the retention-evaporation system. If inaccurate evaporation rates are used to design a wastewater retention pond, it is highly possible that overflow will occur resulting in release of toxic and/or potentially toxic effluents into the environment.

A 20 percent under-estimate of the evaporation rate from a waste pond is no small volume of water to provide storage for; take for example a one-acre waste retention pond in Laramie, Wyoming, where the recorded annual evaporation rate is approximately 46 inches per year. An under-estimate of 20 percent in the evaporation rate at Laramie would result in

approximately 250,000 gallons more of wastewater per year that is not accounted for if the average annual value were used as the design value. If a sufficient factor of safety is not provided in design standards, real problems exist in the disposal of wastewaters from oil shale development, clean coal developments and other industrial processes. This amount of water also indicates the tremendous area that would be needed for evaporation ponds (0.13 inches/day average over the year for Laramie means 2833 acres or 4.43 sq. mi. of land area to evaporate approximately 200,000 barrels of wastewater per day).

Evaporation estimates are generally derived from empirical models using mass balance, energy budgets, or a combination of these two methods. These models were essentially developed for use with fresh water. The use of these evaporation models may not be completely applicable for estimating evaporation from oil shale process waters where significant reductions in fluid vapor pressures may exist because of high concentrations of chemical constituents. Given the possible high rates at which oil shale process waters could be produced on an industrial scale as indicated above, accurate estimates of the evaporation behavior of these waters is critical for planning and design of evaporation retention ponds.

Process waters can contain a complex of compounds including many organics and inorganics. The characteristics of process waters vary not only with the processes used to extract the oil, but also with the type of shale retorted (Fox et al., 1978). These waters are typically high in pH, and they have high concentrations of ammonia, bicarbonate, carbonate, sodium, chloride, and sulfate (Stuber and Leenheer, 1978).

Many of the compounds found in these process waters have high vapor pressures and low water solubilities indicating a potential for high volatilization rates from the wastewater into the atmosphere (Hawthorne, 1984). Since a proposed disposal practice for process waters is the use of evaporation ponds, the rate of emissions of the volatile compounds from the wastewater into the atmosphere should be investigated. These rates can be either measured or estimated using mathematical models.

The accurate estimation of evaporation for western oil shale process waters and the resulting emissions that may occur need to be assessed in greater detail to address engineering and environmental concerns associated with these waters in evaporation ponds so that proper disposal can occur. Western oil shale process waters are the major concern since the amount of evaporation compared to precipitation is highly positive only in the arid western United States. Open evaporation ponds are not a viable alternative for disposal of oil shale process waters produced in the eastern United States because precipitation is generally greater than evaporation over the course of a year. This study was undertaken to address several of the issues associated with evaporation pond disposal of oil shale process waters.

PURPOSE AND OBJECTIVES OF STUDY

Two primary purposes arise for this research program: (1) to study chemical, microclimatological, and interactive effects on the evaporation

of low-quality oil shale process waters, and to develop more applicable evaporation models and evaporation design criteria for the disposal of oil shale process waters and (2) to analyze the processes associated with the release of potentially toxic emissions from these low-quality effluents. The research program incorporated both field and laboratory studies analyzing climatic and chemical effects on the evaporation of oil shale process waters.

The major objectives accomplished by this project were:

1. Determination of the effects of climatological parameters on the evaporation rate of the process waters.
2. Determination of the effects of chemical composition of the process waters on evaporation rates.
3. Development of a model applicable to the design of oil shale process water control by evaporation.
4. Determination of the chemical composition of emissions from process waters.
5. Assessment of the feasibility of using evaporation as a viable alternative for disposal of oil shale wastewaters.

Each major objective was subdivided into tasks or sub-objectives that defined in more detail the requirements of each objective. Table 1 presents the major objectives with all tasks or sub-objectives indicated under the major objective.

The remainder of this report addresses the approaches used and results obtained for each of the major objectives and sub-objectives. A discussion and conclusions section is contained at the end of the report.

Table 1

Listing of Project Tasks by Objective

- 1.0 Objective: Determination of the effects of climatological parameters on the evaporation rate of process waters.
 - 1.1. Compilation of literature relating to the evaporation of low-quality wastewaters.
 - 1.2. Investigate the effects that important climatological parameters have on evaporation rates in a controlled environment.
 - 1.3. Investigate the effects that important climatological parameters have on evaporation rates in a natural field environment.
- 2.0 Objective: Determination of the effects of chemical composition of process waters on evaporation rates.
 - 2.1. Investigate the effects of water quality on evaporation rates in a laboratory environment.
 - 2.2. Measure the effects of water quality parameters on field evaporation rates.
- 3.0 Objective: Development of a model applicable to the design of oil shale process water control by evaporation.
 - 3.1. Analyze data collected from the research project.
 - 3.2. Test existing evaporation formulas against climatological data collected from the field research site.
 - 3.3. Develop a mathematical model for predicting the evaporation of oil shale wastewater.
 - 3.4. Test the mathematical model against data collected from the field.
- 4.0 Objective: Determination of the chemical composition of emissions from process water.
 - 4.1. In a laboratory environment, investigate the composition of emissions from oil shale wastewater.
 - 4.2. Investigate the concentration of selected emissions being released into the environment from an evaporation pond.
- 5.0 Objective: Assessment of the feasibility of using evaporation as a viable alternative for disposal of oil shale wastewaters.
 - 5.1. Development of design criteria for evaporation ponds.

EVAPORATION AND EMISSIONS

When fresh water, oil shale process water or other types of water evaporate, climatic factors are involved. Additionally, the complex nature of oil shale process waters compared to fresh water have an additional effect on evaporation. The high concentrations of salts and organics in oil shale process waters add to the bonds that must be overcome for water molecules to escape from the liquid. When these molecules of water and other compounds in the process water escape by evaporation into the atmosphere, the rate of evaporation and escape of volatile compounds due to the evaporation process must be investigated to see if the compounds being emitted into the atmosphere are of an environmental and health concern.

The purpose of this review of evaporation and emissions is to indicate the knowledge base of these two areas with regard to this research project.

EVAPORATION TECHNOLOGY

Evaporation is a critical process in the hydrologic cycle. It is the process by which water is transferred from bodies of water, soil and vegetation, and returned to the atmosphere. To accomplish this transfer, the water must change from a liquid state into a vapor. This vapor is then transferred or becomes part of the atmosphere; hence, evaporation is defined as the net rate of vapor transfer (Viessman et al., 1977). As Dunne (1978) states, the process occurs when molecules of the liquid attain sufficient kinetic energy to overcome the forces of surface tension and escape from the surface of the liquid. The molecules of the liquid attain this energy from the sun. Whether the energy is in the form of solar radiation directly, sensible heat transfer from the atmosphere, or other related means, it is in effect all from the sun.

Rates of evaporation vary depending on certain climatological parameters, and on the nature of the evaporating surface. Evaporation from an open water surface is a function of many parameters. The available energy and resulting net radiation have a great effect on evaporation. Related to this is the sensible and latent heat, which in turn help establish the temperatures of the water surface and the air. Another major factor is the vapor pressure and related saturation deficit and vapor pressure gradient that results. Connected with this saturation deficit is the wind speed. If there is no wind present, the air above the water surface will become saturated and there will be no vapor pressure gradient present to drive the evaporation process. The result is zero net evaporation.

Other parameters which affect the rate of evaporation include the composition of the water. The presence of different chemical combinations in the water may affect the chemical and physical reactions that take place in the water, thereby affecting the evaporation rate. This may be seen if the salinity of the water changes, or if chemical monolayers are

formed. These differences in the composition of the water affect the nature of the surface of the water. It may be a change in surface tension or latent heat required for vaporization, or it may affect the reflectance properties of the water.

The altitude or elevation of the water above sea level, the latitude and location, and the barometric or atmospheric pressure surrounding the water, may also affect the rate of evaporation. In analysis, several parameters usually prove to be of importance, but the combination may not always be the same. This is apparent in the various models and equations derived for evaporation. Not all use the same combination of parameters, but that does not reduce their importance or significance.

Methods of Estimating Evaporation

There are several approaches currently used to estimate evaporation. The four main approaches are: the energy or water budget method, the mass transfer or aerodynamic method, the combination method (which is a combination of the first two methods), and measurements taken on evaporation pans. Within each method, various models and estimates have been developed. The differences between the various versions arise from the fact that different assumptions and parameters are used or considered.

Energy or Water Budget Method: In this method, all inflows and outflows are accounted for and balanced so that evaporation can be estimated.

$$E = I + P_r - S_p - O - \Delta S \quad (1)$$

where I is the inflow, P_r is the precipitation, S_p is the seepage, O is the outflow, and ΔS is the change in storage. In theory this is an accurate estimation, but it seldom is in reality. The equipment needed for accurate estimates of all variables is extensive and costly, if they can be measured at all. Errors in measurement can be significant to the final results.

To avoid the problems of the water budget method, a balance or budget of a different kind is generally applied, and is known as the energy budget. The energy budget method uses the energy or heat balance to estimate evaporation. The energy budget approach assumes that any heat not accounted for, if all the heat entering and departing from a body of water were to be measured, was lost from the system as it was removed by evaporation, or the latent heat of vaporization (Garstka, 1978). This vertical energy balance was expressed by Bartholic et al., (1970) as:

$$R_n + E + G + H = 0 \quad (2)$$

or to solve for evaporation:

$$E = - (R_n + G + H) \quad (3)$$

where R_n is the net radiation or energy being added, E is evaporation, G

is soil heat flux, and H is sensible heat.

Morton (1965) used a slightly different form of this balance,

$$E = (1-\alpha)G - B - K \quad (4)$$

where α is albedo, G is the incident insolation expressed in evaporation units, B is the radiant heat transfer to the sky in evaporation units, and K is the sensible heat transfer to the air in evaporation units. Viessman et al., (1977) broke down the parameters for the energy budget equation even further:

$$Q_o = Q_s - Q_r + Q_a - Q_{ar} + Q_v - Q_{bs} - Q_e - Q_h - Q_w \quad (5)$$

where:

Q_o = increase in stored energy by the water
 Q_s = solar radiation incident at the water surface
 Q_r = reflected solar radiation
 Q_a = incoming long-wave radiation from the atmosphere
 Q_{ar} = reflected long-wave radiation
 Q_v = net energy advected into the water body
 Q_{bs} = long-wave radiation emitted by the water
 Q_e = energy used in evaporation
 Q_h = energy conducted from water mass as sensible heat
 Q_w = energy advected by evaporated water

Using the Bowen's ration relationship, B,

$$B = H/E = Q_h/Q_e \quad (6)$$

which can be computed using:

$$B = 0.61 (P/1000)(T_s - T_a)/(e_s - e_a) \quad (7)$$

where P is the atmospheric pressure in mb, T_s and T_a are the water and air temperatures, respectively in °C, e_s and e_a are the saturation and actual vapor pressures, respectively, in mb (Linsley, 1975), and the estimate for Q_w is

$$Q_w = c_p Q_e (T_e - T_b)/L \quad (8)$$

where c_p is the specific heat of water in cal/g °C, T_e is the temperature of evaporated water in °C, T_b is the temperature of an arbitrary datum usually taken as 0°C, and L in the latent heat of vaporization (Viessman et al., 1977), the energy of evaporation can be solved using the following:

$$Q_e = (Q_s - Q_r + Q_a - Q_{ar} - Q_{bs} - Q_o + Q_v)/[1 + B + c_p(T_e - T_b)/L]. \quad (9)$$

Evaporation can then be determined using the equation

$$E = Q_e/\rho L \quad (10)$$

where E is the evaporation in cm^3/cm^2 day, and ρ is the mass density of evaporated water in g/cm^3 (Viessman et al., 1977). Using these relationships, the energy budget equation for evaporation is

$$E = (Q_s - Q_r + Q_a - Q_{ar} - Q_{bs} - Q_o + Q_v) / \{\rho[L(1 + B) + c_p(T_e - T_b)]\} \quad (11)$$

Mass Transfer or Aerodynamic Method: The mass transfer method is based primarily on the concept of the transfer of water vapor from an evaporating surface to the atmosphere (Viessman et al., 1977). Thus, the evaporation from a water surface or the water vapor content and its transport from a water surface are estimated. The consideration of transport, or the function of the wind in this evaporation method, has caused it to be referred to not only as a mass transfer method, but also as an aerodynamic method.

The basis for this method originates from Dalton's estimates established in the 1800's, which were similar in form to:

$$E = (e_s - e_a) f(u) \quad (12)$$

where $f(u)$ is a function of the windspeed (Kohler, 1954). In Dalton's estimate, $f(u)$ was replaced by K , which was a coefficient dependent upon the wind velocity, atmospheric pressure and other parameters. In Harbeck's (1962) analysis $f(u)$ was replaced by Nu , where N was a coefficient of proportionality, generally called a mass transfer coefficient, and u was the wind speed in miles per hour at some height above the water surface. In Morton's (1965) studies, he used the simple mass transfer equation of the type,

$$E = [f(u)/P](e_s - e_a) \quad (13)$$

where P is the atmospheric pressure.

All these methods use a vapor pressure change and a wind function, but differ on other effects included in the equation. They are based on the same concepts, but the simplicity or complexity depend on the assumptions and relationships included. The mass transfer method, like the energy budget method, is limited in its use, due to the measurements or observations necessary to utilize it. The observation that is required in both, which is difficult to measure accurately, is the evaporating surface temperature. Efforts to eliminate this problem led to the combination method.

Combination Method: Penman was one of the first to show that it is possible to eliminate the need for surface temperature measurements under certain conditions by combining the mass transfer and energy balance equations into what is known as the combination method (Morton, 1965). There are assumptions that must apply if the combination method is used. Any combination solution assumes two conditions: first, that the differences between surface values and those taken at the point of measurement are negligible; and second, that the turbulent transfer coefficients for water vapor and sensible heat are substantially equal

(Van Bavel, 1966). These assumptions are generally met as long as measurements are taken over and close to the evaporating surface.

Since the complete derivation of the combination equation is lengthy and involves many micrometeorological concepts, Singh (1981) divided the derivation into steps. The main steps of the derivation are: a) define the vertical energy budget of the surface, b) apply the Dalton-type transport function to obtain Bowen's Ratio, c) apply Penman's psychrometric simplification to eliminate the need for surface temperature values, and d) apply the vertical transport equation obtained from turbulent transport theory.

Bowen developed a combination equation using both the energy budget and mass transfer equations. He used an energy budget equation such as Equation (2) and then used mass transfer equations to develop the Bowen's Ratio, B, such that

$$B = H/E. \quad (14)$$

Bowen used the transfer equations to define H and E as shown below. The turbulent vertical transfer of heat in air is given by,

$$H = \rho c_p K_h [\delta T / \delta z + \Gamma] \quad (15)$$

where Γ is the dry adiabatic lapse rate $dT/dz = -0.01$ °C/m and is neglected in most applications (Bartholic et al., 1970). The equation for the turbulent flux density of latent heat is commonly seen in the following form:

$$E = L_v \rho K_w (0.62/P) (\delta e / \delta z). \quad (16)$$

Substituting the transfer equations into the Bowen Ratio yields

$$B = H/E = [c_p P K_h \delta T / \delta z] / [0.62 L_v K_w \delta e / \delta z]. \quad (17)$$

Assuming $K_h = K_w$, and that the gradients are measured over the same intervals, upon integration

$$B = H/E = \gamma (\Delta T / \Delta e) \quad (18)$$

where $\gamma = c_p P / 0.62 L_v$ and is the psychrometric constant. Substituting (18) into (3) and rearranging gives

$$E = -(R_n + G) / [1 + \gamma (\Delta T / \Delta e)] \quad (19)$$

This evaporation equation has been used extensively by Frisichen and Van Bavel, Pruitt and Tanner, and others, and is generally adequate for determining evaporation (Bartholic et al., 1970).

Penman developed his combination equation by simultaneously solving equations of the two types, energy budget and mass transfer. His equation is

$$E = (R_n \Delta + E_a \gamma) / (\Delta + \gamma) \quad (20)$$

where

$$\begin{aligned} \Delta &= \text{the slope of the saturations vapor pressure} \\ &\quad \text{versus temperature curve } (de_s/dT) \text{ at the air} \\ &\quad \text{temperature } T_a, \\ \gamma &= \text{the psychrometric constant as developed in} \\ &\quad \text{Bowen's Ratio,} \\ E_a &= \text{the aerodynamic portion of the combination} \\ &\quad \text{equation,} \\ E_a &= f(u)(e_{sa} - e_a). \end{aligned} \quad (21)$$

As these two examples show, different forms of the combination equations arise from the different assumptions used in each derivation. The assumptions used determine the degree of physical reality of each model and define the input data required (Stewart, 1983).

Pan Evaporation Method: The alternative to using formulas such as the energy budget, mass transfer, or combination formulas is to actually measure the evaporation. Since it is not feasible for most applications, for practical, theoretical, or financial reasons, to directly measure evaporation, pan evaporation is used. Evaporation from a pan is measured as an index of the evaporation from the actual surface of interest (Stewart, 1983). It was found by experience that pans tend to evaporate more water than do lakes or reservoirs during most months of the year. This increased rate is attributed to several conditions.

One of the most important considerations is what type and size of pan is used. Standards have been set and established as to the size and placement of pans, and results have been established for each. Sunken pans tend to more closely indicate lake results directly. The physical conditions in which they are set up are more representative of a natural body of water (Kohler, 1954). The major drawbacks to this plan are the cost and placement problems. Floating pans were developed to simulate actual conditions, but problems of wave action into the pan, and difficulty in measuring rates, has kept this type of pan from being widely used. The other main alternative is the above ground pan, which is subject to convective and radiant heat transfer to and from the sides and bottom. The major advantage of these pans is the ease of placement and maintenance. Another condition is the large difference in heat capacities of the pan and lake. In the case of a pan, the effect of a particular weather event on evaporation is relatively independent of previous weather conditions, mainly because of its limited heat capacity. On the other hand, the lake evaporation occurring on a particular day is not independent of previous conditions because the temperature of the lake is a function of the energy exchange over a considerable period of time (Kohler, 1954). Another point to consider is that evaporation measured

from pans is frequently greater than true pan evaporation. Water may be lost from pans due to heavy rain, or hail, or high winds, which cause water to splash out or blow out of the pans.

All these conditions or factors must be considered in using pan evaporation to predict lake evaporation. Taking these conditions into account, pan coefficients have been developed. Pan coefficients are applied to the pan evaporation losses measured to reduce them to an assumed lake evaporation equivalent (Garstka, 1978). Pan coefficients are generally established on an annual basis, and it is generally accepted that reliable estimates of annual lake evaporation can be obtained from pan data (Nordenson, 1963). If data are broken down into shorter time periods, some variations or adjustments may have to be considered. According to Dunne and Leopold (1978), the difference between pan and lake evaporation will vary through the year because of seasonal differences in radiation, air temperature, wind, and heat storage within the larger body of water. If these seasonal differences are noticeable, a coefficient that varies accordingly must be applied to measurements of pan evaporation in order to estimate water loss from a lake. The pan evaporation method can be a good indication of larger scale evaporation, as long as the pan coefficient used is indicative of the surrounding conditions.

Effects of Different Waters on Evaporation

Several studies have indicated that the chemical composition of a water will affect its evaporation rate. One of the major components studied has been the effect of salinity on evaporation. Evaporation from a saline water surface is less than that from a fresh water surface because dissolved salts lower the free energy of the water molecules (Salhotra et al., 1985). The resulting effect is that the saturation vapor pressure is reduced or decreased. In general, the saturation vapor pressure decreases as the surface salinity increases. The specific relationship between saturation vapor pressure and salinity depends on the particular salt in solution (Salhorta et al., 1985). These relationships have been established for several salts individually, but information on mixtures of salts is very limited.

The lower vapor pressure over saline water permits less energy to escape as latent heat, thus causing an increase in temperature within the water and an increase in sensible heat loss and back radiation to the atmosphere (Salhotra et al., 1985). This effect was shown in the evaporation study done by Salhotra et al., for waters of different salinity. The pans with the highest evaporation rate had the highest temperature and vice versa. The general approach in dealing with the effects of salinity, until recently, has been to ignore them. It is still generally accepted, especially when considering effects on a large scale, that salinity effects are negligible (Linsley, 1975).

Other effects on evaporation related to the chemical composition deal with surface films and monolayers. Research has been done in this area, mainly in an attempt to develop a monolayer to reduce evaporation in arid

areas where water loss is great. Varying results have been reported for films and monolayers. For a film or monolayer to affect evaporation it must act as a diffusion barrier and damp out small waves (Beard and Gainer, 1970). The monolayer may also affect the reflectance of the surface, thereby lowering the solar energy reaching the water to drive evaporation. Linsley (1975) stated that any foreign material which tends to seal the water surface or change its vapor pressure or albedo will affect evaporation.

In Beard and Gainers' (1970) studies, they found that evaporation was reduced for waters with monolayers as a function of a reflectance ratio. They also cited other studies that showed a 25-percent reduction of evaporation when cetyl alcohol was used on a pond. These other studies also noted that the surface temperature of the monolayer-covered pond was, on the average, more than 5°F higher than similar ponds without monolayers. This reaction is similar to that of the salinity on the evaporation rate. Rideal (1925) found that the rate of evaporation of water from a surface is considerably diminished by the presence of a unimolecular film of fatty acid upon the surface. He also found that the decrease in rate was affected by the compression or surface concentration of the film.

Beard and Gainer (1970) did an analysis of various materials that form films and monolayers on a water surface and found that only one of the monolayers tested had a significant effect on evaporation. This was a special Union Carbide experimental silicone, S-1362-91-2. It acted as a diffusion barrier, increased the solar energy reflectance, plus it had good spreading properties and was very difficult to remove from the water surface. The last two properties are qualities which have kept many films and monolayers from effectively decreasing evaporation. Often the film or monolayer does not spread easily or evenly over the surface and those that do spread initially are often moved, shifted and separated by wind and wave movement. Many monolayers or films may have one or two of the desired qualities, but unless they have a combination of several, they will not be effective. Any of the properties may affect evaporation slightly, but the effect will not be uniform and consistent. This may account for some of the differences in results and opinions as to the effectiveness of one type of film or monolayer in comparison to another.

The effect of color of the water on evaporation may also cause a difference in evaporation rate. The amount of heat adsorbed and reflected by a body of water can be affected by its color. Adsorption of energy has been found to be a function of color with a black body being a highly adsorbing surface, while a white body is highly reflective. Viessman et al., (1977) mentions color and states that energy budget equations for evaporation can be in error by 3 to 15 percent if the incoming long wave radiation estimate is off by less than 2 percent, while estimates of reflected long wave radiation affect results much less; an error of 10 percent in reflected solar radiation may cause errors of only 1 to 5 percent in evaporation rate averaged over a month. Since oil shale process waters have a dark color, the effect on evaporation may be significant.

EMISSIONS FROM EVAPORATING WATERS

State and federal regulations require that waste effluents meet set water quality standards before being released into open water bodies. Often, treating waste effluents to meet discharge standards is difficult and expensive. Hence, evaporation ponds have become an attractive alternative for the ultimate disposal of wastewaters. A problem associated with the evaporation of low quality waters is the release of noxious and toxic pollutants into the atmosphere. Although there are regulations controlling emission of pollutants directly vented to the atmosphere through vents, flues and smoke stacks, evaporation ponds have largely been ignored.

Methods of Estimating Emissions

Emissions from evaporation ponds are classified into two groups: organic and inorganic compounds. Detailed analysis of compounds from these groups require various sampling and analytical techniques. Below follows a discussion of prescribed gas sampling techniques to determine emissions from evaporating surfaces.

Basically, there are four methods available for collecting gaseous pollutants (Painter, 1974). These are (1) absorption, (2) adsorption (3) condensation and (4) grab sampling.

Each method has inherent limitations such as accuracy range, cost, and personnel training, and each is applicable to collecting only certain gases.

Absorption sampling is a process by which gas is brought in contact with a reactive liquid. The gaseous pollutant then forms a nongaseous substance. A standard chemical solution is prescribed for each gas to be sampled. A common device using the absorption technique is called a 24-hour bubbler. A bubbler can simultaneously sample for a number of gases, depending on its size. Commonly, bubblers are used to sample for NO_2 , SO_2 , and H_2S .

Adsorption samplers work through a process by which gases are attracted and retained on the surface of a solid. Activated carbon is widely used in absorption samplers, along with silica gels and specialized resins. Gases commonly collected by this method are NH_3 , NO_x compounds, CO and CO_2 .

Condensation sampling is widely used to collect hydrocarbons and other insoluble or nonreactive vapors (Painter, 1974). The sampler works by drawing gases through a series of chambers which are progressively lower in temperature. When the condensation temperature of the gas is met, it will change into a liquid state. After the gases have been collected, they can be analyzed using mass spectroscopy, infrared detection, or gas chromatography.

A grab sample is a sample taken at a particular time within an interval of a few seconds. Grab sampling is particularly useful in conjunction with absorption when reaction times are slow. Grab samples can be taken by several different means, such as syringe, evacuated flask, or gas displacement cylinder. Grab samples are limited to detecting only relatively high concentrations of gases because the gas sample cannot be concentrated over a long time period.

The other method of estimating emissions from evaporation pond surfaces is through emission rate models. These models require the compounds being evaporated from the wastewater to be known which requires sampling by the above methods to determine these compounds.

Five chemical transfer processes exist for a water atmosphere system. These processes include volatilization, absorption, wet deposition, dry deposition and dissolution (Mackay and Shiu, 1984). Mackay and Paterson (1986) have modeled all of these processes; however, volatilization will be the only process considered as a part of this report.

The most common model utilized to determine mass transfer across the air-water boundary is the two resistance model applied to environmental conditions by Liss and Slater (1974). The model consists of the bulk water phase, a liquid film which produces liquid resistance to transfer, an interface, the gas film which produces gas resistance to transfer, and the gas phase. The solute diffuses from the water to the interface, then through the interface, and finally from the interface to the air phase. The basic assumption of this model is that the solute is at equilibrium between the water and air phases at the interface.

The mass flux across the phase boundary has been modeled as

$$N = K_{ol}(C_w - P/H_c) \quad (22)$$

and

$$K_{ol} = 1/(1/k_L + RT/Hck_G) \quad (23)$$

where N is the mass flux ($\text{gmol/m}^2/\text{h}$), and k_L and k_G are the liquid and gas phase mass transfer coefficients (m/h), K_{ol} is the overall mass transfer coefficient (m/h), H_c is the Henry's Law Constant (HLC) ($\text{atm}\cdot\text{m}^3/\text{gmole}$), C_w is the solute concentration in the liquid phase (gmole/m^3), P is the solute partial pressure in the atmosphere (atm), T is the absolute temperature (K) and R is the gas constant ($\text{m}^3\cdot\text{atm/gmole/K}$). If this model is to be used, both K_{ol} and H_c must be known for the system. Cohen et al., (1978) indicate that this model may be too simple to use for environmental conditions due to the effects of other contaminants and emulsions, however, it does produce an estimate. The limitations of this model should be studied in detail (Cohen et al., 1978) when estimating emissions from process waters because they have many contaminants such as oil and grease, dissolved solids and emulsions which would retard the actual emission rates.

Mackay and Paterson (1986), Mackay and Yeun (1983), Dilling (1977), and others (Doskey and Andren, 1981; Gowda and Lock, 1985; Mackay and Leinonen, 1975; Rathbun and Tai, 1982; Rathbun and Tai, 1986; Smith et al., 1980) have all used the two film resistance concept to either measure or estimate the volatilization rates of various compounds in water. The emission rates have been measured in a number of ways (Dilling et al., 1975; Smith et al., 1983). One method that can be used in the field involves placing a "bubble" over an evaporation pan and controlling the climatological parameters that would affect evaporation and emissions. Sensors would be used to measure not only the climatological parameters, but also the concentration of the compounds of interest in the vapor above the liquid over a period of time (Eklund et al., 1985). These measurements would provide the emission rates of the compounds.

Many physical and climatological parameters affect the emission rates of compounds from evaporation ponds. The major parameters include pond depth, wind speed, water turbulence and Henry's Law Constant (HLC). Some other parameters are the presence of emulsions, suspended solids and other contaminants. The main problem in designing an evaporation pond is that it is usually designed for maximum evaporation. The method for maximizing evaporation also maximizes emissions, so a balance will have to be maintained so that acceptable levels of both emissions and evaporation can be obtained. This means that the emissions should be measured and estimated so that accurate models of the actual emissions can be developed.

Whether the volatilization of a compound is measured or estimated, knowledge of HLC is critical to determining the emission rates. Some of the methods of measuring emissions do not require a knowledge of HLC values. However, if models of the emissions are to be developed from the measured values, the HLC values will still be required. It is therefore necessary to measure the HLC for the compounds in the process waters to obtain accurate values of HLC and emissions.

The accuracy required for HLC values, however, depends on the magnitude of the HLC. If the HLC is very large (H_c greater than $9.87 \times 10^{-4} \text{ atm}\cdot\text{m}^3/\text{mol}$ at 25°C), then N is insensitive to errors because $1/H_c$ has become very small, and the flux is controlled by the liquid diffusion rate. In contrast, the gas diffusion rate controls when the HLC is very small (H_c less than $9.87 \times 10^{-6} \text{ atm}\cdot\text{m}^3/\text{mol}$ at 25°C) and the sensitivity of N is directly proportional to the errors in measuring H_c . If the HLC value is in between this range, then the sensitivity of N on the errors in measuring H_c varies between the two limits because both the liquid and gas diffusion rates are controlling the flux (Mackay and Shiu, 1981).

Oil Shale Water Emissions

Dobson et al., (1985) have identified the major organic compounds found in an Australian oil shale process water. They found carboxylic acids, alkyl substituted benzenes, straight chain alkanes, ketones and nitrogen heterocyclic compounds. Of the nitrogen heterocyclic compounds, pyridines and quinolines were dominant. Some phenols were also found in the process water.

The three waters that were studied as a part of this project were Rio Blanco, Geokinetics-17 and Paraho 75/76. Rio Blanco and Geokinetics-17 are produced with modified in-situ processes, and Paraho 75-76 is produced with an above ground retorting process. The Rio Blanco is a pumped water from the burned out in-situ retort from groundwater inflow. A list of the water quality characteristics of these waters is shown in Table 2. This table indicates that the Rio Blanco water is not as complex or concentrated as the Geokinetics and Paraho waters, but it is extremely high in pH. The Geokinetics and Paraho waters are generally quite complex and contain many compounds, and they are especially high in pH, ammonia, nitrogen, sulfate, chloride, alkalinity, organic and inorganic carbon and total dissolved solids. This list is not at all inclusive of all constituents found in these waters, however, it does provide an indication of the types of chemical constituents that may be found in oil shale process waters.

Hawthorne (1984) used the two resistance model of Liss and Slater (1974) to estimate emission rates for a few compounds in oil shale process water. He calculated volatilization rates in terms of half lives with the following equation:

$$t_{1/2} = .69(Z/Ko1) \quad (24)$$

where $t_{1/2}$ is the half life and Z is the pond depth (meters). For a pond depth of 1 meter, a wind speed of 3.6 meters/sec and HLC values ranging from 10^{-2} to 10^{-5} $m^3 \cdot atm/gmole$, the half lives ranged from 3 to 8 days. These half life values indicate that the emissions of volatile organic compounds would be significant in process water holding ponds.

Table 2 Water quality characteristics of oil shale process waters
(mg/l unless otherwise noted).*

Parameter	Oil shale process water		
	Rio Blanco	Paraho 75/76	Geokinetics-17
Alkalinity	45	1920	12900
Carbon, total dissolved	26.7	5925	5010
Carbon, dissolved inorganic	9.7	68	2890
Carbon, dissolved organic	15.9	5856	2120
COD	84	19000	NM
Conductivity (micromhos/cm)	5910	7820	19000
Nitrogen, ammonia (as N)	7	1050	1350
Nitrogen total Kjeldahl	9	1700	1500
pH (S.U.)	9.6	8.16	8.69
Oil and grease	<2	1100	1360
Solids, total dissolved	5447	16495	14000
Sulfate	4900	1540	1100
Phenols	7.01	26	37.3
Chloride	47	2020	3180
Sodium	1.66	360	4830
Potassium	1.74	37	138
Calcium	2.37	200	4.1
Magnesium	3.73	130	7.4

* Mean values of lab measurements performed in 1985

NM - not measured

S.U. - standard units

EXPERIMENTAL FIELD SITE

The field operations in this study were performed from July 1985 through August 1988. A description of the field site location, layout and instrumentation and data handling are discussed in this section as they pertained to the entire project.

LOCATION

The field site was located northwest of Laramie, Wyoming on the grounds of the City of Laramie's municipal wastewater treatment system, and was first established (set up) during May and June of 1985. Laramie is located in the southeast portion of Wyoming in the midst of the semi-arid high plains of the Rocky Mountains. The site is located in Section 20 of Township 16 North and Range 73 West, lies at a latitude of 41° and 20' and longitude of 105° 36', and is at an elevation of approximately 7200 feet msl. The field location was favorable for several reasons: it was easily accessible, yet in an area where any emissions from the waters would not be a problem; it was located adjacent to a long established climatological weather monitoring station (Laramie 2NW) that also monitored Class A pan evaporation; and it was situated in a good location for evaporation monitoring because the site has a long unbroken wind fetch to the west and southwest, the directions of the prevailing winds in the area.

FIELD LAYOUT

The field site was equipped to monitor climatic data and evaporation and was arranged as shown in Figure 1. Three anemometers were installed to measure the wind speed. These were installed at heights of 3 meters, 2 meters, and pan level. Wind direction, air temperature, relative humidity, atmospheric pressure, and incoming and reflected solar radiation were also monitored. Four stainless steel Class A pans were installed at the site to measure evaporation. These pans were the standard 47.5 inches (4 foot pans) in diameter by 10 inches deep, and were mounted on a lattice platform constructed of 2 foot by 4 foot lumber (Peck and Pfankuch, 1963) which permits air to flow under the pan relatively unrestricted. The pans were situated so that each could have the maximum exposure to prevailing winds. One adaptation made to the pans was the addition of a stilling well built into the pan to house the probes used to measure evaporation. The pans also had temperature probes located at the bottom and at surface water level in each pan. The orientation of the pans was in a row running generally north and south, with a distance of approximately ten feet between the pans. The pans were numbered for reference, Pan 1 to Pan 4, with Pan 1 farthest south, in order up to Pan 4 which was farthest to the north. In addition, an 11-foot diameter stock tank 2.5 feet deep (implanted with lip at ground level) was located on the site, which had bottom and surface temperature probes, plus a series of thermistors located in the ground surrounding the tank. A potentiometer was set within the tank to measure surface height and change, and a net radiometer was placed above the water surface. A raingage was also installed at the site to measure precipitation.

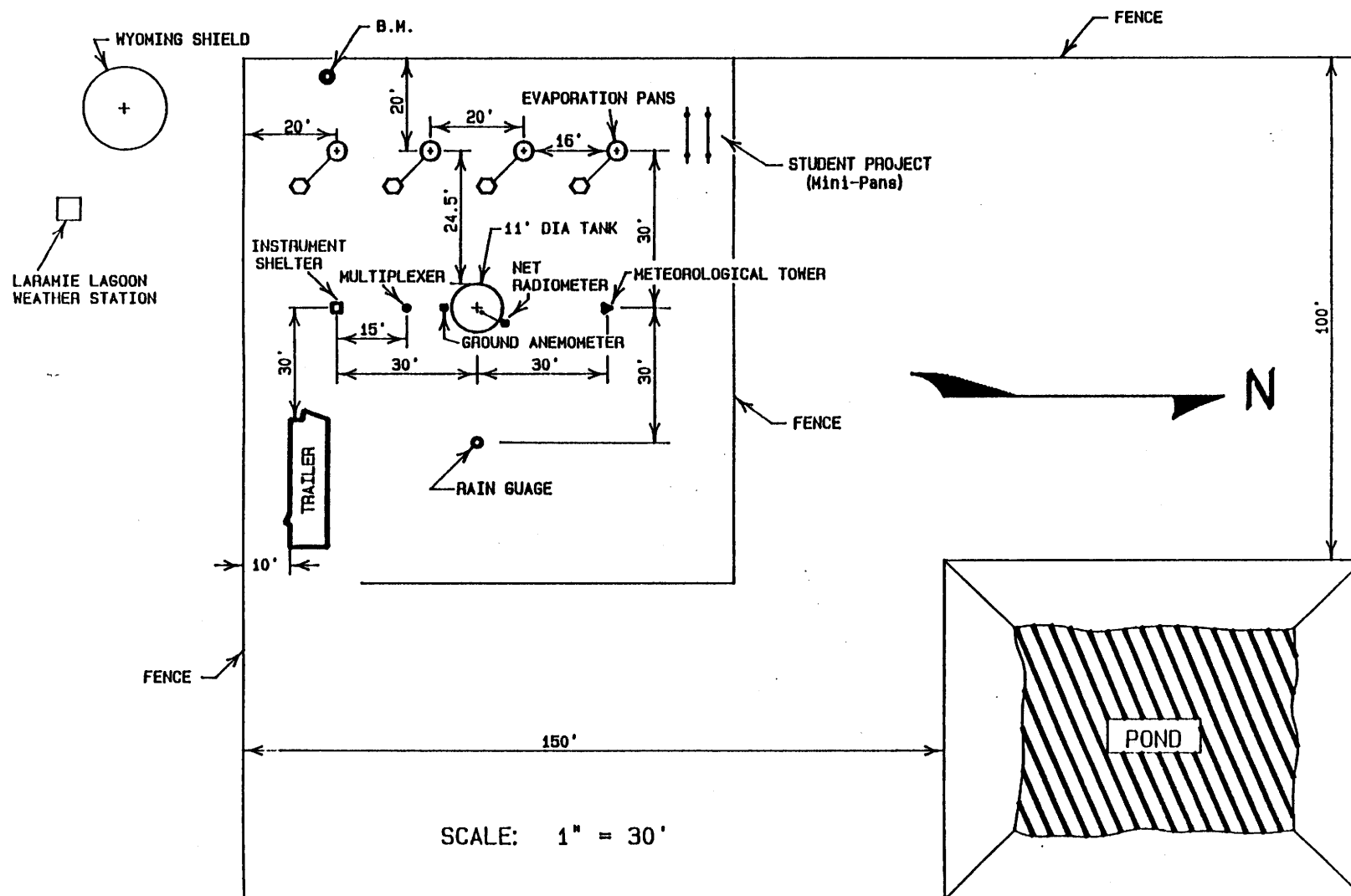


Figure 1. Oil Shale Evaporation Field Site.

All the equipment was connected to a Campbell Scientific CR-21X datalogger which was housed in a trailer (Figure 1) and was programmed with the respective corrections or calibration factors pertaining to each instrument.

An undergraduate student project was performed at the field site during 1985 through 1987 on the use of a thermodynamically designed Mini Class A evaporation pan. Figure 1 shows the location of this study done only with fresh water. Four minipans with different thicknesses of outside insulation were studied. The minipans were placed on 1 inch by 4 inch boards with the boards spaced 1 inch apart. Appendix A contains a summary of this study.

Each pan was filled with a different type of water to determine what effect the quality or composition of oil shale process waters would have on evaporation. Pan 1 was filled with "fresh water" obtained from the Laramie municipal water supply system. Pan 2 was filled with a post process water obtained from the Rio Blanco modified in-situ retort near Rifle, Colorado several years after the actual retorting had occurred and groundwater had infiltrated into the retorted area and the water from the retorted area had been pumped to surface evaporation ponds on more than one occasion. This water was obtained in May 1985 and was pumped directly from the Rio Blanco in-situ retort area directly into a stainless steel tank truck. This water was then hauled to the Western Research Institute North Site near Laramie where it was stored in a tank approved for storage of low-hazard toxic wastewater. Pan 3 was filled with process water from the Paraho above ground retort, produced in 1979. The water for this pan as well as for Pan 4 was stored in a research archive maintained in cold storage by the Western Research Institute. The water was stored in polyethylene lined 30 gallon drums which were kept at a temperature of approximately 4°C to prevent microbial degradation. Pan 4 was filled with water from the Geokinetics horizontal modified in-situ retort which was produced in 1975-76. The large 11-foot diameter evaporation tank was filled with the Rio Blanco water during 1985 and with fresh water from 1986 through 1988.

INSTRUMENTATION

The instrumentation used at the field site is state-of-the-art in terms of equipment and probes for sensing climatological and evaporation measurements. Several measuring device schemes were developed during the project for special needs in collecting diurnal data for evaporation rates. Following is a discussion of the special climatological and evaporation pan instrumentation used with the project.

Climatological

The Campbell Scientific CR-21X datalogger was developed to handle directly several climatological instruments which were already calibrated for use with the datalogger. These instruments were anemometers, a wind direction sensor, thermistors for measuring air temperature, water temperatures and ground temperatures, incoming solar radiation

pyranometer, tipping bucket precipitation gage and relative humidity sensor. A barometer sensor to measure atmospheric pressure and the net radiometers had to be field calibrated and tested for correct voltage signal readings to the datalogger as well as one of the anemometers used with the evaporation pans. As a quality control measure, a strip chart, hygrothermograph (temperature and relative humidity) and maximum and minimum thermometers were installed in a standard Weather Service shelter with the air temperature and relative humidity probes that were hooked to the datalogger as a check on the accuracy of the probes to ensure that accurate measured data were being collected. A standard strip chart pyranometer and precipitation gages and other measurements from the Laramie 2NW weather station located 100 feet south of the evaporation site were also utilized for control on the climatic data being logged into the datalogger.

Surface reflectance or albedo was measured over each of the evaporation pans as well as at several other points on the field site using a photometer and later (1987 and 1988) with a net radiometer which was moved between the Class A pans at regular intervals. The photometer readings were not connected to the datalogger equipment being used, but were measured and recorded independently. These readings were taken over a range of times and conditions to give a good representation of the albedo of each pan water.

During the winter months, climatological data was continuously recorded even though the evaporation pans were inoperative. Maintenance on climatological equipment was performed over the winter months so that any problems were corrected before the next evaporation season.

Evaporation Pans

Evaporation in the Class A pans was measured using an automated system connected to the datalogger. The initial system (Figure 2) consisted of a set of water level sensing probes located within the stilling well of each pan, and solenoid valves installed in the fill and drain lines for each pan. The water level sensing probes (Figure 3) consisted of four stainless steel resistance probes which extended to different depths in the pan. The system was connected so that when the water had evaporated to the point that the low water level sensor was no longer in contact with the water it caused a loss of current. This in turn signaled the solenoid valve on the line from the reservoir to open, thus, filling the pan. When the water reached the proper water level sensor, the additional current signaled the solenoid valve to close. The high water level sensor triggered the opening of the overflow drain line solenoid valve, so that when the water level rose close to the top of the Class A pan due to precipitation, the excess water was drained off to prevent pan overflow. The distance between probes was established by laboratory testing and again in the field when installed and the amount of water which was added or drained from the Class A pan due to the addition or draining of water was known from the installation tests. Each time either valve was triggered it was recorded by the datalogger, with

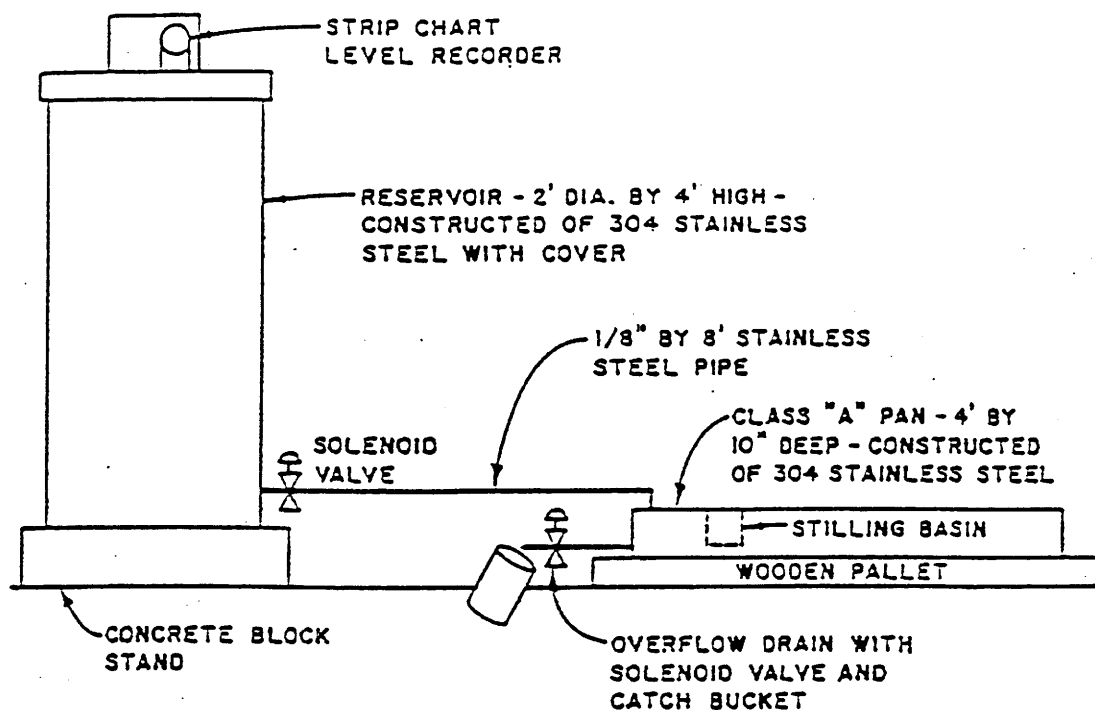


Figure 2. Diagram of Class A Pan and Holding Reservoir Arrangement.

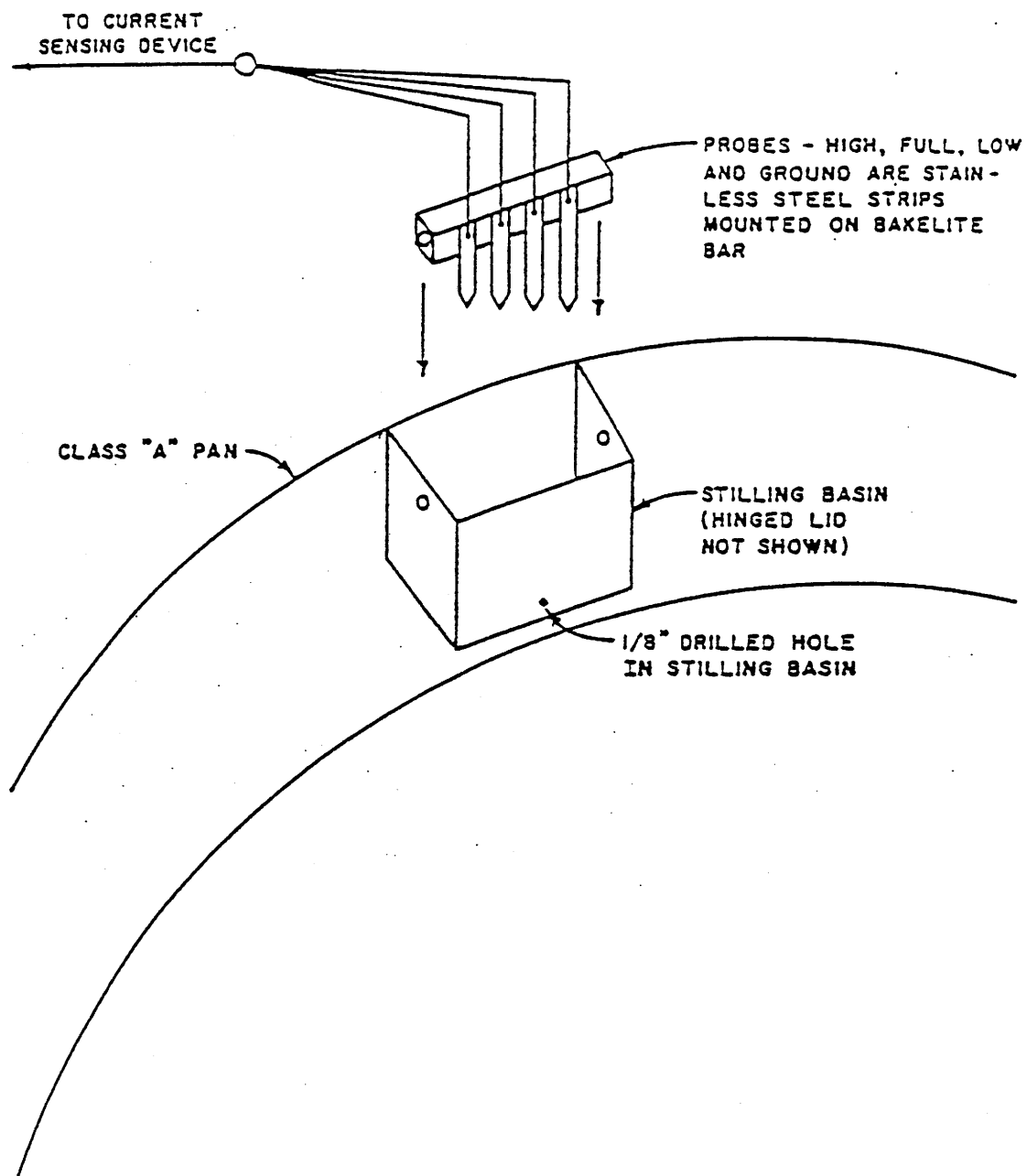


Figure 3. Detail of Stilling Basin and Level Sensing Probes.

different voltage set values representing a fill or a drain. Using this method and by knowing the number of fills and drains, the amount of water evaporated or drained could be determined for each pan.

The system was tested in the Hydraulics Laboratory in the College of Engineering for approximately one month before it was placed in the field at the end of June 1985. The laboratory testing went reasonably well and the indications were that the system should function so that a diurnal cycle of evaporation would be produced. The time history of fills (0.05 inches decrease in water level per fill) would allow for the determination of average evaporation rates for different periods of the day.

Once the system was set-up in the field and placed in operation, it was plagued with problems. Several parts of the electronics equipment malfunctioned, chemical deposits adhered to the sensors, and debris in the stilling well area caused sensor problems at different times resulting in system data being suspect.

A backup system of measuring evaporation was also operated during the same time frame. This consisted of strip chart recorders mounted on the pan reservoirs (Figure 2). The strip charts recorded the change of height of the water level in the reservoirs over time. The reservoirs were sealed as well as possible so that any drop in water level in the reservoirs would be due to water evaporating from the pans. Thus, knowing the change in water height in the reservoirs and the diameters of the reservoirs and pans, both total evaporation and evaporation rate during the day for the pans could be evaluated from the strip charts. Some problems also existed with the backup system because it was dependent on the electronic sensors for opening the valve to fill the pan from the reservoir and the strip chart ink pens did not function (dry out) at times to give a good trace of evaporation rate. The backup system did provide relatively accurate data on total evaporation and some periods when evaporation rates could be determined on a diurnal basis. During the months of October and November, when freezing became common, it was necessary to protect the electronics and valves. Therefore, standard hook gage readings were made on a daily basis for this period and the pans were filled by hand with a bucket.

As a result of the failure of the water level sensing monitoring system during 1985, a redesign of the system was necessary in order to obtain the diurnal variations needed to look at evaporation rates of ponds. The new system tapped the stilling well area well below the water surface with a small diameter pipe which had attached to the end away from the evaporation pan a very sensitive pressure transducer which measured pressure differential compared to atmospheric pressure (gage pressure). This pressure differential measures the water depth in the evaporation pan. The pressure transducer was a Transamerica brand from England with a 35 millibar (mb) range (14 inches of water) with a sensitivity of 0.1 mb. The pressure transducer was adapted to the datalogger for continuous recording of water level (in cm) in the pan with differences over time indicating evaporation rate and total evaporation for the period of interest.

This design required that someone go to the field site each day to refill the pan due to evaporation loss. This was done each day at approximately the same time and standard hook gage readings were taken at this time as a backup system for total evaporation for comparison to the pressure transducer readings. Thin sponges were used inside the stilling well, in front of the opening into the pressure transducer, to filter large particles and debris from reaching, coating or damaging the sensitive membrane within the transducer.

The system was installed in late July of 1986 and worked very satisfactorily for the rest of the project. The main problem encountered with this system was air bubbles in the line to the transducer. This problem could be recognized by looking at the transducer readings on the datalogger on a daily basis and bleeding the line when an air bubble was indicated. The only other problem encountered was freezing weather. The pressure transducers are very susceptible to damage from even small ice formations in and around the inlet pipe extension to the transducer.

The 11-foot diameter evaporation tank used a converted Fl-Type recorder fitted with a potentiometer which was calibrated to water level depth in a still well area and the signal sent to the datalogger. Daily readings on a staff gage were used as a backup system to the potentiometer measurements.

MEASUREMENTS AND DATA HANDLING

Beside the evaporation and climatic parameter measurements being collected at the field site, water quality or composition of the waters in each pan were analyzed on a regular basis. The waters used (Table 2) represent a wide range of properties and the composition of these waters is important to the evaporation rate.

Weekly analyses included temperature, pH, salinity, conductivity, dissolved oxygen, total organic carbon (TOC), carbonate alkalinity, total dissolved solids (TDS), chlorides, and sulfates.

Monthly analyses also included ammonia, color, specific gravity, Kjeldahl nitrogen, and oil and grease. In addition, each process water sample was characterized by an initial analysis at the beginning and end of each evaporation season which included the most common metals, phenols, and EPA priority pollutants (EPA methods 624 and 625 analyses).

The datalogger recorded readings from each instrument (climatic and evaporation pan) every 30 seconds. These 30-second readings were then averaged (or totaled depending on the reading) to form 30-minute readings, which were then permanently recorded by the datalogger to cassette tape. The datalogger could record up to nine days of data before any data would be deleted by being recorded over. The data were dumped to a cassette tape recorder at least every nine days so that a continuous record of the data could be obtained. These data in turn were loaded through an interface system onto the Cyber computer system at the University of Wyoming for use and manipulation in modeling and analysis. The data were recorded and processed in whatever units were most compatible with the

measuring devices. For example, temperature measurements are all in terms of Celsius degrees, while barometric pressure is in inches of mercury, wind speed is in miles per hour, and solar radiation is in watts per square meter.

The recorded climatic, evaporation and chemical data were checked when placed on the computer database for errors in reading of the instruments by the datalogger. Any errors or missing data were corrected to the extent possible using the backup system measurements to fill in where necessary. The database was then utilized in modeling and analysis throughout the project to address the main objectives of this study.

EFFECTS OF CLIMATOLOGICAL PARAMETERS ON EVAPORATION RATE OF PROCESS WATERS

A literature review on evaporation of low quality wastewaters was developed during the first year of this project which was the basis for much of the research performed on this project. The results of this literature review helped define the field and laboratory studies that were performed on climatological parameters that effect evaporation rate.

LITERATURE REVIEW

A topical report (DOE/LC/11049-2205 (DE87001011)), produced as a portion of this project entitled "State-of-the-Art Evaporation Technology" by Hasfurther and Haass, was published by the Office of Fossil Energy of DOE in September 1986. This report was a literature review on evaporation of low quality wastewaters. The abstract of this report is given below as a reference of what is contained in the topical report. For details, please refer to the report.

"This report discusses evaporation theory, measurement and estimation as well as the effects of water quality on evaporation. Emissions from waste effluents is also mentioned.

The theory and equations to represent evaporation using energy balances, mass transport and the combination of these two methods of analysis are presented in detail. Evaporation meters and other techniques for measuring evaporation are reviewed. A discussion of ways to estimate a real evaporation is presented along with criteria which affects evaporation pond design.

The effects of chemical monolayers and salinity on the rate of evaporation is cited and discussed to indicate problems associated with most industrial waste effluents. The problem of monitoring emissions resulting from evaporation ponds associated with industrial waste emissions is also presented."

CLIMATOLOGICAL PARAMETERS AFFECTING EVAPORATION RATE

The study of climatological parameters affecting evaporation rate was performed in the field with more detailed control performed in a laboratory environmental chamber. A description of the experimental designs, methodology used and analyses performed are given in the following sections.

Field and Laboratory Experimental Design

A description of the field study site and associated equipment for monitoring climatological parameters and evaporation rate was presented as a portion of the previous chapter of this report. The field study site was designed to monitor all significant climatological parameters identified. These parameters, as well as the evaporation rate from the

three oil shale process waters were monitored on a microclimate basis. These data were used to identify significant effects of climatological parameters acting on the evaporation of these oil shale process waters under confounded field conditions.

Using the results of the first summer of data collected, laboratory studies were designed to isolate and describe significant climatological and interactive effects on evaporation and its rate under controlled conditions. A controlled environmental chamber in the Civil Engineering Department in the College of Engineering at the University of Wyoming was used to conduct the laboratory studies. This allowed for the chemical parameters which may affect evaporation to be held constant and the climatological parameters to be controlled and replicated to determine individual climatological effects on evaporation.

Six mini-evaporation pans (Vassar, et al., 1987) were used in the laboratory study. The mini-evaporation pan is 12 inches in diameter, 10 inches deep, and constructed of stainless steel. The pans are insulated around the sides with 0.25 inches of polyurethane foam between inner and outer shells. Three pans were filled with the Paraho process water and three were filled with fresh tap water. In the environmental chamber, ambient temperature, relative humidity and air flow above the water surface were measured.

Methodology

A one-way analysis of variance and Scheffe multiple range tests were used for statistical comparison between the evaporation rates of fresh water and the three oil shale process waters from Class A pans. Mean evaporation rates, standard deviations and coefficients of variation for the means were determined for analysis purposes.

The climatological parameters measured (data collected on them) at the field study site were used to help explain the evaporation rate for each of the three process waters. All possible subsets multiple regression, using Mallows C_p and Adjusted R^2 criteria, was used to identify the significant climatological parameters affecting the evaporation rates of these process waters.

Once the significant climatological parameters affecting evaporation rate were determined from the field data, the laboratory was used to design experiments to look at individual and interactive effects of these parameters on evaporation rate. Temperature was analyzed at three levels: 5°C, 25°C, and 35°C. Relative humidity was analyzed at two levels: 20 percent and 80 percent; and air flow across the water surface was studied at two levels: 0 mph and 15 mph. Evaporation from the minipans was measured using a hook gage every two days. Evaporation was observed for each set of experimental conditions for approximately ten days and each ten-day period (i.e. each set of experimental conditions) was replicated. The environmental chamber was allowed to equilibrate for 48 hours when ambient conditions were changed.

Utilizing this procedure, the laboratory environmental study of climatological parameters analyzed using a factorial analysis of variance (ANOVA) design. A further ANOVA analysis was performed on the orthogonal components of the design to determine interactive affects between climatological parameters on the evaporation rate.

Analysis and Results

Field data from, 1985, 1986 and 1987 were analyzed to determine daily evaporation, evaporation rates and the affect of climatological parameters on evaporation and its rate. Figure 4 shows measured evaporation with time for fresh water and each of the three oil shale process waters for the summer field season of 1987. Table 3 presents mean evaporation on a daily basis along with the standard deviation for 1986 for the different waters. Table 4 presents mean evaporation rates for Julian days 218-264 during 1985 along with standard deviations and coefficients of variation for this same period of 1985 for each of the process waters and fresh water.

One-way analysis of variance and the Scheffe multiple range test for statistical comparison of mean evaporation rate and mean daily evaporation from fresh water and the three oil shale process waters for 1985 and 1986 were run on the data. No difference at a significance level of 0.05 was found for the F-statistic between the mean evaporation rate during 1985 for fresh water and the three process waters.

However, Table 4 indicates that significant variation occurs during the day in the evaporation rate as indicated by the size of the standard deviation and coefficient of variation. The 1986 data for mean daily evaporation also indicated no significant difference between fresh water and the process waters at the 0.05 significance level. Figure 4 shows the seasonal trend of total evaporation for each of the different waters for 1987. The differences in total evaporation as shown on Figure 4 indicate essentially the same result for 1987, in that mean daily evaporation between waters and in total are visually not greatly different.

The fact that no significant difference is indicated between fresh water and the three different oil shale process waters was unexpected. It was initially felt that fresh water would evaporate at a higher rate than the oil shale process waters. The following paragraphs present results of the interactive affects of meteorological parameters on evaporation rate. Chemical composition interactions are presented in another section of this report which indicated other reasons for this unexpected result.

All possible subsets multiple regression, using Mallows C_p and Adjusted R^2 criteria for model selection, was used to identify significant climatological parameters affecting evaporation rates of the different waters using the 1985 field data. These results are presented in Tables 5 through 8. In general, relative humidity or barometric pressure, wind speed, and energy-type parameters (radiation intensity, ambient air

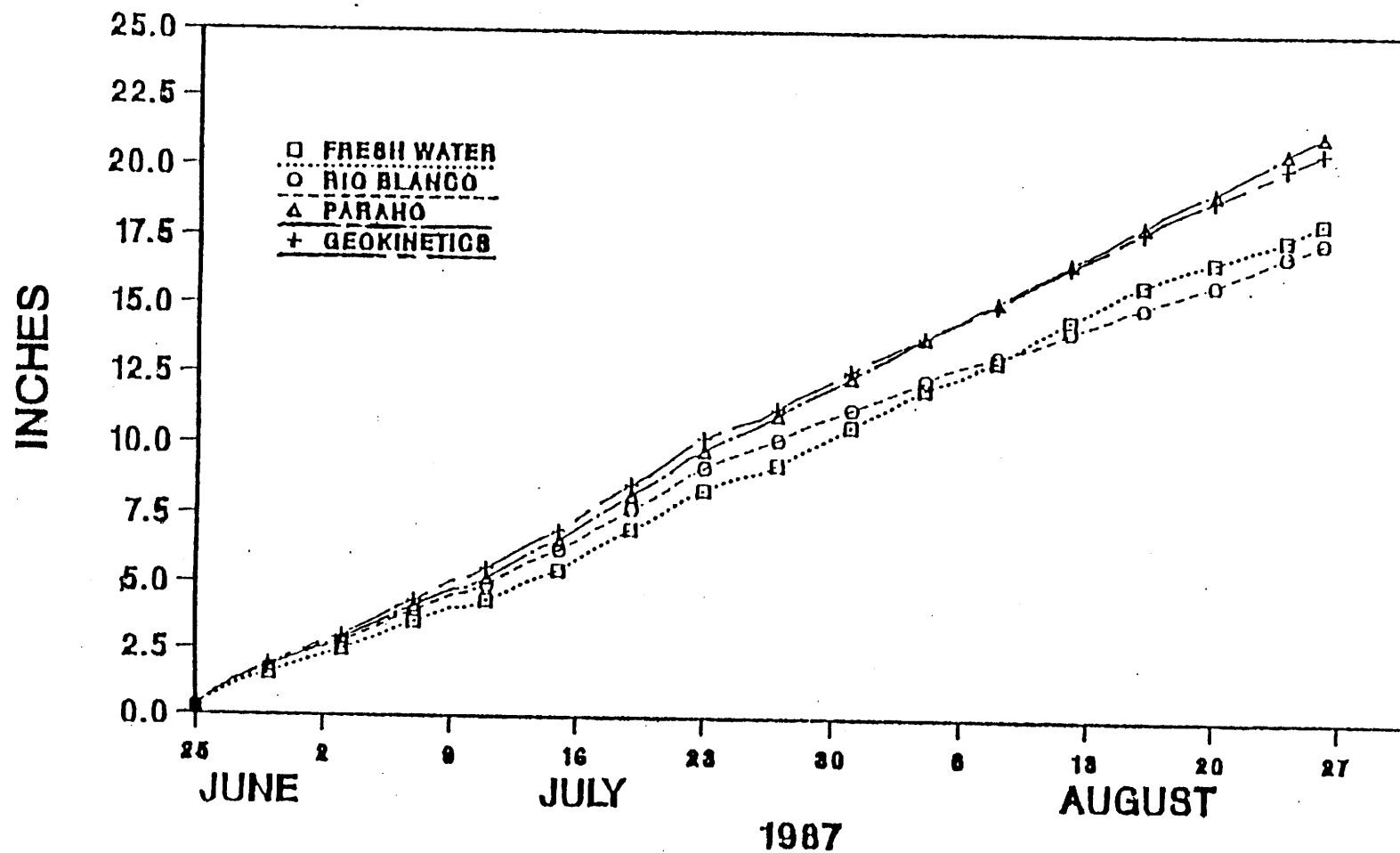


Figure 4. Total Measured Evaporation for Fresh Water and the Three Process Waters for the 1987 Field Season.

Table 3. Descriptive Statistics for Mean Daily Evaporation.

<u>1986 Julian Days 142-262</u>			
Process Water	Sample Size	Mean Evaporation (in./day)	Standard Deviation (in.)
Fresh Water	110	0.273	0.082
Rio Blanco	113	0.285	0.089
Paraho	114	0.299	0.093
Geokinetics	113	0.297	0.096

Table 4. Descriptive Statistics for Process Water Evaporation Rates.

<u>1985 Julian Days 218-264</u>				
Process Water	Sample Size	Mean Evaporation Rate (in/hr)	Standard Deviation (in)	Coefficient of Variation
Fresh Water	87	.0146	0.0106	0.73
Rio Blanco	68	.0142	0.0091	0.64
Paraho	61	.0161	0.0150	0.93
Geokinetics	87	.0161	0.0087	0.54

TABLE 5. Climatological Variables Significantly Affecting Process Water Evaporation Rate
Results From All Possible Subsets Regression Analysis (fresh water).

PROCESS WATER	RH^2	ADJ. R^2	VARIABLE	REGRESSION COEFFICIENT	T-STATISTIC
FRESH WATER	0.63	0.60	ZRH	-0.001710	-3.37
			ZRH ²	0.000014	2.83
			BASE H ₂ O TEMP	0.001088	1.78
			WIND SPEED (3m)	-0.002323	-1.32
			WIND SPEED (gnd)	0.006573	2.42
			INTERCEPT	0.048932	

TABLE 6. Climatological Variables Significantly Affecting Process Water Evaporation Rate
Results From all Possible Subsets Regression Analysis (Rio Blanco).

PROCESS WATER	R^2	ADJ. R^2	VARIABLE	REGRESSION COEFFICIENT	T-STATISTIC
RIO BLANCO	0.78	0.76	ZRH	-0.001734	-3.54
			ZRH ²	0.000014	2.69
			BASE H ₂ O TEMP	0.000879	1.54
			WIND SPEED (3m)	0.002430	5.04
			WIND SPEED (gnd)	0.006573	-1.66
			INTERCEPT	0.049558	

TABLE 7. Climatological Variables Significantly Affecting Process Water Evaporation Rate
Results From All Possible Subsets Regression Analysis (Paraho).

PROCESS WATER	R^2	ADJ. R^2	VARIABLE	REGRESSION COEFFICIENT	T-STATISTIC
PARAHO	0.66	0.64	NET RADIATION	0.055454	3.84
			WIND SPEED (3m)	0.001466	1.26
			WIND SPEED (2m)	0.002725	3.69
			INTERCEPT	0.001924	

TABLE 8. Climatological Variables Significantly Affecting Process Water Evaporation Rate
Results From All Possible Subsets Regression Analysis (Geokinetics).

PROCESS WATER	R^2	ADJ. R^2	VARIABLE	REGRESSION COEFFICIENT	T-STATISTIC
GEOKINETICS	0.32	0.27	NET RADIATION	0.031120	2.84
			WIND SPEED (3m)	-0.006917	-3.01
			WIND SPEED (2m)	0.000845	1.41
			WIND SPEED (gnd)	0.009445	2.68
			INTERCEPT	0.012902	

temperature and water temperature) were found to significantly affect evaporation rate. These data confirm results from the literature review. It is interesting that for fresh water and Rio Blanco waters (Table 5 and 6), a curvilinear or higher order (squared term) relationship between evaporation rate and relative humidity was found to be significant. Analysis of the coefficients of the two relative humidity terms (linear and squared) in Tables 5 and 6 show that their effect on increasing evaporation rate is opposite (linear is negative and squared is positive). No explanation can be given for this result. Water temperature (measured at the base of the pan) was shown to have a significant effect on the evaporation rate of fresh water and Rio Blanco process water (Tables 5 and 6). The energy-related effects were also expressed as net radiation and were significant for Paraho and Geokinetics process waters (Tables 7 and 8). It is believed that these energy-type effects on evaporation rate are the same, however, the variables indicated (i.e., water temperature or net radiation) show more accurate predictive capability for the evaporation rates of the particular process waters.

Using the results of the field data analysis and the procedures described above, for controlled laboratory analysis of the field indicated significant climatological parameters, the laboratory climatic study used a four-factor ANOVA design analyzing ambient air temperature at three levels, relative humidity at two levels, and wind speed at two levels for both the fresh and process waters. Tables 9 through 14 indicate some of the data from the laboratory tests for the different controlled climatological parameter affects on evaporation rate. ANOVA results (Table 15) indicated significant effects due to temperature, relative humidity, and wind at the 0.05 significance level. No significant difference could be noted between process waters and fresh water at even the 0.30 significance level. Significant interaction at the 0.05 significance level were noted between temperature and relative humidity, temperature and wind speed, and relative humidity and wind speed. No three-way interactions were found to be significant.

A further ANOVA analysis was then performed on the orthogonal components of these results. Tables 16 and 17 indicate some of these results for the interaction of temperature and relative humidity with the wind on and wind off. In this manner, the interactive effects were broken down to determine the significance of the linear and quadratic (squared) terms of the ambient temperature. This aided in quantifying and modeling temperature effects and determine the significance of quadratic effects for ambient temperature. Results from this analysis showed significant linear and quadratic effects for ambient air temperature at the 0.05 significance level and these components were also significant as interactive effects with other components. These results indicate that in modeling or predicting evaporation from these waters, ambient temperature in both the linear and quadratic terms should be used and are significant. These results also back up findings from the field studies in which temperature in both the linear and quadratic terms were found to be significant in a predictive regression model that is discussed in a later section.

Table 9. Laboratory Evaporation Rates At 20°C And 80 Percent Relative Humidity With No Wind.

TARGET CONDITIONS:

20°C

WIND - 0 MPH

RELATIVE HUMIDITY 80Z

JULIAN DAY	TIME HOURS	TIME DIFFERENCE	POSITION #1		POSITION #2		POSITION #3	
			PAN #1 HOOK GAGE (in)	PAN #2 HOOK GAGE (in)	PAN #3 HOOK GAGE (in)	PAN #4 HOOK GAGE (in)	PAN #5 HOOK GAGE (in)	PAN #6 HOOK GAGE (in)
295	15:46	0.000	3.743	3.632	3.704	3.655	3.756	3.363
301	15:50	144.003	3.298	3.074	3.234	3.178	3.307	2.906
GAGE DIFFERENCE (in)			0.445	0.558	0.470	0.477	0.449	0.457
EVAP. RATE (in/hr)			0.003	0.004	0.003	0.003	0.003	0.003
EVAP. RATE (mm/hr)			0.078	0.098	0.083	0.084	0.079	0.081

*NOTE: Minipans 1, 3, 5, were filled with tap water. Mini Pans 2, 4, 6 were filled with Paraho process water. Position is a blocking factor used because of suspected differences in air circulation within the Incubator Room. On 298 @ 15:00 the exact location of Pans 1 & 2, Pans 3 & 4, and Pans 5 & 6 were switched within their respective position block.

Table 10. Laboratory Evaporation Rates At 35°C And 80 Percent Relative Humidity With No Wind.

TARGET CONDITIONS:

35 DEGREES C

WIND - 0 MPH

RELATIVE HUMIDITY 80Z

JULIAN DAY	TIME HOURS	TIME DIFFERENCE	POSITION #1		POSITION #2		POSITION #3	
			PAN #1 HOOK GAGE (in)	PAN #2 HOOK GAGE (in)	PAN #3 HOOK GAGE (in)	PAN #4 HOOK GAGE (in)	PAN #5 HOOK GAGE (in)	PAN #6 HOOK GAGE (in)
304	16:30	0.000	3.560	3.494	3.511	3.557	3.563	3.461
310	16:50	143.983	2.495	2.345	2.580	2.665	2.677	2.575
GAGE DIFFERENCE (in)			1.065	1.149	0.931	0.892	0.886	0.386
EVAP. RATE (in/hr)			0.007	0.008	0.006	0.006	0.006	0.006
EVAP. RATE (mm/hr)			0.188	0.203	0.164	0.157	0.156	0.156

*NOTE: Minipans 1, 3, 5, were filled with tap water. Minipans 2, 4, 6 were filled with Paraho process water. Position is a blocking factor used because of suspected differences in air circulation within the Incubator Room. On 307 @ 15:00 the exact location of Pans 1 & 2, Pans 3 & 4, and Pans 5 & 6 were switched within their respective position block.

TARGET CONDITIONS:

JULIAN DAY	TIME HOURS	TIME DIFFERENCE	POSITION #1		POSITION #2		POSITION #3	
			PAN #1	PAN #2	PAN #3	PAN #4	PAN #5	PAN #6
			HOOK GAGE (in)	HOOK GAGE (in)	HOOK GAGE (in)	HOOK GAGE (in)	HOOK GAGE (in)	HOOK GAGE (in)
315	16:06	0.000	3.325	3.370	3.619	3.217	3.344	3.460
321	16:00	143.996	2.579	2.553	2.668	2.305	2.288	2.325
GAGE DIFFERENCE (in)			0.746	0.817	0.951	0.912	1.056	1.135
EVAP. RATE (in/hr)			0.005	0.006	0.007	0.006	0.007	0.008
EVAP. RATE (mm/hr)			0.132	0.144	0.168	0.161	0.186	0.200

Table 12. Laboratory Evaporation Rates At 35°C And 80 Percent Relative Humidity With Wind.

TARGET CONDITIONS:

JULIAN DAY	TIME HOURS	TIME DIFFERENCE	POSITION #1		POSITION #2		POSITION #3	
			PAN #1	PAN #2	PAN #3	PAN #4	PAN #5	PAN #6
			HOOK GAGE (in)	HOOK GAGE (in)	HOOK GAGE (in)	HOOK GAGE (in)	HOOK GAGE (in)	HOOK GAGE (in)
326	16:05	0.000	3.238	3.115	2.901	2.962	2.831	2.998
332	16:06	144.001	2.130	1.954	1.443	1.462	1.067	1.138
GAGE DIFFERENCE (in)			1.108	1.161	1.458	1.500	1.764	1.860
EVAP. RATE (in/hr)			0.008	0.008	0.010	0.010	0.012	0.013
EVAP. RATE (mm/hr)			0.195	0.205	0.257	0.265	0.311	0.328

46

Table 13. Laboratory Evaporation Rates At 5°C And 80 Percent Relative Humidity With No Wind.

TARGET CONDITIONS:

20 DEGREES C

WIND - 0 MPH

RELATIVE HUMIDITY 80%

JULIAN DAY	TIME HOURS	TIME DIFFERENCE	POSITION #1		POSITION #2		POSITION #3	
			PAN #1	PAN #2	PAN #3	PAN #4	PAN #5	PAN #6
			HOOK GAGE (in)	HOOK GAGE (in)	HOOK GAGE (in)	HOOK GAGE (in)	HOOK GAGE (in)	HOOK GAGE (in)
343	16:17	0.000	3.354	3.007	3.448	2.807	3.795	3.106
349	16:00	143.988	3.171	2.804	3.225	2.622	3.602	2.978
	GAGE DIFFERENCE (in)		0.183	0.203	0.223	0.185	0.193	0.128
	EVAP. RATE (in/hr)		0.001	0.001	0.002	0.001	0.001	0.001
	EVAP. RATE (mm/hr)		0.032	0.036	0.039	0.023	0.034	0.023

*NOTE: Minipans 1, 3, 5, were filled with tap water. Minipans 2, 4, 6 were filled with Paraho process water. Position is a blocking factor used because of suspected differences in air circulation within the Incubator Room. On 346 @ 16:00 the exact location of Pans 1 & 2, Pans 3 & 4, and Pans 5 & 6 were switched within their respective position block.

Table 14. Laboratory Evaporation Rates At 5°C And 80 Percent Relative Humidity With Wind.

TARGET CONDITIONS:

20 DEGREES C

WIND - 0 MPH

RELATIVE HUMIDITY 80Z

JULIAN DAY	TIME HOURS	TIME DIFFERENCE	POSITION #1		POSITION #2		POSITION #3	
			PAN #1 HOOK GAGE (in)	PAN #2 HOOK GAGE (in)	PAN #3 HOOK GAGE (in)	PAN #4 HOOK GAGE (in)	PAN #5 HOOK GAGE (in)	PAN #6 HOOK GAGE (in)
12	16:00	0.000	3.319	3.192	3.189	2.828	2.755	2.447
18	16:00	144.000	2.913	2.797	2.713	2.414	2.291	1.970
	GAGE DIFFERENCE (in)		0.406	0.395	0.476	0.414	0.464	0.477
	EVAP. RATE (in/hr)		0.003	0.003	0.003	0.003	0.003	0.003
	EVAP. RATE (mm/hr)		0.072	0.070	0.084	0.073	0.082	0.084

*NOTE: Minipans 1, 3, 5, were filled with tap water. Minipans 2, 4, 6 were filled with Paraho process water. Position is a blocking factor used because of suspected differences in air circulation within the Incubator Room. On 346 @ 16:00 the exact location of Pans 1 & 2, Pans 3 & 4, and Pans 5 & 6 were switched within their respective position block.

Table 15. Laboratory Evaporation Analysis of Variance Interactions *

Components	SS	DF	MS	F
MEAN	28.9296	1	28.9296	3732.04
WATER (W)	.0012	1	.0012	.16
TEMPERATURE (T)	3.6827	2	3.6827	475.08*
RELATIVE HUMIDITY (RH)	.0357	1	.0357	4.60*
WIND (FLOW) (F)	.8322	1	.8322	107.36*
WXT	.0069	2	.0069	.44
WXRH	.0000	1	.0000	.00
TXRH	.1934	2	.0967	12.48*
WXF	.0003	1	.0003	.04
TXF	.1091	2	.0546	7.04*
RHXF	.0677	1	.0677	8.73*
WXTXRH	.0002	2	.0001	.01
WXTXF	.0005	2	.0002	.03
WXRHXF	.0046	1	.0046	.59
TXRHXF	.0052	2	.0026	.34
WXRHXTXF	.0036	2	.0018	.23
ERROR	.1860	24	.0078	

*Significant at 0.05 level

Table 16. Analysis of Variance for Orthogonal Component of Temperature and Relative Humidity With No Wind

Components	SS	DF	MS	F
RH	0.1007	1	0.1007	24.38
Temp	2.9773	2	2.4887	360.34
Linear	2.9235	1	2.9235	707.65
Quadratic	0.0538	1	0.0538	13.03
T X R	0.0680	2	0.0340	8.23
T (Linear) x R	0.0276	1	0.0276	6.68
T (quadr.) x R	0.0405	1	0.0405	9.79
Error	0.0744	18	0.0041	
Total	3.2205	23		

Table 17. Analysis of Variance for Orthogonal Components of Temperature and Relative Humidity

	SS	DF	MS	F
RH	0.0025	1	0.0025	0.35
Temp	4.4968	2	2.2484	313.96
Linear	4.1878	1	4.1878	584.77
Quadratic	0.3091	1	0.3091	43.16
T X R	0.1306	2	0.0653	9.12
T (Linear) x R	0.0607	1	0.0607	8.47
T (quadr.) x R	0.0699	1	0.0699	9.76
Error	0.1289	18	0.0072	
Total	4.7589	23		

EFFECTS OF CHEMICAL COMPOSITION OF PROCESS WATERS ON EVAPORATION RATES

Oil shale process waters are chemically very complex. It is a well established fact that certain types of chemicals in water can either help to increase or decrease the rate of evaporation of water. Studies were designed to primarily investigate and assess the gross effects that chemicals in oil shale process waters have on evaporation.

LABORATORY EVAPORATION STUDIES

To assess the effects of chemical composition of the three oil shale process waters on evaporation, a laboratory study was designed in the environmental engineering laboratory in the Civil Engineering Department. Climatological parameter effects on the evaporation rate of oil shale process waters was held constant by using a laboratory environmental chamber. This study was undertaken following the first year of field investigations.

EXPERIMENTAL DESIGN

The laboratory design used a sealed box container (4' x 4' x 8') which exhibited all the properties of an actual controlled environmental chamber. Two mini evaporation pans were used in the study for replication purposes. Each minipan was filled with Geokinetics process water. This water was chosen over the other two process waters because of its high chemical complexity and high concentration of dissolved solids.

The sealed box container (environmental chamber) was maintained at laboratory room temperature which had a very small fluctuation in average air temperature. The chamber maintained the process water at an average air temperature of 25°C and 35 percent relative humidity for the duration of the experiment.

METHODOLOGY

The sealed box container was operated for a period of approximately six months. The amount of water loss by each of the minipans was measured every two days with a hook gage to assess the average rate of evaporation and then the minipans had additional Geokinetics water added. The Geokinetics water added was thoroughly mixed in the sample barrel before being added to the minipans. The reason for this particular experimental design was to simulate increased chemical composition with time, similar to what would occur in the field in order to observe this effect on evaporation rate. Samples of the minipan water were obtained and analyzed for total dissolved solids (TDS) and total organic carbon (TOC).

Rate of evaporation was observed for five different chemical concentration levels for the Geokinetics water. These concentration levels were achieved by heating the Geokinetics process water from the

previous experimental run to force evaporation from the process water to a new chemical concentration level. Experimental runs were continued and evaporation measured at each different concentration level until the TDS and TOC concentration of the process water was twice that observed in the field at the end of a summer field season. Hook gage measurements were taken every two days over the six-month period.

Analysis and Results

Tables 18 through 22 indicate the results of the measurements taken for the five (5) different chemical concentration levels using the Geokinetics water. Figure 5 is a plot of the average evaporation rate at each chemical concentration for the two minipans. Table 23 is a regression fit of the data shown in Figure 5. The slope of the line is essentially zero (Table 23) indicating that chemical concentration does not increase or decrease the rate of evaporation. The variance in the data do not show a small enough variability to indicate a trend of any type in the data for evaporation.

As a result, the laboratory chemical study indicated that no significant effects caused by the increasing concentrations of chemical constituents could be stated on process water evaporation rates compared to fresh water. The range of concentrations studied were based on two (2) times the range of TDS and TOC concentrations observed in the field study over one field season. These data indicate that in large scale evaporation, increasing chemical concentrations (at the levels studied) do not show a trend or affect on evaporation rates of oil shale process waters compared to fresh water.

FIELD EVAPORATION STUDIES

Field measurements were taken during each of the evaporation seasons (May through October) of this project (1985-1988) to obtain the change in chemical composition of the evaporating waters over the season. These field measurements were designed to evaluate the affects of chemical concentration on evaporation rate under field conditions to help develop an evaporation rate equation and to determine those chemical parameters which affect oil shale process water evaporation.

Experimental Design

The field research site was used to look at possible changes in chemical composition on evaporation rates. The Class A evaporation pans and the large tank were used to obtain field samples of the three oil shale process waters and fresh water. Standard EPA procedures were followed for obtaining field samples for laboratory analysis. Field techniques and instrumentation were used to obtain some chemical parameters in the field. Sampling occurred during the entire field season during each year of the project.

Methodology

Chemical analyses for water quality was made using several frequency schedules and the measurements were taken generally at times during the

Table 18. Laboratory Chemical Concentration Effects on Evaporation Rate at the Lowest or Level One Chemical Concentration.

EVAPORATION RATE SUMMARY (in/hr)

Pan #1		Pan #2		Total	
AVG =	0.00240	AVG =	0.00251	AVG =	0.00246
STD =	0.00022	STD =	0.00018	STD =	0.00020
N calc. =	6.690	N calc. =	2.610	N calc. =	34.000

(N calc. = Necessary samples to obtain statistical adequacy at P = .05)

JULIAN DAY	TIME (HOURS)	TIME DIFFERENCE	PAN #1		PAN #2		EVAPORATION RATE	
			HOOK GAGE (in)	GAGE DIFFERENCE	HOOK GAGE (in)	GAGE DIFFERENCE	PAN #1 (in/hr)	PAN #2 (in/hr)
260	11:38	0.000	3.096	0.000	3.247	0.000	--	--
266	11:38	144.000	2.701	0.395	2.842	0.405	0.0027	0.0028
268	11:40	48.001	2.590	0.111	2.712	0.130	0.0023	0.0027
272	13:45	96.087	2.358	0.232	2.468	0.244	0.0024	0.0025
274	12:09	47.933	2.254	0.104	2.357	0.111	0.0022	0.0023
275	11:58	23.992	2.199	0.055	2.300	0.057	0.0023	0.0024
276	12:13	24.010	2.133	0.066	2.241	0.059	0.0027	0.0025
279	14:00	72.074	1.974	0.159	2.067	0.174	0.0022	0.0024

* Note: Water used was Geokinetics. The waters used were taken directly from barrels in cool storage. (5°C).
Original chemical concentration.

Table 19. Laboratory Chemical Concentration Effects on Evaporation Rate at Level Two Chemical Concentration.

EVAPORATION RATE SUMMARY (in/hr)

Pan #1		Pan #2		Total	
AVG =	0.00252	AVG =	0.00218	AVG =	0.00235
STD =	0.00005	STD =	0.00017	STD =	0.00022
N calc. =	0.284	N calc. =	2.969	N calc. =	21.534

(N calc. = Necessary samples to obtain statistical adequacy at P = .05)

JULIAN DAY	TIME (HOURS)	TIME DIFFERENCE	PAN #1		PAN #2		EVAPORATION RATE	
			HOOK GAGE (in)	GAGE DIFFERENCE	HOOK GAGE (in)	GAGE DIFFERENCE	PAN #1 (in/hr)	PAN #2 (in/hr)
293	09:50	0.000	3.598	0.000	3.466	0.000	0.0000	0.0000
295	09:25	47.983	3.475	0.123	3.363	0.103	0.0026	0.0021
297	09:50	48.017	3.357	0.118	3.265	0.098	0.0025	0.0020
299	09:45	47.997	3.237	0.120	3.151	0.114	0.0025	0.0024
301	09:45	48.007	3.115	0.122	3.047	0.104	0.0025	0.0022

* Note: Water used was Geokinetics. Chemical concentration level 2. After completion of Lab Run #1, minipan #1 was force evaporated under the hood at 35 degrees C until 2.4" depth remained. Minipan #2 was force evaporated until 2.3" depth remained. Minipans were then refilled to proper levels.

Table 20. Laboratory Chemical Concentration Effects on Evaporation Rate at a Medium Level (Level Three) Chemical Concentration.

EVAPORATION RATE SUMMARY (in/hr)

Pan #1		Pan #2		Total	
AVG =	0.00243	AVG =	0.00230	AVG =	0.00236
STD =	0.00005	STD =	0.00008	STD =	0.00009
N calc. =	0.170	N calc. =	1.180	N calc. =	12.900

(N calc. = Necessary samples to obtain statistical adequacy at P = .05)

JULIAN DAY	TIME (HOURS)	TIME DIFFERENCE	PAN #1		PAN #2		EVAPORATION RATE	
			HOOK GAGE (in)	GAGE DIFFERENCE	HOOK GAGE (in)	GAGE DIFFERENCE	PAN #1 (in/hr)	PAN #2 (in/hr)
310	08:30	0.000	3.237	0.000	3.255	0.000	0.0000	0.0000
312	08:37	48.005	3.120	0.117	3.151	0.104	0.0024	0.0022
315	09:00	72.016	2.948	0.172	2.982	0.169	0.0024	0.0023
317	08:30	47.979	2.832	0.116	2.871	0.111	0.0024	0.0023
319	08:40	48.007	2.713	0.119	2.757	0.114	0.0025	0.0024

* Note: Water used was Geokinetics. Chemical concentration level 3. After completion of Lab Run #2, minipan #1 was force evaporated under the hood at 35 degrees C until 3" depth remained. Minipan #2 was force evaporated until 3.2" of depth remained. Minipans were then refilled to proper levels.

Table 21. Laboratory Chemical Concentration Effects on Evaporation Rate at Level Four Chemical Concentration.

EVAPORATION RATE SUMMARY (in/hr)

Pan #1		Pan #2		Total	
AVG =	0.00277	AVG =	0.00245	AVG =	0.00261
STD =	0.00062	STD =	0.00031	STD =	0.00049
N calc. =	38.442	N calc. =	13.569	N calc. =	52.539

(N calc. = Necessary samples to obtain statistical adequacy at P = .05)

JULIAN DAY	TIME (HOURS)	TIME DIFFERENCE	PAN #1		PAN #2		EVAPORATION RATE	
			HOOK GAGE (in)	GAGE DIFFERENCE	HOOK GAGE (in)	GAGE DIFFERENCE	PAN #1 (in/hr)	PAN #2 (in/hr)
328	09:20	0.000	3.260	0.000	3.316	0.000	0.0000	0.0000
330	08:40	47.972	3.128	0.132	3.190	0.126	0.0028	0.0026
332	08:45	48.003	2.957	0.171	3.055	0.135	0.0036	0.0028
334	08:50	48.003	2.858	0.099	2.945	0.110	0.0021	0.0023
336	09:20	48.021	2.732	0.126	2.845	0.100	0.0026	0.0021

* Note: Water used was Geokinetics. Chemical concentration level 4. After completion of Lab Run #3, minipan #1 was force evaporated under the hood at 35 degrees C until 2.9" depth remained. Minipan #2 was force evaporated until 3.3" of depth remained. Minipans were then refilled to proper levels.

Table 22. Laboratory Chemical Concentration Effects on Evaporation Rate at the Highest Level or Level Five Chemical Concentration.

EVAPORATION RATE SUMMARY (in/hr)

Pan #1	Pan #2	Total
AVG = 0.00210	AVG = 0.00213	AVG = 0.00211
STD = 0.00028	STD = 0.00024	STD = 0.00024
N calc. = 12.298	N calc. = 10.208	N calc. = 1.209

(N calc. = Necessary samples to obtain statistical adequacy at P = .05)

JULIAN DAY	TIME (HOURS)	TIME DIFFERENCE	PAN #1		PAN #2		EVAPORATION RATE	
			HOOK GAGE (in)	GAGE DIFFERENCE	HOOK GAGE (in)	GAGE DIFFERENCE	PAN #1 (in/hr)	PAN #2 (in/hr)
343	16:08	0.000	3.216	0.000	3.301	0.000	0.0000	0.0000
345	16:00	47.994	3.108	0.108	3.216	0.085	0.0023	0.0018
347	16:09	48.006	2.998	0.110	3.113	0.103	0.0023	0.0021
349	16:00	47.994	2.916	0.082	3.004	0.109	0.0017	0.0023
351	16:10	48.007	2.815	0.101	2.893	0.111	0.0021	0.0023

* Note: Water used was Geokinetics. Chemical concentration level 5. After completion of Lab Run #4, minipan #1 was force evaporated under the hood at 35 degrees C until 2.9" depth remained. Minipan #2 was force evaporated until 3.3" depth remained. Minipans were then refilled to proper levels.

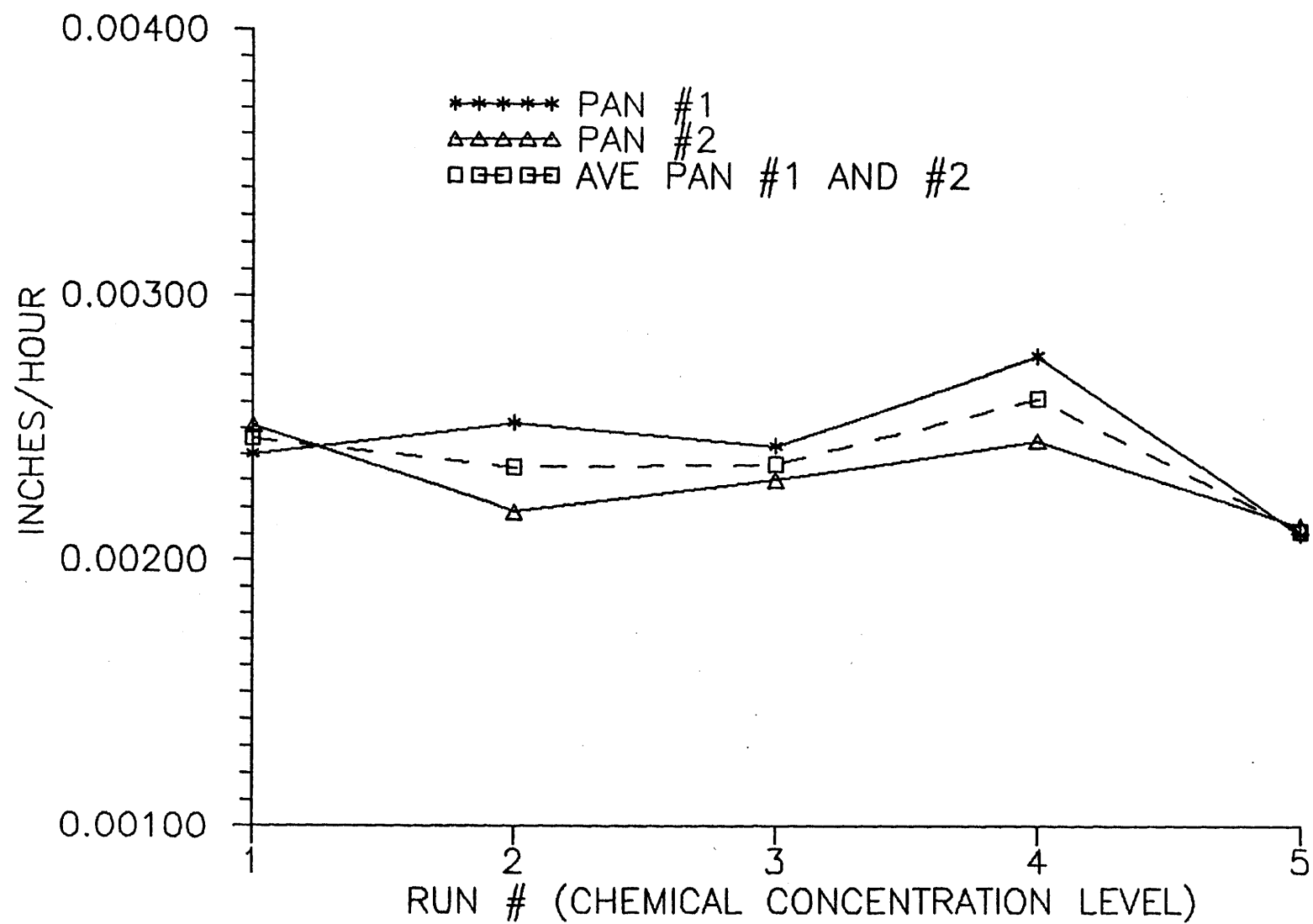


Figure 5. Average Evaporation Rate for Each Chemical Concentration Level.

Table 23. Regression Analysis of Evaporation Rates Versus Chemical Composition.

RUN#	PAN #1 (in/hr)	PAN #2 (in/hr)	AVG P1 P2 (in/hr)
1	0.00240	0.00251	0.00246
2	0.00252	0.00218	0.00235
3	0.00243	0.00230	0.00236
4	0.00277	0.00245	0.00261
5	0.00210	0.00213	0.00211

Regression Output: EVAP RATE BY RUN NUMBER (AVERAGE VALUES)

Constant	0.00251
Std Err of Y Est	0.000195
R Squared	0.145
No. of Observation	5
Degrees of Freedom	3

X Coefficients(s) -0.000044

day other than when the evaporation and climatic data were being manually observed. In general, the chemical composition of the oil shale process waters and the fresh water were sampled on the average of three times per week in the field for pH, conductivity, and temperature from all Class A pans and the tank. On a weekly basis, water samples were obtained in the field and brought into the laboratory for analysis of TDS, dissolved oxygen (DO), chloride, oil and grease, and alkalinity from all the Class A pans. Twice during the summer period (at the beginning and at the end), a more complete chemical composition analysis was taken and included EPA Method 624 and 625 analysis for organic priority pollutants. A subcontract with the Western Research Institute (WRI) for certain constituents of the chemical analysis was a part of the process on the weekly samples plus WRI performed the EPA Method 624 and 625 analysis. Monthly sampling was also performed and WRI was used for some of these analyses. The monthly analyses included total organic carbon (TOC), TDS, pH, alkalinity, chloride ion, sulfate ion, oil and grease, ammonia, total Kjeldahl-nitrogen (TKN), specific gravity and color. In addition, during the first summer each monthly sample was submitted to WRI for an induction coupled plasma (ICP) analysis for iron, magnesium, sodium, calcium and aluminum. The standard laboratory techniques used to analyze for the chemical constituents are defined in Koontz (1986).

Each of the oil shale process waters and fresh water were sampled as indicated above. Sampling frequency on all important chemical parameters was based on a statistical analysis of variance of the particular parameter being measured during the first summer of study. The chemical data were also analyzed periodically during the first year to find if certain parameters were not relevant or that an increased or decreased frequency of analysis could occur.

Based on a statistical analysis of the measured chemical parameters with respect to evaporation rate and amount, the chemical parameters which are significant in determining field evaporation rates can be defined. All possible subsets regression, using Mallows C_p and adjusted R^2 criteria were used to identify those chemical parameters that significantly affect evaporation rate.

The major inorganic contaminants were determined using ion ratios of the major ionic species found from laboratory analysis and substituting these ratios into the computer program WATEQ which uses an iteration procedure and thermodynamic equations to determine equilibrium proportions for the most common species in solution to obtain the amount of each inorganic contaminant.

Graphical analysis of several of the chemical parameters was used to also visualize if any trends are considered significant for those particular chemical parameters.

Analysis and Results

Tables 2 and 24 illustrated the mean values of laboratory measurements of chemical parameters taken at different times during the 1985 field season. The variability in concentration at these different times is indicated for selected parameters for the three different process

TABLE 24. Descriptive Statistics for Chemical Concentrations of
Oil Shale Waters. Time Period: Julian Days 183-312 of 1985.

PROCESS WATER	CHEMICAL CONSTITUENT	SAMPLE SIZE	MEAN CONCENTRATION (ppm)	STANDARD DEVIATION	COEFFICIENT OF VARIATION
RIO BLANCO	TOTAL ORG. CARB.	16	40.1	8.00	0.19
	TOTAL DIS. SOLIDS	16	9145.6	1078.73	0.12
	pH	16	7.4	0.19	0.02
	TOTAL ALKALINITY	16	49.7	18.48	0.37
	CL ⁻	16	51.5	10.35	0.20
	SO ₄ ⁼	16	9061.2	1699.10	0.19
PARAHO	TOTAL ORG. CARB.	14	12167.1	3094.89	0.25
	TOTAL DIS. SOLIDS	14	23320.7	5715.61	0.25
	pH	14	6.7	0.15	0.02
	TOTAL ALKALINITY	14	3149.6	585.16	0.19
	CL ⁻	14	1581.2	446.02	0.28
	SO ₄ ⁼	14	7207.9	1602.43	0.22
GEOKINETICS	TOTAL ORG. CARB.	12	3615.5	657.36	0.18
	TOTAL DIS. SOLIDS	12	26822.5	6154.30	0.23
	pH	12	8.9	0.17	0.02
	TOTAL ALKALINITY	12	15760.3	1813.23	0.12
	CL ⁻	12	3517.2	1074.07	0.31
	SO ₄ ⁼	12	4900.8	1418.76	0.29

waters (Table 24) by the standard deviation and coefficient of variation. Table 25 gives the range for each chemical parameter measured for each of the different process waters during the 1986 field season. Similar type results were obtained in 1987 and 1988. It can be seen from Tables 2 and 25 that the three oil shale process waters are quite different in chemical composition.

Chemical analyses of the three process waters were done twice each year (beginning and end of each field season) for EPA priority pollutants (EPC 624 and 625 methods). The EPA 624 analysis is for volatile organic compounds, and the EPA 625 analysis is for semi-volatile organics. The priority pollutants listed in Table 26 are the only ones found at the detection limits set for the WRI equipment of the 103 organic compounds included in the two analyses. No compounds were identified as being volatile organic. Several semi-volatile compounds were identified as indicated by Table 26 but it was noted by the WRI laboratory technician that levels of several of these semi-volatile compounds were below the detection levels set for the compound which means they could be present but were not detectable. Failure to reach these detection levels may have been due to the large dilution factors used by WRI when analyzing the oil shale process waters.

Major inorganic chemicals of the oil shale process waters were determined using the computer program WATEQ. Table 27 illustrates the WATEQ printout for the Geokinetics process water summarized as ion ratio tables for the major inorganic constituents. Results of the WATEQ analyses for all three oil shale process waters are contained in a Master of Science thesis by Koontz (1986). Figures 6 and 7 depict the ion distribution and relative TDS of the process waters on two different dates in 1985. The area of the pie charts is proportional to the relative TDS. The top half of each chart represents cations and the bottom half anions. It is shown that very little change in ion distribution occurs with chemical concentration.

Sampled concentrations of chemical constituents and pH from the 1985 field season are graphically represented in Figures 8 and 9. Figure 8 generally shows an increasing concentration of the chemical constituents caused by evaporation over the field season. Concentrations of total dissolved solids, total organic carbon, and total alkalinity appear to show the largest increases and be the most affected by evaporation. Figure 9 indicates that pH is almost insensitive to concentration. Problems were associated with the Class A pan instrumentation and filling mechanism during 1985 as described earlier. On several occasions, the automatic controllers allowed the pans to drain and refill resulting in a significant dilution of the process waters. This factor complicated the analyses designed to test the significant effects of chemical concentrations on the evaporation rate of the process waters during the first year. The years that followed (1986-88), however, indicated the same trends as shown by Figure 8 without the pan overflow.

A literature review showed that water quality data of at least three types is necessary to predict evaporation rates. These data are dissolved solids, surface properties and color. The water quality data that were measured in this project were assigned to one or more of these categories (Table 28).

Table 25. Range of Chemical Composition of the Oil Shale Process Waters During 1986. (Range of Parameters Given in mg/l Except Where Noted*)

Parameter	Rio Blanco	Paraho	Geokinetic
Alkalinity	52-160	1741-4520	13266-28000
Chloride	89-200	430-1616	420-1090
Sulfate	9000-16824	3717-9760	3117-12300
TDS	13910-108190	22940-67510	3 3860-77300
TOC	85-140	12200-17896	3615-7500
pH*	7.61-8.87	6.53-6.98	8.5-9.49
Conductivity*	69-140	92-145	165-260
Salinity	4-10	6-10	11-19
Total Kjeldahl Nitrogen	21-23	3700-4300	690-980
Oil & Grease	1-40	660-3300	120-270
Ammonia	11-14	1900-3500	120-270
Sodium	1770-3240	822-1360	10200-14030
Potassium	295-4120	73-139	207-281
Calcium	27-572	162-301	12-16
Magnesium	15-30	315-456	18-27
Boron	5-10	7-10	219-316
Arsenic	<1	61-95	17-54
Strontium	8-24	2-4	1-2

*(pH is unitless and conductivity is measured in μ mhos).

Table 26. EPA Priority Pollutants Found in Oil Shale Process Waters.

Constituent	Concentration	Source
Toluene	0.6 ug/L	Pan 2
Phenol	15,000 ug/L	Pan 4
Aniline	1,400 ug/L	Pan 4
2-Methylphenol	2,300 ug/L	Pan 4
Bis (2chloroisoprophyl) ether	1,000 ug/L	Pan 4
4-Methylphenol	2,300 ug/L	Pan 4
Phenol	16,000 ug/L	Pan 3
4-Methylphenol	3,200 mg/L	Pan 3
2, 4-Dimethylphenol	600 ug/L	Pan 3
Methylene chloride	290 ug/L	Pan 3
Phenol	7,500 ug/L	Pan 3
4-Methylphenol	1,600 ug/L	Pan 3

Table 27. WATEQ Computer Printout of Inorganic Constituents on Geokinetics Oil Shale Process Water.

Geokinetics Process Water, Sept 6, 1985

WATEQ Analysis

Sample ID 1511

Sample Coordinates X = 1.0000 Y = 1.0000 Z = 1.0000

Temperature = 2.52 Degrees C PH = 8.720 Dissolved Oxygen = 1.30 MG/L

Specific Conductance = 19500.0000 Lab-Measured Ph = 8.7200

Measured EH = 0.0000 Volts PE = 0.000

*****TOTAL CONCENTRATIONS OF INPUT SPECIES*****

SPECIES	TOTAL MOLALITY	LOG TOTAL MOLALITY	TOTAL MG/L
AL 3+	2.482101E-05	-4.6052	6.700000E-01
CA	8.628972E-03	-2.0640	3.460000E+02
CL -	7.587023E-02	-1.1199	2.691000E+03
HCO3 -	2.811091E-01	-.5511	1.716000E+04
IRON	4.116600E-05	-4.3855	2.300000E+00
K +	1.559343E-03	-2.8071	6.100000E+01
MG 2+	1.393765E-02	-1.8558	3.390000E+02
NA +	3.786985E-02	-1.4217	8.710000E+02
N2 AQUEOUS	1.4986293-01	-.8243	4.200000E+03
SIO2 TOTAL	1.663589E-04	-3.7790	1.000000E+01
SO4 2-	4.040436E-02	-1.3936	3.883000E+03

*****DESCRIPTION OF SOLUTION*****

CATION MILLIEQUIVALENTS	57.403	PH	8.720	ACTIVITY H2O = .9902
ANION MILLIEQUIVALENTS	410.684	TEMPERATURE	2.52 DEG C	PCO2 = 1.717851E-02
RATIO CATIONS/ANIONS	.140	IONIC STRENGTH	2.861261E-01	PH2S = 0.
				P02 = 2.133364E-02
				PCH4 = 2.543427E-58
				CO2 TOTAL = 2.683770E-01
				DENSITY = 1.030
				TDS = 29563.97MG/L

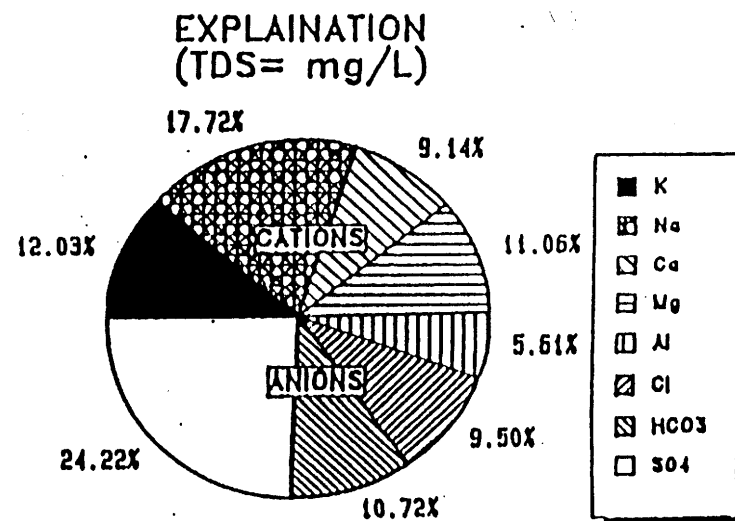
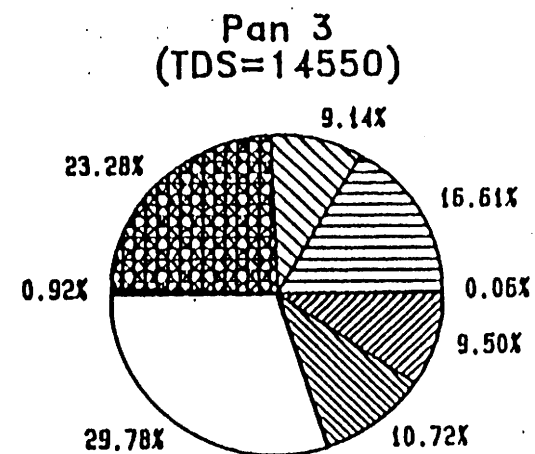
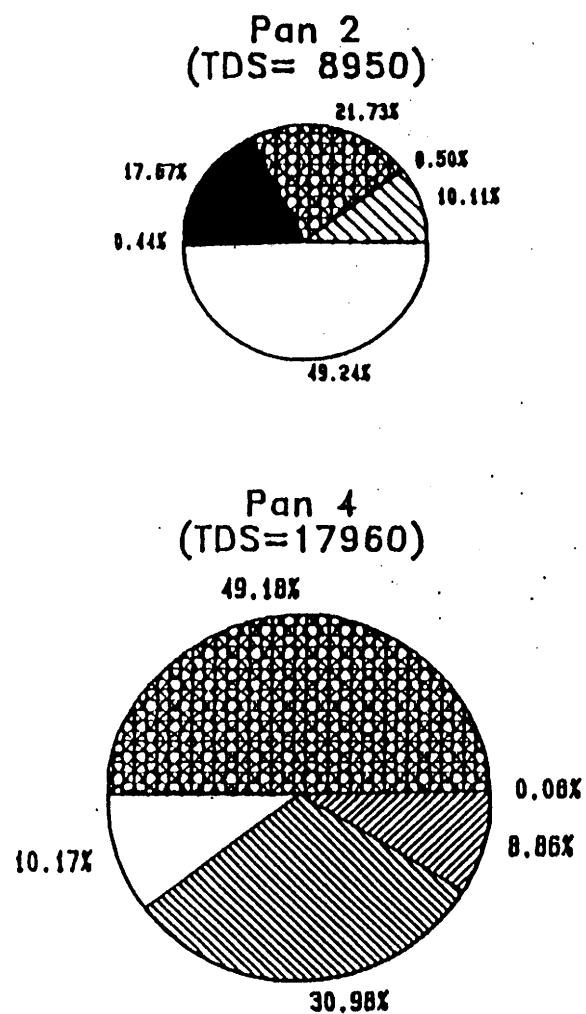
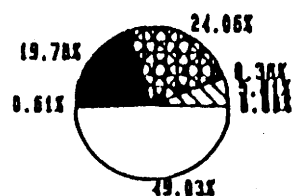
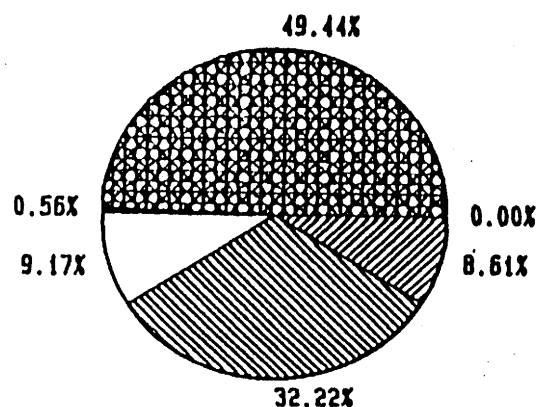


Figure 6. Major Ion Distribution August 8, 1985 (Julian Day 220)

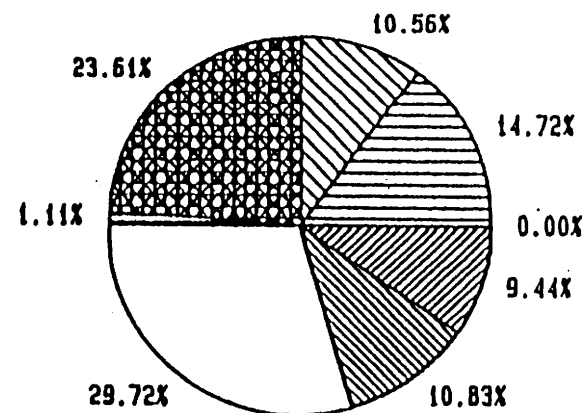
Pan 2
(TDS= 8420
mg/L)



Pan 4
(TDS=24000 mg/L)



Pan 3
(TDS=28010 mg/L)



EXPLANATION
(TDS= mg/L)

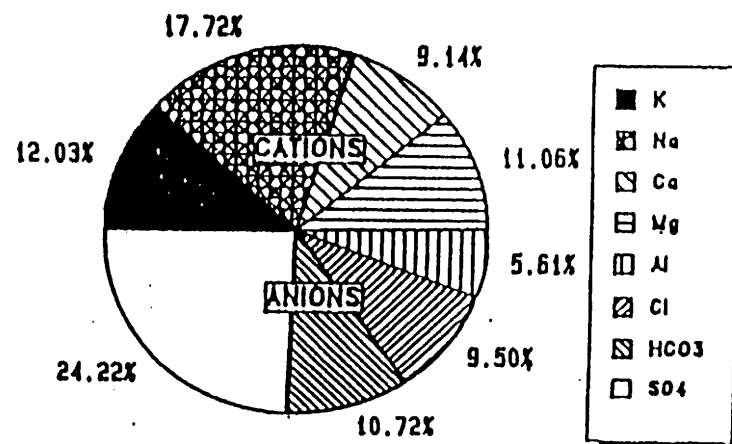


Figure 7. Major Ion Distribution September 6, 1985 (Julian Day 249)

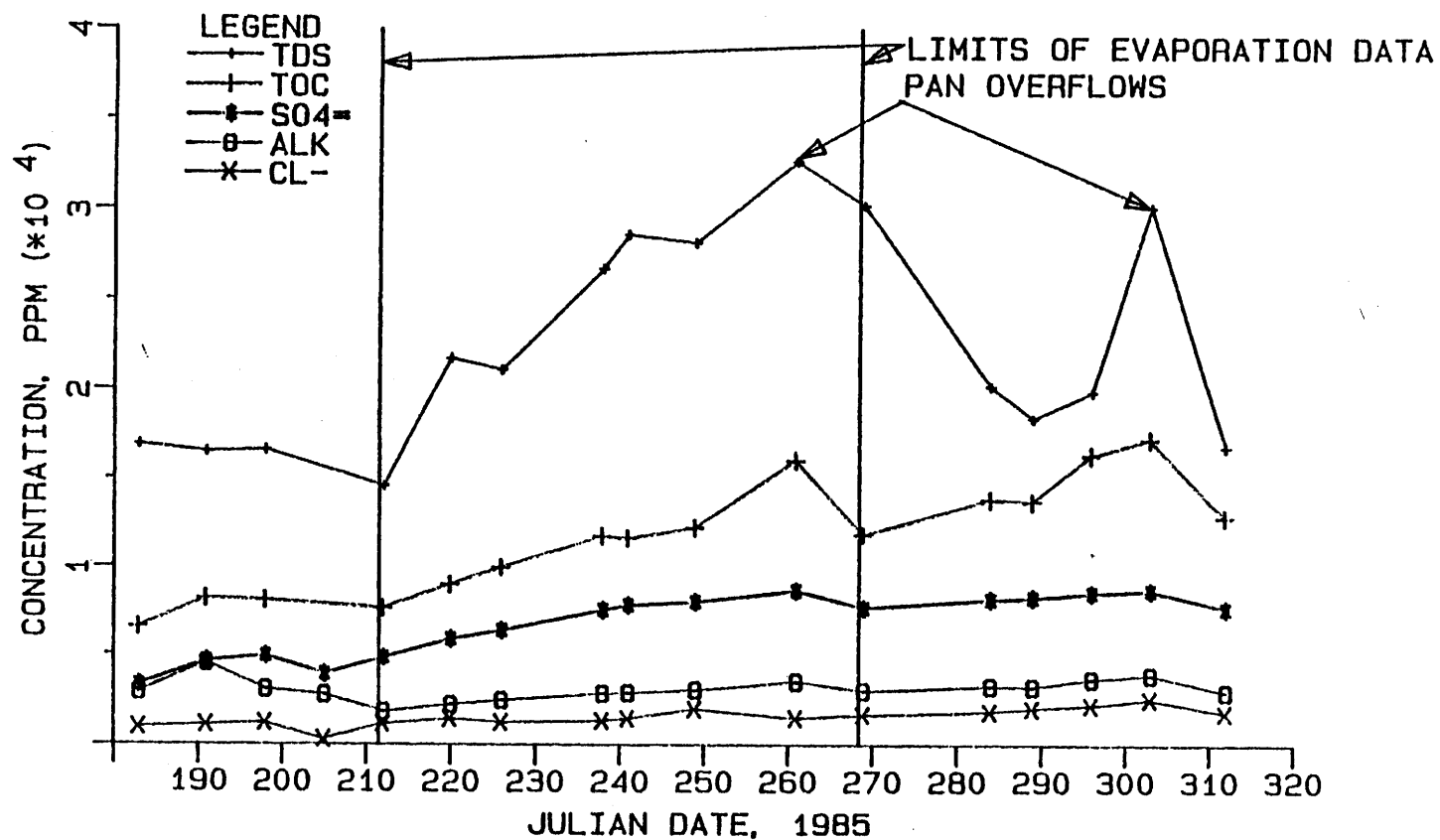


Figure 8. Chemical Constituent Concentration with Time During 1985 for the Paraho Process Water.

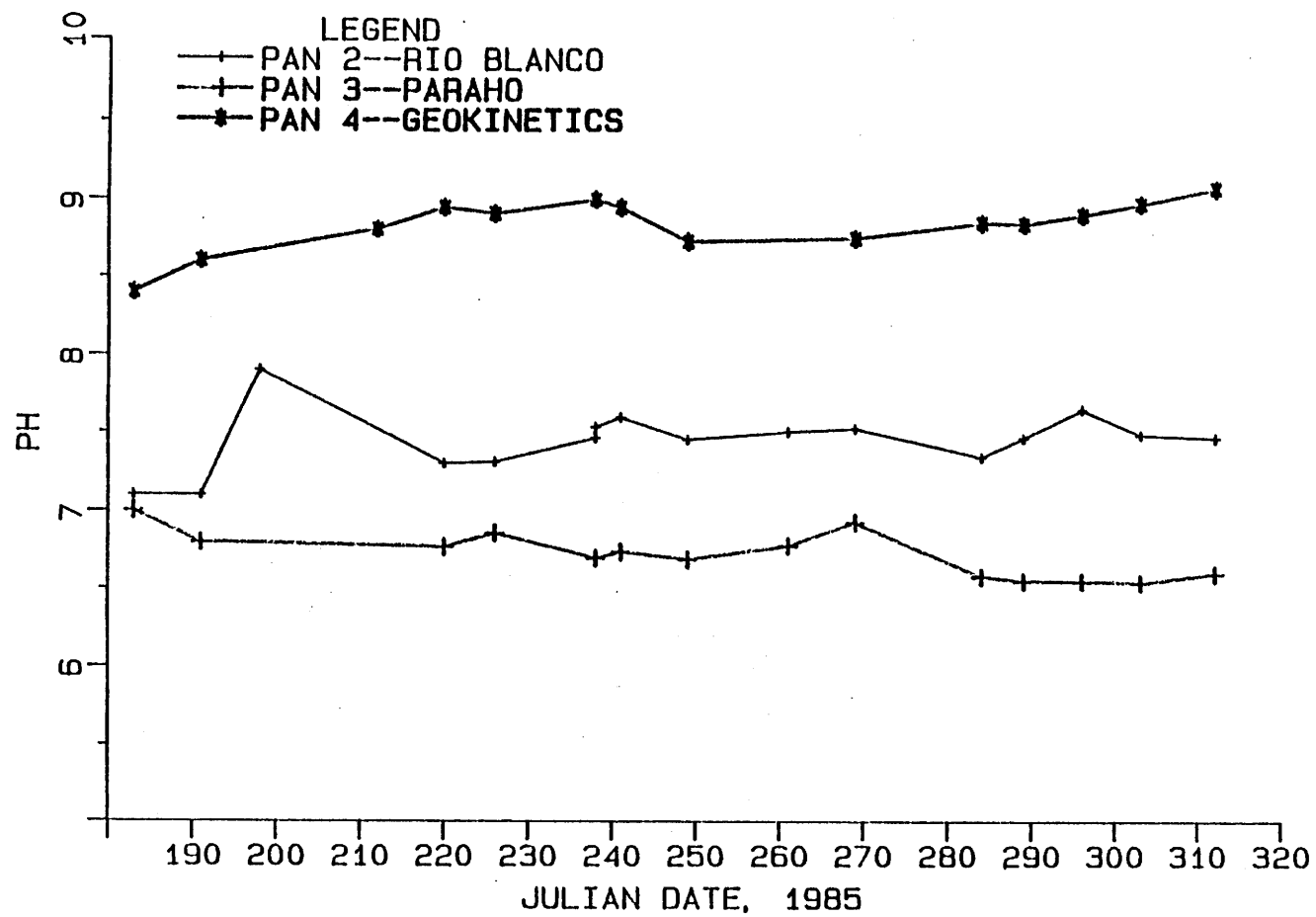


Figure 9. pH Concentration with Time During 1985.

Table 28. Categories of Water Quality Data.

Factors which may influence evaporation rate:

Dissolved solids (water activity coefficient)

Total Dissolved Solids (TDS)
Alkalinity
Chloride Ion
Sulfate Ion
Ammonia (NH_4)
Total Kjeldahl Nitrogen (TKN)
Salinity
Conductivity
Specific Conductance

Surface Properties (immiscible film)

Total Organic Carbon (TOC)
Oil and Grease
Total Kjeldahl Nitrogen (TKN)

Color (light absorbance)

Total Organic Carbon (TOC)
Total Dissolved Solids (TDS)
Oil and Grease
Color

Factors not expected to influence evaporation rate:

pH
Dissolved Oxygen (DO)

Several of the chemical constituents are considered in two categories. TOC, for instance, might indicate dark oily hydrocarbons that would form a surface film but would increase light absorbance. Chemical analysis from water samples were performed on all parameters shown in Table 28. Light transmittance or color was reported in terms of percent of light transmitted through a sample using 340 nm wavelength monochromatic light for a 1 cm light path. Each sample was diluted 50:1 with distilled water, with distilled water being used as the standard measure (transmittance of distilled water was assumed to be 100 percent). Low transmittance indicates a high absorbance or a dark color. Light transmittance was found to decrease (low transmittance) with increasing chemical concentration of the process waters.

It was speculated that light transmittance or color might be highly correlated with another chemical parameter. Investigations of light transmittance and TOC data for all three process waters produced a very high correlation (98.5 percent). A regression equation was developed between these two parameters following the first year of the study. This regression relationship allowed for only TOC to have to be measured beyond the first year of the study because light transmittance could be predicted from the regression equation.

Using the chemical analysis data for those quantities in Table 28, a statistical program combining polynomial regression and significance testing was used to screen each measured chemical parameter relative to its affect on evaporation of process waters. These data were used to provide an indication of the significance that each independent variable may have in a complex interactive model and to indicate if polynomial effects may exist for that variable. All possible subsets regression, using Mallows Cp and adjusted R^2 criteria for model selection, was used to identify significant variables thus affecting evaporation.

Results of these analyses showed that six chemical parameters were found to have significant effects on process water evaporation. The six chemical parameters are alkalinity, chloride ion, sulfate ion, TDS, TOC and pH. All the parameters listed above were significant at the $\alpha = 0.05$ level. Regression analysis, however, indicated that no significant affect on evaporation rate could be attributed to increasing concentration of the chemical constituents in the water.

COMPARISON OF LABORATORY AND FIELD STUDIES - CONCLUSIONS

The field studies on chemical parameter effects on evaporation indicated that individual chemical parameters (six were found significant) have an affect on evaporation. However, no significant affect on evaporation could be attributed to increasing concentrations of chemical constituents in the process waters. This second conclusion was verified by both the field and laboratory studies. The effect of films on the surface of the Class A pans did not show a significant affect on

evaporation rate which was surprising. The physics of the interactions suggest that color and increasing chemical concentration result in increased heating and molecular activity of the process waters in such a manner that no discernable affect due to films or other molecular bonding activity could be measured which would result in a change in evaporation rate or amount compared with fresh water. In general, however, most highly chemical waters result in a decrease in evaporation rate compared to fresh water as indicated in the literature review.

EVAPORATION MODELS FOR ASSESSMENT/DEVELOPMENT AND DESIGN OF OIL SHALE PROCESS WATER DISPOSAL

Emperical, statistical and theoretical models were assessed and developed for evaporation of oil shale process waters and are described in this section of the report. Modeling of the diurnal variation of evaporation of oil shale process waters is also described.

SELECTION AND ASSESSMENT OF EXISTING EVAPORATION MODELS

A description of methods for estimating evaporation was presented earlier. Four main methods to the estimation of evaporation were given. Three of these methods (energy budget, mass transfer and combination method) have theoretical and/or empirical equations associated with the methods. This section presents the results of analysis made on several of these equations for oil shale process waters.

Evaporation Models Selected

Several evaporation models were chosen to test their effectiveness in estimating daily evaporation of oil shale process waters. The models chosen were: 1) Penman (two versions) (PM1, PM2), 2) Priestly-Taylor (PT), 3) Kohler-Nordenson-Fox (KNF), 4) Linacre (LIN), 5) Meyer (MEY), 6) U.S. Geological Survey (USGS), 7) Harbeck (HARB), 8) Salhotra (SAL), and 9) Haass. These models vary in complexity and in the data required to operate them due to the simplifying assumptions made in each case. A description of the models can be found in Eyre (1987). The parameters or input required for each model are shown in Table 29.

In most cases the models selected estimate the evaporation from a body of fresh water, such as a lake or pond. These models will be compared with evaporation rates measured from the Class A evaporation pans at the field site.

Table 29. Parameters Required to Predict Evaporation for Established Models.

MODEL	EQ NO	RAD	ALBEDO	WIND	AIR TEMP	SURF TEMP	RH	ATM PRESS	AREA	LAT	ELEV	S
PM1	38	*	*	*	*		*	*				
PM2	45			*	*	*	*					
PT	47	*	*		*			*				
KNF	50	*	*	*	*		*	*				
LIN	63				*					*	*	
MEY	64			*	*	*	*					
USGS	67			*	*	*	*					
HARB	70			*	*	*	*		*			
SAL	71			*	*	*	*					*
HAASS	74	*		*	*		*					

To compare the models to the pan measurements, a pan coefficient, K_p , will be applied.

$$E = K_p E_p \quad (25)$$

where E_p is the pan evaporation and E is the estimate of evaporation. The generally accepted annual coefficient for the Class A pan is approximately 0.70 (Nordenson, 1963; Linsley, 1958; Dunne and Leopold, 1978). However, the pan coefficient can vary due to climatological conditions. The annual pan coefficient may be 0.80 or higher for humid climates where the pan water temperature is greater than the ambient air temperature, or 0.60 or less for arid areas where the pan water temperature is less than the ambient air temperature (Nordenson, 1963). In Wyoming, a semi-arid area, where the site is located, 0.70 is a reasonable pan coefficient. The effects of advected energy and the change in heat storage are the major sources causing variability in the pan coefficient. Energy goes into storage during spring months decreasing evaporation, and comes out of storage in the fall which results in increasing evaporation. Climatological data and pan evaporation were only measured from May to September for this study, so variations that may apply due to seasonal changes are avoided.

Field Data Used in Analysis

Comparison and analyses performed on the evaporation models were based on field site data measured for climatological parameters and the measured pan evaporation from the fresh water pan and three process water pans. Analyses on the models were performed using 38 days of data from 1985, 122 days of data from 1986 and 63 days of data from 1987. All ten evaporation models were tested with the 1985 and 1986 data. Only the Penman, Priestly-Taylor, Kohler-Nordenson-Fox and Haass models were evaluated with the 1987 data.

Analyses and Results

Using 1985 and 1986 data, the daily estimates of evaporation generated for the ten models were compared with the measured daily evaporation using the statistical package MINITAB. The correlation between the predicted evaporation of each model and the measured evaporation was calculated for each pan and for all waters combined.

When analyzing the estimates for the individual pans, normal score plots (NSCORES) were prepared to determine if the data was normally distributed. All of the data were plotted against the normal distribution to determine if the data fit a normal distribution (data should plot around a normal distribution line), with some small variations occurring with a few of the model data results. The models by Harbeck, Meyer, Salhotra, and the second version of the Penman equation all indicated variation from normal distributions for several of the pans. This variation could cause the correlation coefficient for these models to be higher than usual, but since these models did not turn out to be the best predictors of evaporation, this problem was not significant. The correlation coefficient, the coefficient of determination (R^2), and the adjusted coefficient of determination (R^2 adjusted), were then compared to find which models would more closely predict an evaporation amount corresponding to measured values.

For the fresh water in pan 1, the best estimates were achieved by the Kohler-Nordenson-Fox (KNF), the Priestly-Taylor (PT), and the Haass models. Correlation with the KNF model supports the conclusions for fresh water evaporation made by Warnaka (1985). The Haass, the Penman combination equation (PM1) and the PT models more closely correlated with measured evaporation in all three of the pans containing the process waters with the KNF method a close fourth. An analysis made on the average evaporation of all waters combined (fresh water and the three process waters) indicated that the same models that were selected for the separate process water pans were also the best estimators₂ for all of the waters combined. The coefficients of correlation, R^2 , and R^2 adjusted coefficients for each model, in comparison with measured evaporation, are shown in Tables 30 and 31.

The top four models all had correlation coefficients that were reasonably close to each other and they were all significantly greater in correlation coefficient than were the other six. These four models incorporate similar parameters for estimation of evaporation which would indicate that these parameters would be the most important in prediction of process water evaporation. They are many of the same climatological parameters that were found to be significant in affecting evaporation as indicated previously. In analyzing the ten models, the four models which best estimated measured evaporation were the only models which used radiation (net or incoming) as a parameter. Models which simplified this parameter through the use of coefficients or simply eliminating it from further consideration were not as effective in estimating evaporation for these process waters. Therefore, this parameter, which is also included in all of the regression models, is determined to be a major parameter and should be measured and included when estimating evaporation. Since net radiation data was not always recorded during this project or reliable for all waters due to signal noise or data logger malfunction, the ten models used a calculated (estimated) rather than measured net radiation. Since the effect of solar radiation was established to be critical for evaporation estimation, improvement in net radiation instrumentation or estimation could help improve evaporation estimates and correlation with measured evaporation.

Each of the ten models were used to estimate daily evaporation for the four different waters. The primary difference in evaporation estimates between waters for the ten models occurred when albedo and water temperature were included as parameters, because these parameters differed between pans. The estimate for each model was compared with measured evaporation. An example of the estimates of evaporation computed for each model is shown, by pan, in Table 32.

The two Penman equations, a combination (PM1) and a mass transfer (PM2), were compared. Estimates of evaporation for PM1 correlated well with measured evaporation, having the second highest correlation for the three process waters and all waters combined, and the fourth highest correlation for the fresh water pan. PM2 on the other hand was much less correlated with measured evaporation, being 20 to 30 percent less correlated than the best model. The better evaporation estimates produced by PM1 could be due to the parameters required as input. Net radiation, wind speed, temperature, relative humidity and atmospheric pressure are all required, while PM2 only requires wind speed, temperature, and relative humidity.

Table 30. Coefficients of Correlation for the Ten Models.

Model	Pan1	Pan2	Pan3	Pan4	All Waters
PM1	0.672	0.695	0.777	0.760	0.722
PM2	0.394	0.506	0.433	0.498	0.450
PT	0.686	0.702	0.757	0.755	0.721
KNF	0.686	0.684	0.730	0.735	0.704
LIN	0.455	0.429	0.439	0.392	0.360
MEY	0.397	0.514	0.441	0.497	0.454
USGS	0.422	0.519	0.417	0.479	0.452
HARB	0.426	0.516	0.417	0.480	0.452
SAL	0.387	0.477	0.457	0.484	0.446
HAASS	0.682	0.705	0.786	0.764	0.730

Table 31. R^2 , and R^2 Adjusted Coefficients for the Ten Models.

Model	Pan1		Pan2		Pan3		Pan4		All Waters	
	R^2	R^2 ADJ	R^2	R^2 ADJ	R^2	R^2 ADJ	R^2	R^2 ADJ	R^2	R^2 ADJ
PM1	0.452	0.448	0.484	0.479	0.604	0.601	0.577	0.574	0.522	0.521
PM2	0.155	0.148	0.256	0.250	0.187	0.180	0.248	0.242	0.202	0.201
PT	0.470	0.466	0.493	0.489	0.574	0.570	0.570	0.566	0.520	0.519
KNF	0.470	0.466	0.482	0.477	0.533	0.529	0.540	0.536	0.500	0.499
LIN	0.207	0.200	0.184	0.172	0.193	0.186	0.154	0.147	0.130	0.128
MEY	0.158	0.151	0.264	0.258	0.194	0.187	0.247	0.241	0.206	0.205
USGS	0.178	0.171	0.269	0.263	0.174	0.169	0.229	0.223	0.204	0.203
HARB	0.182	0.175	0.267	0.261	0.174	0.167	0.231	0.224	0.205	0.203
SAL	0.150	0.142	0.227	0.221	0.208	0.202	0.235	0.228	0.199	0.197
HAASS	0.465	0.460	0.497	0.493	0.617	0.614	0.584	0.581	0.533	0.532

Table 32. Evaporation Estimates by Method Compared to Pan Evaporation for Each of the Four Pans (inches/day).

JDAY	PM1	PM2	PT	KNF	LIN	MEY	USGS	HARB	SAL	HAASS	MEASURED
Freshwater Pan:											
205	0.20	0.22	0.30	0.27	0.24	0.18	0.22	0.22	0.07	0.12	0.28
206	0.09	0.06	0.10	0.21	0.26	0.05	0.07	0.06	0.04	0.08	0.20
207	0.14	0.14	0.20	0.29	0.20	0.12	0.13	0.13	0.06	0.10	0.23
208	0.15	0.10	0.20	0.26	0.21	0.08	0.09	0.09	0.04	0.10	0.17
209	0.16	0.13	0.20	0.30	0.21	0.11	0.11	0.11	0.07	0.11	0.21
210	0.21	0.20	0.30	0.31	0.23	0.17	0.16	0.16	0.10	0.13	0.24
Rio Blanco Pan:											
205	0.20	0.25	0.30	0.27	0.29	0.21	0.25	0.25	0.08	0.12	0.26
206	0.09	0.08	0.10	0.21	0.26	0.06	0.07	0.07	0.04	0.08	0.19
207	0.14	0.15	0.20	0.29	0.25	0.13	0.14	0.14	0.06	0.10	0.24
208	0.15	0.11	0.20	0.26	0.26	0.09	0.10	0.10	0.04	0.10	0.20
209	0.16	0.14	0.20	0.30	0.26	0.12	0.12	0.12	0.07	0.11	0.24
210	0.21	0.22	0.30	0.31	0.29	0.18	0.17	0.17	0.10	0.13	0.26
Paraho Pan:											
205	0.20	0.23	0.30	0.27	0.38	0.20	0.23	0.23	0.08	0.12	0.28
206	0.09	0.07	0.10	0.21	0.33	0.06	0.06	0.06	0.04	0.08	0.20
207	0.14	0.14	0.20	0.29	0.32	0.12	0.13	0.13	0.06	0.10	0.24
208	0.15	0.09	0.20	0.26	0.33	0.07	0.08	0.08	0.03	0.10	0.19
209	0.16	0.13	0.20	0.30	0.33	0.11	0.11	0.11	0.06	0.11	0.24
210	0.21	0.19	0.30	0.31	0.37	0.15	0.15	0.15	0.09	0.13	0.27
Geokinetics Pan:											
205	0.20	0.31	0.30	0.27	0.37	0.26	0.31	0.31	0.09	0.12	0.28
206	0.09	0.08	0.10	0.21	0.33	0.07	0.07	0.07	0.04	0.08	0.19
207	0.14	0.17	0.20	0.29	0.32	0.14	0.15	0.15	0.06	0.10	0.24
208	0.15	0.13	0.20	0.26	0.33	0.11	0.12	0.12	0.04	0.10	0.21
209	0.16	0.18	0.20	0.30	0.33	0.14	- .15	0.15	0.07	0.11	0.17
210	0.21	0.25	0.30	0.31	0.37	0.21	0.20	0.20	0.11	0.13	0.28

Estimates of evaporation using the PT method also correlated well with measured evaporation. The PT method had one of the better correlations with fresh water (Table 30), the third highest correlation with the three process waters and when all of the waters were combined together. This method, like PML, required net radiation and atmospheric pressure as input variables, which could be a factor in it's effectiveness to estimate evaporation.

The KNF method is one of the best methods for estimating fresh water evaporation in the Rocky Mountain area which was the conclusion arrived at by Warnaka (1985). For the process waters and all of the waters combined, KNF was considered fourth in terms of having the best correlation with measured evaporation. The KNF method contains four of the five parameters required in PML. This included net radiation and atmospheric pressure, which are parameters common to three of the four best models for estimating evaporation for oil shale process waters.

Estimates using the Haass equation tended to be slightly lower than measured evaporation, but the correlation was good. Estimates using this method had the best correlation for the three process waters and all of the waters combined and had the third highest correlation for fresh water evaporation. Good correlation with the process waters was not surprising since the model was developed for similar oil shale process waters. This method included four of the five parameters required for PML and was derived using data from similar waters.

The other five models (LIN, MEY, USGS, HARB and SAL) either greatly over- or underestimated pan evaporation and the coefficients of correlation were low (40 to 50 percent) in comparison to the other models. In general, these models did not contain the appropriate climatological parameters (solar radiation, relative humidity, etc.) which were a part of the best estimating models.

Only the four models which proved to be the best from the analysis with 1985 and 1986 data were used to analyze the 1987 data for comparison purposes. The results of these comparisons for the Geokinetics process water are shown on Figure 10. Similar results were obtained for the other two process waters and fresh water. Figure 10 indicates a relatively good match between measured and predicted values on a daily basis for all four models.

Figure 11 shows the cumulative mass plots of the four predictive models, and indicates a very strong relationship between the Penman, KNF, and Haass models. The Priestly-Taylor equation, however, overestimates evaporation. Statistical comparison of each of the models compared to the cumulative measured evaporation of each of the four waters gave R^2 values on the order of .99 for all cases.

These results indicate that evaporation can be predicted on a daily basis with reasonable accuracy using the calibrated Penman, KNF or Haass model equations knowing the climatological parameters for that particular day. Additionally, over a period of weeks, the three models above give very accurate estimates of total evaporation for the period.

Figure 10. Daily Evaporation Pan #4 Geokinetics.

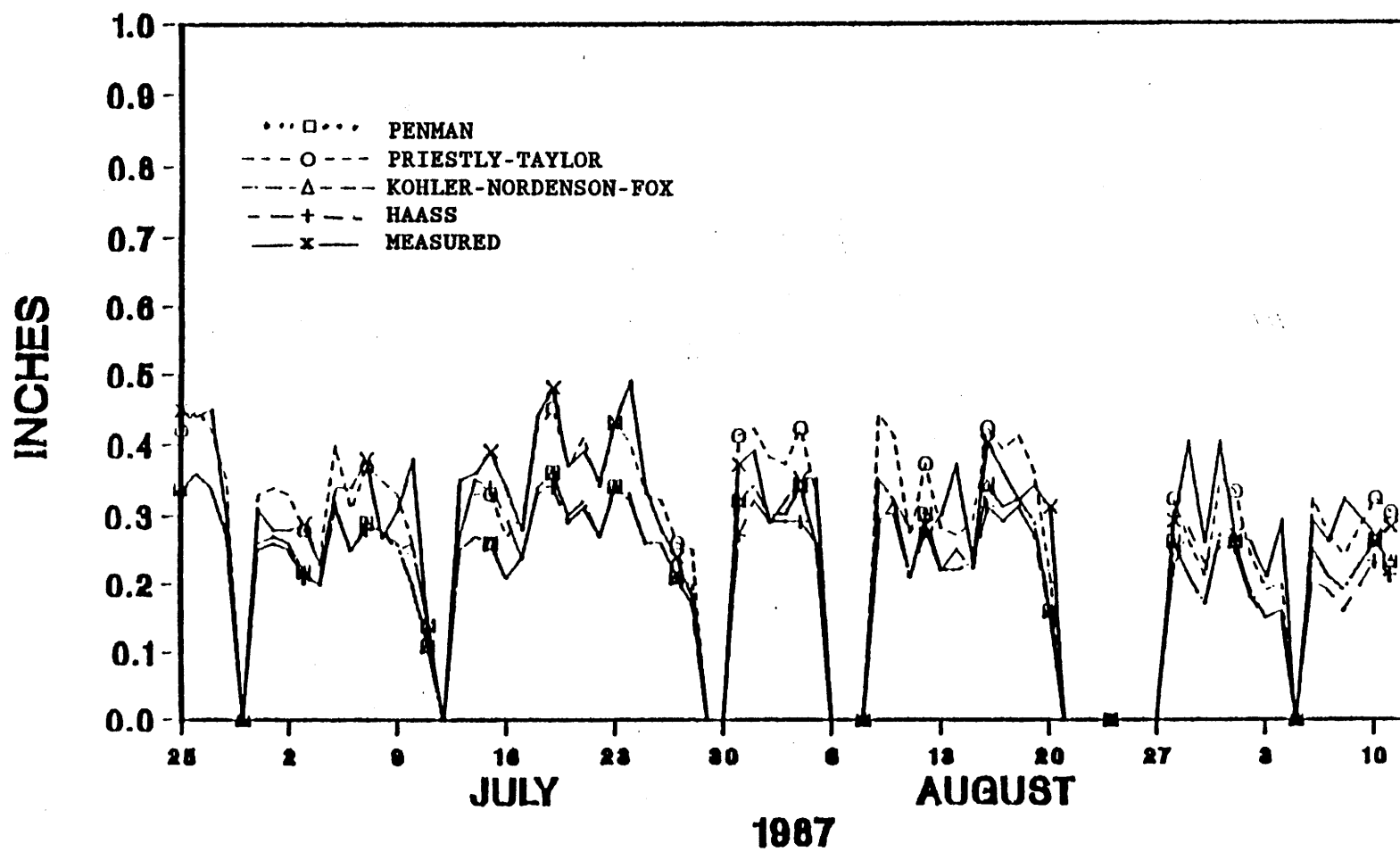
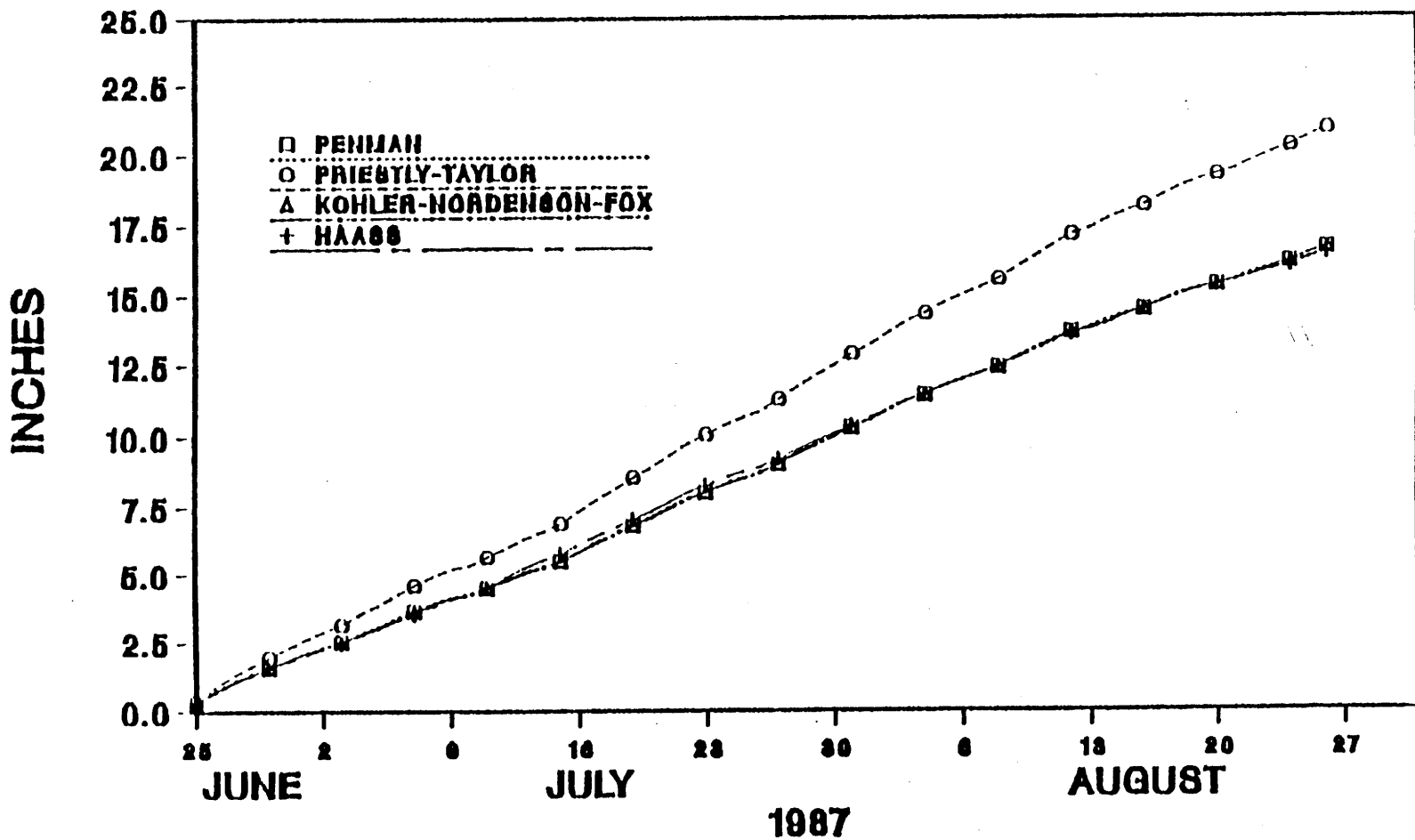


Figure 11. Total Evaporation Estimated During 1987 for the Four Established Models.



MATHEMATICAL/STATISTICAL MODELS

Regression analysis was used to develop mathematical/statistical models for each of the process waters and for all waters combined. The purpose of this mathematical/statistical model study was an attempt at developing a model(s) which could more accurately predict evaporation rate and amount in the western United States for process waters compared to existing evaporation models.

Methodology

Regression analysis to develop a daily evaporation model using the climatological and chemical parameter data for 1986 was performed for fresh water and the three process waters (pans), and for all waters combined using the statistical package BMDP. Regression analysis was done using BMDP9R, which is an all-possible subsets regression. All possible subsets of the measured parameters input were compared using the Mallows C_p criteria, which pertains to the total squared error of observations. R^2 adjusted criteria was also examined. The best subset was chosen using these criteria for each water and all the waters combined. The subset with the smallest C_p in theory has the smallest total squared error.

Parameters input as independent variables were each independently analyzed to determine if they were constant or if they changed over time. Constant parameters were not input for regression analysis since they did not change with time. Parameters which showed a change over time were input and also analyzed independently with evaporation data to see if they exhibited a significant curvilinear effect. If a curvilinear effect was noted, higher power terms were analyzed and included in the regression analysis. The parameters which showed this effect were the temperature measurements (air, surface and bottom water). After analysis of each, it was determined to include squared parameters for each of these temperatures. Some of the chemical components shown in Table 25 were not included as parameters due to an insufficient amount of data.

The parameters in the best subset were also checked to ensure that they made sense logically. If the models included squared parameters, the original parameter, or parameter to the first power, was also included. This regression analysis was done to determine which parameters have more effect on evaporation. By identifying and measuring these parameters, evaporation at other locations in the same geographic region or for other waters can be more closely estimated. The parameters used in these developed regression equations are shown in Table 33 and are those that were indicated previously as important climatological and chemical parameters associated with evaporation. This analysis was based on daily values, but produced evaporation estimates were in mm/hour. The unit mm/hour was used because of the number of significant digits beyond the decimal for evaporation rate if inches per hour were used (a simple conversion factor will permit a change of units). This philosophy is used throughout the rest of the report. To obtain a daily evaporation model, the developed models can be multiplied by 24 hours.

Table 33. Parameters Required to Estimate Evaporation in Regression Models.

REGRESSION MODEL	RAD	WIND	AIR TEMP	SURFACE TEMP	BOTTOM TEMP	ATM PRESS	ALK	CL	SO ₄	TDS	TOC	pH
1	*	*	*	*	*							
2	*	*	*	*			*					
3	*	*			*	*	*					
4	*	*	*	*			*					
All Waters	*	*	*	*	*	*	*	*	*	*	*	*

Validation of Developed Models

As a result of regression analysis for each pan, it was found that for the fresh water pan that ambient air temperature (T_a) to the first and second power, the surface and bottom pan temperature (T_s and T_b), the ground wind speed (W_g), and the incoming solar radiation (R_s) were the key parameters in evaporation. The regression equation for the best estimate of evaporation for fresh water (EF) is:

$$EF = 0.035918 T_a - 0.002518 T_a^2 - 0.086271 T_s + 0.083288 T_b + 0.006539 W_g + 0.0004563 R_s - 1.10594 \quad (26)$$

where all temperatures are in °F, W_g is in mph, and R_s is in ly/day. The parameters included in this regression model are similar to those required in most fresh water evaporation models. Including the squared air temperature parameter in the model accounts for the curvilinear effect due to air temperature and relates to the effect of the wind profile and temperature change that occur above the pan. Including both bottom and surface temperature accounts for temperature variations throughout the water depth. Wind and incoming solar radiation are generally determined to be important in evaporation so their inclusion was not surprising.

For the Rio Blanco process water (ER), T_a to the first and second power, T_s to the first and second power, W_g , R_s , and the alkalinity (ALK), had the major influence on evaporation. The regression equation for Rio Blanco process water evaporation is:

$$ER = -0.061254 T_a + 0.0057421 T_a^2 + 0.045015 T_s - 0.00035375 T_s^2 + 0.014001 W_g + 0.0005127 R_s + 0.0001609 ALK + 0.020164 \quad (27)$$

where ALK is in mg/l. In this regression model, wind, incoming solar radiation and both surface water and air temperature to the first and second power are included as well as alkalinity. Comparing parameters of the fresh water and Rio Blanco regression equations shows that chemical composition of the Rio Blanco process water has an effect on evaporation that is probably associated

with surface tension and temperature. Alkalinity was also included, which supports the supposition that chemical composition effects evaporation.

For the Paraho process water (EP), T_b , W_g , R_s , the barometric pressure, P, and ALK had the major influence on evaporation^s. The resulting regression equation for Paraho process water evaporation is:

$$ER = 0.0052173 T_b + 0.0057421 W_g + 0.00055197 R_s - 0.172436 P + 0.000017259 ALK + 3.5816 \quad (28)$$

where P is in inches Hg. This regression model again found wind and incoming solar radiation significant, but includes only the bottom water temperature. Since this water is darker, the water absorbs more solar energy which causes the surface temperature to fluctuate a great deal while allowing the water at the bottom of the pan to change more gradually. This more stable change would tend to make the bottom water temperature a better indication of the changes in water temperature than the surface water temperature. Alkalinity, as a parameter, again indicates that chemical composition does effect evaporation, and the inclusion of barometric pressure relates to the effect of atmosphere on evaporation. Atmospheric pressure can increase evaporation or, as in this case, reduce the evaporation rate.

For the Geokinetic process water (EG), evaporation was influenced by T_a to the first and second power, T_s , W_g , r_s , and ALK. The best evaporation regression equation is:

$$EG = -0.27473 T_a + 0.00024022 T_a^2 + 0.0034408 T_s - 0.0061358 W_g + 0.00049334 R_s + 0.0000047246 ALK + 0.44744 \quad (29)$$

The parameters in this regression model are similar to those in the other two process waters analyzed, especially the Rio Blanco process water. The only difference in parameters from the Rio Blanco process water is the fact that surface water temperature squared is not included. The curvilinear effect of surface water temperature may not have as great an effect on evaporation for this type of water.

The best model for all waters combined had many factors that influenced evaporation. They include T_a to the first and second power, T_s and T_b , W_g , R_s , P, ALK, chlorine (CL), sulfate (SO_4), total dissolved solids (TDS), total organic carbon (TOC), and the pH. This regression model for evaporation is represented by the equation:

$$E = -0.017175 T_a + 0.0001464 T_a^2 + 0.0021304 T_s + 0.006171 T_b + 0.010918 W_g + 0.00035796 R_s - 0.15074 P - 0.85426 \times 10^{-5} ALK + 0.00017286 CL + 0.000015014 SO_4 - 0.22181 \times 10^{-5} TDS + 0.000019938 TOC + 0.1428 pH + 2.20 \quad (30)$$

Where CL, SO_4 , TDS, and TOC are measured in mg/l. This regression model includes many of the climatological and chemical parameters that were investigated earlier in this report as inputs to the model. Since the parameters often vary more from one water to another than they do within one water, many more parameters are included. The differences that are seen between pans can be accounted for by including this range of parameters. For those regression equations for each process water where only ALK was significant in the regression model compared to the regression model for all waters combined, several other chemical parameters were also found to be significant in prediction of evaporation.

Assessment of Developed Models

A strict level of tolerance (tolerance = $1 - R^2$) between independent parameters was used in the multiple regression analyses so that statistically redundant independent parameters would be excluded from the model. Multicollinearity, however, may still exist between some of the parameters. High multicollinearity can cause inaccuracies in the coefficients of the parameters involved. It is suspected that in the development of these regression models some multicollinearity exists between the chemical parameters and that inaccuracies exist in the coefficients. This hypothesis is based on data showing high correlations between the chemical parameters.

The correlation coefficients, coefficients of determination, and adjusted coefficients of determination for these regression models are shown in Table 34. In statistical terms, R^2 represents the portion of variation in the model which can be explained by the linear regression relationship between the measured evaporation and the regression model. The adjusted R^2 term is adjusted to take into account the degrees of freedom involved. In comparing the R^2 or the adjusted R^2 terms, the values for the regression analysis in Table 34 are generally higher than those for the comparison of models shown in Table 31. The one exception being for the Paraho process water where the estimates using the PML or the Haass methods are more highly correlated with measured evaporation. The estimates using these models are closer to the measured evaporation than the regression model. These results indicate that the regression models may be better estimators of evaporation for the waters concerned than the established existing models.

Table 34. Correlation Coefficients, R^2 , and R^2 Adjusted Values for Regression Models.

Water	Correlation Coefficient	R^2	R^2 Adjusted
Fresh Water	0.791	0.626	0.606
Rio Blanco	0.783	0.614	0.590
Paraho	0.769	0.591	0.573
Geokinetics	0.801	0.642	0.619
All Waters Combined	0.788	0.620	0.606

DIURNAL VARIATION OF EVAPORATION

The diurnal variation of evaporation is important to overall evaporation on a daily basis and will identify during what portion of the day the evaporation rate is the highest. Maximizing the evaporation rate during a given day, for example, by mechanical or electrical input of energy to an evaporation pond when it will produce the maximum benefit should be important to industry as a management practice (also knowing that certain portions of a day are not productive with energy input would be equally as important). A discussion of the analysis of the diurnal variation of oil shale process waters associated with Class A evaporation measurements is presented below along with a model evaluation.

Field Data Utilized in Analysis

Hourly evaporation data for the Rio Blanco, Paraho, and Geokinetic oil shale process waters were carefully reviewed and verified for accuracy and any potential inconsistencies. The data set consisted of hourly evaporation data for 99 days from June 24 (Julian day 175) through September 30 (day 273), 1987. Data beyond September 16 (day 259) were incomplete for some of the process waters leaving an 85-day period of evaporation data available for analysis.

This same 85 day period was used to visually inspect the hourly climatological data (air temperature, solar radiation, relative humidity, etc.). The visual inspection indicated occasional erratic readings in the data set (i.e., air temperature). Elimination of days with missing values and erratic daily climatological data reduced the usable diurnal daily record to 33 days of hourly data. Table 35 gives a listing of the 33 days retained with the total daily evaporation value for the given process water.

Analysis of Meteorological Parameters

The occurrence of erratic readings within the climatological data set on an hourly basis was relatively frequent. The erratic behavior of when these readings occur on an individual climatological parameter made it very difficult to develop a technique for correcting individual hourly values or several hourly values in succession. As a result, days with apparent erratic hourly readings were visually screened and discarded from the usable data set.

Analysis of Pan Evaporation Diurnal Data

Review of the evaporation data indicated errors during hours when the pans were filled and during precipitation events. All such obvious errors were identified and corrected where possible or the data for these hours were shown as missing data. Corrections were based on straight-line interpolation using the data for the hours immediately preceding and following the hour in question. When a series of hours were in error, for example due to precipitation events, then the data were simply shown as missing data. Table 36 gives an example set of data value corrections made showing the initial values and corrected values for each of the three process waters.

Table 35. Usable 33 Days of Hourly Evaporation Data.

Date	Day Number	Evaporation (inches)		
		Rio Blanco	Paraho	Geokinetics
Jun 25	176	0.307	0.28	0.387
Jun 27	178	0.350	0.319	0.364
Jun 28	179	0.258	0.240	0.212
Jul 6	187	0.281	0.275	0.268
Jul 8	189	0.263	0.251	0.253
Jul 16	197	0.272	0.434	0.415
Jul 17	198	0.157	0.190	0.203
Jul 18	199	0.198	0.398	0.397
Jul 19	200	0.261	0.346	0.377
Jul 20	201	0.209	0.233	0.278
Jul 21	202	0.198	0.339	0.356
Jul 23	204	0.193	0.428	0.456
Jul 25	205	0.214	0.361	0.398
Jul 26	206	0.253	0.346	0.298
Jul 27	207	0.169	0.279	0.276
Jul 28	208	0.144	0.215	0.227
Aug 5	217	0.227	0.361	0.360
Aug 6	218	0.186	0.272	0.224
Aug 11	223	0.153	0.221	0.252
Aug 14	226	0.206	0.407	0.394
Aug 17	229	0.137	0.331	0.367
Aug 18	230	0.126	0.322	0.309
Aug 19	231	0.228	0.352	0.351
Aug 20	232	0.149	0.263	0.320
Aug 29	241	0.182	0.303	0.293
Aug 30	242	0.130	0.261	0.241
Sep 3	246	0.131	0.196	0.217
Sep 4	247	0.253	0.317	0.283
Sep 7	250	0.271	0.344	0.266
Sep 9	252	0.150	0.270	0.231
Sep 10	253	0.259	0.278	0.275
Sep 13	256	0.144	0.266	0.296
Sep 14	257	0.111	0.156	0.195

Table 36. Hourly Evaporation Initial and Corrected Values (in cm) for the Three Oil Shale Process Waters.

Julian Day	Hour	Rio Blanco		Paraho		Geokinetics	
		Initial Value	Corrected Value	Initial Value	Corrected Value	Initial Value	Corrected Value
175	8	0.121*	0.026	0.175	0.086	0.150	0.002
175	9	-.999*	0.033	-.999	0.119	-.999	0.002
176	8	0.318	0.021	0.281	0.022	0.214	0.078
176	9	-.999	0.021	-.999	0.022	-.999	0.078
176	10	0.101	0.022	0.128	0.023	0.158	0.078
177	8	0.178	0.005	0.266	0.000	0.287	0.033
178	8	0.226	0.008	0.253	0.000	0.213	0.032
178	9	-.999	0.012	-.999	0.000	-.999	0.016
179	8	0.167	0.030	0.252	0.018	0.299	0.022
179	9	-.999	0.030	-.999	0.018	-.999	0.022
179	10	0.238	0.031	0.216	0.018	0.172	0.023
180	1	0.517	-.999	0.516	-.999	0.524	-.999
180	11	0.749	-.999	0.750	-.999	0.788	-.999
181	9	0.141	0.040	0.141	0.063	0.141	0.010
185	8	-.999	0.039	-.999	0.036	-.999	0.030
186	8	0.235	0.064	0.229	0.037	0.192	0.045
187	8	0.174	0.030	0.170	0.032	-.999	0.038
187	9	-.999	0.015	-.999	0.016	0.156	0.001
188	8	0.277	0.010	0.284	0.001	0.189	0.032
189	8	0.208	0.039	0.218	0.039	-.999	0.000
190	9	-.999	0.017	-.999	0.016	0.217	0.038

*-0.999 indicates a missing value in the data.

Further review of the evaporation data indicated that hour-to-hour, and some day-to-day, inconsistencies were present beyond the above corrections. The most pronounced of these inconsistencies were the low (often zero) readings for the 12:00 o'clock noon hour. Figure 12 shows a sample daily plot for each of the three process waters for Julian Day 230. Figure 13 gives a plot of average evaporation over the 85-day (June 24 through September 16) period indicating the noon hour problem. No logical explanation for the hour-to-hour variations were determined for the data.

In order to reduce the hour-to-hour variations of the evaporation data, 3- and 5-hour running averages were calculated. Multiple linear regressions were later performed for the hourly evaporation versus climatological data with the best results achieved from the 5-hour running averages. Thus, most of the remaining analyses were performed using the 5-hour running averages of the evaporation data.

Visual inspection of the 5-hour running averages and of plots of the evaporation data indicated that the diurnal cycles of the Rio Blanco data often did not follow closely those of the Paraho and Geokinetics data. Overall, the Rio Blanco data had a slightly lower average daily evaporation. In addition, multiple linear regressions between hourly Rio Blanco evaporation and climatological data produced lower correlation coefficients than regressions between either the Paraho or the Geokinetic evaporation and climatological data.

Model Evaluation for Diurnal Variation

Two approaches were used in attempting to develop a predictive equation for hourly evaporation for the various process waters. The Kohler-Nordenson-Fox equation was investigated for its ability to predict hourly evaporation. The equation was then calibrated for each wastewater through calculation of new coefficients. Multiple linear regression equations were also calculated for each process water using hourly air temperature, relative humidity, wind speed, and solar radiation as the independent variables. Both the Kohler-Nordenson-Fox and multiple linear regressions were investigated with and without air temperature and solar radiation data being lagged (shifted) to more accurately represent these parameters with respect to the hourly evaporation data.

The Kohler-Nordenson-Fox equation (Kohler et al., 1958) is the empirical model most widely used for estimating evaporation. The model is an adaptation of the Penman equation for estimating Class A pan evaporation. The complete model is given as:

$$\begin{aligned}
 ES &= 3.377 * \text{EXP}((-7482.6/((1.8 * x1) + 430.36)) + 15.674) \\
 GAMMAP &= .001568 * ((1013-.1093 * 1195) * .0296 * 3.377) \\
 TD &= .556 * (-7482.6/(\text{LOG}(.296 * X2 * ES) - 15.674) - 430.36) \\
 DELTA &= (ES-X2 * ES)/(X1-TD) \\
 UP &= X3 * (.5/2) .2 \\
 RN &= (154.4 * \text{EXP}((1.8 * X1 - 180) * (A1 + A2 * \text{LOG}(.239 * X4)))) + \\
 &\quad A3/DELTA \\
 EA &= 25.4 * ((.296 * (ES-X2 * ES)) .88) * (A4 + A5 * UP) \\
 Y &= ((RN * DELTA) + (EA * GAMMAP))/(DELTA + GAMMAP)
 \end{aligned}$$

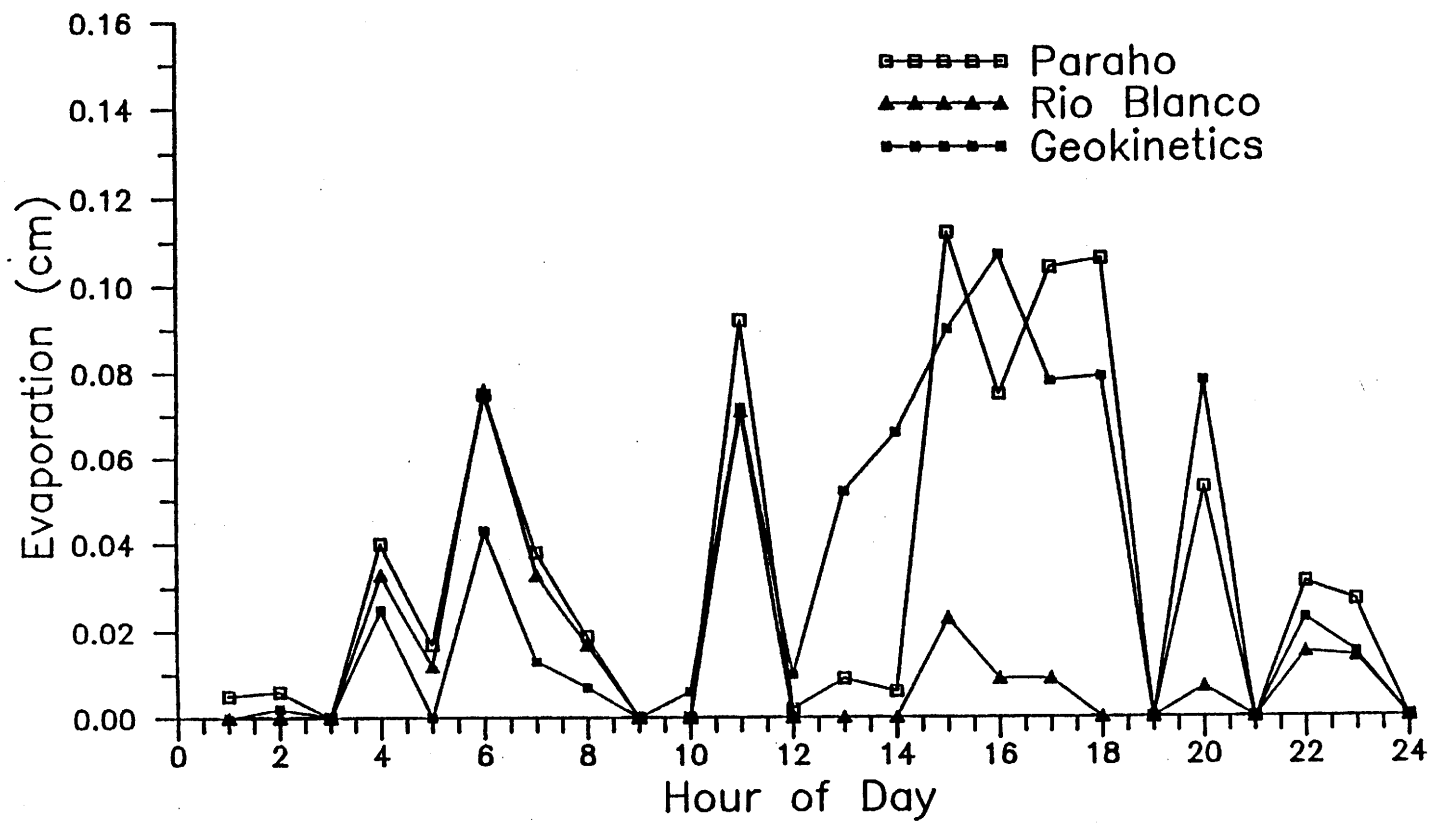
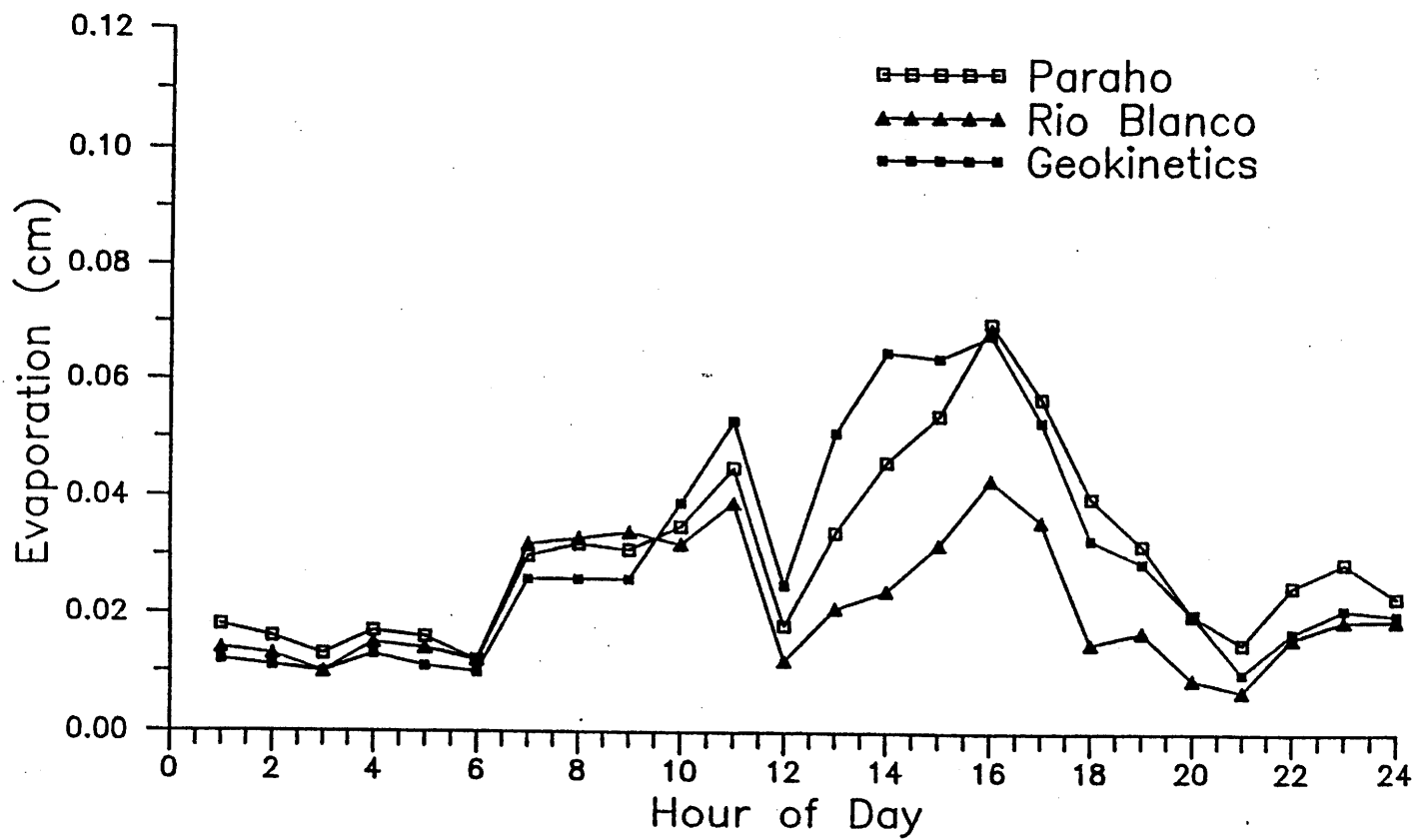


Figure 12. Evaporation data, August 18, 1987 (day 230).

Figure 13. Overall averages of evaporation data, June 24-September 16, 1987 (days 175-259).



where Y is pan evaporation in mm/h, ES is the saturated vapor pressure in KPa, GAMMAP is the psychrometric constant in KPa/°C, DELTA is the slope of the saturation vapor pressure versus temperature curve at the air temperature in KPa/°C, TD is the dew point temperature in °C, UP is the wind run at pan height in km for an hour, RN is the net radiation for a pan in units of equivalent depth of evaporation in mm/h, EA is an aerodynamic function also in units of mm/h, X1 is air temperature in °C, X2 is relative humidity expressed as a decimal, X3 is wind run at a height of two meters in km/h, X4 is the solar radiation in J/cm²h, and A1, A2, A3, A4, and A5 are empirical coefficients.

For calculation of daily evaporation, values and units for evaporation, wind run, solar radiation, heat radiation, and the aerodynamic term are used in units of days rather than hours. Thus, in SI units the values of the five empirical coefficients as given by Kohler-Nordenson-Fox were:

A1 = 0.1024
A2 = -0.01066
A3 = -0.01544
A4 = 0.37
A5 = 0.00255

A difficulty arises in using the equation for hourly data. In particular, conversion of hourly solar radiation to an equivalent radiation on a daily basis results in very large radiation values for the mid-day hours. As shown later, recalibration of the equation for hourly data was found to be necessary.

The Texas Tech computer program MERV was used for calibration of the Kohler-Nordenson-Fox equation. MERV is a computer program for analyzing both linear and nonlinear functions and provides estimates of unknown coefficients, 95 percent confidence ranges for those coefficients, R² values for goodness of fit measures, and the significance of the fit with and without data clustering.

MERV is capable of estimating up to five unknown coefficients, while the Kohler-Nordenson-Fox contains six empirical coefficients. These include three each in the net radiation and aerodynamic terms. The three in the aerodynamic term include two coefficients in the wind function and a third coefficient as an exponent on the vapor pressure deficit term. The calibration approach selected was to estimate new coefficients for the radiation term and the wind function. Calibration was performed both with and without a 0.88 exponent on the vapor pressure deficit. The five empirical coefficients are shown above in the model as A1 through A5.

MERV will permit a sample size of up to 100 data sets. Thus, calibration was limited to the use of four days of hourly data which provided a sample size of 96. The 4 days used were selected more or less at random from the 33 days retained but with some consideration to selecting days spaced so as to represent the entire measurement period. This selection process resulted in days 178 (July 27), 205 (July 25), 230 (August 18), and 256 (September 13)

being selected initially for calibration of the Kohler-Nordenson-Fox equation. Further inspection of the data, and performance of the calibration process, indicated that the Rio Blanco evaporation data for each of these four days were inconsistent with reasonable diurnal cycles. Thus, four other days were selected for the Rio Blanco process water. These included days 176 (July 25), 199 (July 18), 223 (August 11), and 247 (September 4).

The multiple linear regressions were performed using MINITAB. Regressions were performed for both the selected 4-day data sets and for the entire 33-day data set. The analyses on the 33-day data set, using Paraho data, was used to identify the effect of lagging either or both air temperature and solar radiation with respect to the hourly evaporation. Lags from one to four hours were investigated.

Discussion of Results

In an attempt to verify the overall accuracy of evaporation measurements and/or estimates, measured and estimated seasonal values were compared as shown in Table 37. Daily estimates using the Kohler-Nordenson-Fox equation, without calibration, were calculated (a) using daily averages or totals of the climatological data and (b) by summing the hourly estimates for each day. These totals are compared with both the evaporation from the three process waters for the 33-day record and from a fresh water evaporation pan for a 22-day record.

The 22-day averages from the Kohler-Nordenson-Fox estimates using daily data and the fresh water evaporation are nearly the same (0.361 inches per day versus 0.362 inches per day). On the other hand, the estimates using the sum of hourly Kohler-Nordenson-Fox estimates are much higher than pan evaporation. This depicts the problems in using the Kohler-Nordenson-Fox equation in its original form for estimating hourly evaporation rates. Comparison of actual process water evaporation rates shows that for both the 22-day and 33-day records, the Rio Blanco average evaporation was lower than the Paraho and Geokinetic averages. Estimated evaporation using daily data averaged approximately 10 to 15 percent higher than measured Paraho and Geokinetic evaporation. In general, the Rio Blanco average from this data set seems low.

The first approach to calibrating the Kohler-Nordenson-Fox equation was to calculate hourly ratios between measured process water evaporation and estimated evaporation. The intent of this approach was to develop correction coefficients which would vary during the day much in the same manner that crop coefficients are used for predicting crop water use from a reference evapotranspiration estimate. Crop coefficients vary during a season, accounting for changes in crop conditions.

The diurnal ranges of the calculated ratios for the various process waters were much greater than would be acceptable. The average ratios, using a 29-day period of record--that is, the 33-day record minus the 4 days later used for the multiple linear regressions and model calibrations are shown in Table 38. In general, this approach was not successful in calibrating the Kohler-Nordenson-Fox equation for estimating hourly evaporation from the process waters.

Table 37. Comparison of Measured and Estimated Evaporation.

Date	Day Number	Process Water Evap			Estimated Evap**		Fresh Water Evap
		RB	PR	GK	Daily	Summed	
Jun 25	176	0.307	0.280	0.387	0.389	0.566	--
Jun 27	178	0.350	0.319	0.364	0.464	0.722	0.38
Jun 28	179	0.258	0.240	0.212	0.302	0.461	0.38
Jul 6	187	0.281	0.275	0.268	0.310	0.485	0.28
Jul 8	189	0.263	0.251	0.253	0.284	0.505	0.33
Jul 16	197	0.272	0.434	0.415	0.392	0.633	0.35
Jul 17	198	0.157	0.190	0.203	0.246	0.401	0.30
Jul 18	199	0.198	0.398	0.397	0.444	0.661	0.23
Jul 19	200	0.261	0.346	0.377	0.438	0.721	0.41
Jul 20	201	0.209	0.233	0.278	0.341	0.610	0.42
Jul 21	202	0.198	0.339	0.356	0.364	0.622	0.34
Jul 23	204	0.193	0.428	0.456	0.508	0.830	0.37
Jul 25	205	0.214	0.361	0.398	0.529	0.813	0.49
Jul 26	206	0.253	0.346	0.298	0.373	0.566	0.44
Jul 27	207	0.169	0.279	0.276	0.307	0.468	0.28
Jul 28	208	0.144	0.215	0.227	0.229	0.358	0.29
Aug 5	217	0.227	0.361	0.360	0.370	0.604	0.36
Aug 11	223	0.153	0.221	0.252	0.267	0.430	0.37
Aug 14	226	0.206	0.407	0.394	0.350	0.549	0.21
Aug 17	229	0.137	0.331	0.367	0.409	0.704	0.60
Aug 18	230	0.126	0.322	0.309	0.379	0.662	0.44
Aug 19	231	0.228	0.352	0.351	0.405	0.708	0.36
Aug 20	232	0.149	0.263	0.320	0.309	0.461	--
Aug 29	241	0.182	0.303	0.293	0.328	0.556	--
Aug 30	242	0.130	0.261	0.241	0.246	0.419	--
Sep 3	246	0.131	0.196	0.217	0.266	0.374	--
Sep 4	247	0.253	0.317	0.283	0.166	0.259	--
Sep 7	250	0.271	0.344	0.266	0.165	0.271	--
Sep 9	252	0.150	0.270	0.231	0.288	0.465	--
Sep 10	253	0.259	0.278	0.275	0.165	0.306	--
Sep 13	256	0.144	0.266	0.296	0.252	0.425	--
Sep 14	257	0.111	0.156	0.195	0.239	0.367	--
<hr/>							
Avgs.: n = 22		0.213	0.315	0.320	0.361	0.585	0.362
n = 38		0.205	0.299	0.304	0.326	0.525	--

* All values are in units of inches.

** Estimated evaporation is from the Kohler-Nordenson-Fox model.
Daily used daily climatological data while summed used the sum of
hourly

Note: RB = Rio Blanco, PR = Paraho, GK = Geokinetics.

Table 38. Ratios of Measured Evaporation vs. Kohler-Nordenson-Fox
Estimates*.

Hour	Rio Blanco	Paraho	Geokinetics
0100	1.704	2.309	1.550
0200	2.226	2.586	1.742
0300	2.733	3.274	2.229
0400	2.999	3.474	2.405
0500	5.355	4.813	3.859
0600	8.351	6.134	5.209
0700	7.621	6.047	5.145
0800	2.911	2.762	2.586
0900	1.209	1.215	1.273
1000	0.577	0.617	0.683
1100	0.358	0.394	0.503
1200	0.228	0.292	0.406
1300	0.170	0.268	0.363
1400	0.149	0.305	0.369
1500	0.157	0.525	0.576
1600	0.246	0.643	0.698
1700	0.330	0.651	0.635
1800	0.354	0.720	0.654
1900	0.459	0.912	0.791
2000	0.564	1.215	0.981
2100	0.870	1.659	1.267
2200	1.161	2.171	1.570
2300	1.313	2.229	1.456
2400	1.489	2.217	1.530

* Estimates are from the uncalibrated Kohler-Nordenson-Fox equation. The evaporation data used was that from the 5-hour running averages. All ratios are averages for the 29-day record.

The results of the calibration of the Kohler-Nordenson-Fox equation using MERV are shown in Table 39. Results are shown for each of the process waters for calibrations with and without the vapor pressure deficit exponent and with and without the radiation data lagged two hours with respect to evaporation. The 2-hour lag was determined from a multiple linear regression analysis to be discussed later.

The Kohler-Nordenson-Fox equation was calibrated with evaporation in units of mm/h, meaning other parameters such as radiation were also on an hourly basis. As mentioned above, the Kohler-Nordenson-Fox equation as normally presented requires daily units.

The coefficients of determination for the various calibrations of the Kohler-Nordenson-Fox equation using MERV were generally in the range of 0.5 or greater for the Paraho and Geokinetic wastewaters. However, the coefficients of determination were low for all calibrations using Rio Blanco data. The coefficients of determination were, in general, slightly higher when the 0.88 exponent for the vapor pressure deficit term of the Kohler-Nordenson-Fox equation was omitted as compared to when it was included. The differences, however, were small. Lagging solar radiation two hours improved the results for the Paraho data but decreased the coefficients of determination for regressions using the Geokinetics data.

The calibrated Kohler-Nordenson-Fox equations for the three process waters were used to estimate hourly evaporation for each of the 29 days not used to develop the calibrations. The calibrated equations were the ones without a solar radiation lag and with the 0.88 exponent on the vapor pressure deficit term. The resulting hourly evaporation estimates were then used to calculate average ratios of measured to estimated hourly evaporation, as shown in Table 40. As compared to the previous ratios, which had been calculated using the uncalibrated Kohler-Nordenson-Fox equation, the current ratios were more reasonable. Although calibrations based on four days of data do not produce equations which will predict average diurnal cycles perfectly, the results using the calibrated equations are a great improvement over those using the uncalibrated equation.

Linear and multiple linear regressions of evaporation versus air temperature, relative humidity, wind speed at two meters, and solar radiation were performed for the selected 4 days and for the 33 days of hourly data. Regressions were performed to determine the effects of lagging air temperature and/or solar radiation with respect to evaporation and of smoothing the evaporation data with 3-hour and 5-hour running averages. Results are shown in Tables 41 and 42 for the 33 days and 4 days, respectively.

Regressions were initially performed on the 33 days of hourly Paraho data. The correlations between evaporation and climatological data were very low when hourly evaporation data were used without any smoothing. Use of 3-hour running averages for the evaporation data improved the results somewhat, while use of 5-hour running averages produced the best results. However, even with the use of 5-hour running averages, the coefficients of determination were low, ranging in magnitude to slightly above 0.400.

Table 39. Results of MERV calibration of the Kohler-Nordenson-Fox Equation.

Retort Water	Coefficients					R^2
	A1	A2	A3	A4	A5	
Rio Blanco ¹	.326005	-.056732	.030100	.014158	.000490	.079
Paraho	.230889	-.036458	.030346	.014415	.001223	.486
Geokinetics	.174310	-.025880	.036797	.009321	.001273	.601
Rio Blanco ²	.354216	-.063117	.020449	.018787	.000232	.084
Paraho	.281405	-.047053	.032429	.015014	.001252	.492
Geokinetics	.172644	-.025322	.038071	.009572	.001342	.606
Rio Blanco ³	.344734	-.063147	.026415	.018259	.000246	.131
Paraho	.285655	-.048844	.029305	.015802	.001121	.505
Geokinetics	.251628	-.041274	.020818	.029955	.000366	.562
Rio Blanco ⁴	.352019	-.064669	.027884	.021761	.00035	.128
Paraho	.340275	-.060920	.032715	.014752	.001219	.511
Geokinetics	.202671	-.030919	.030335	.021247	.000799	.572

¹No radiation lag and with the exponent on the vapor term.

²No radiation lag and w/o the exponent on the vapor term.

³Radiation lagged two hours and with the exponent on the vapor term.

⁴Radiation lagged two hours and w/o the exponent on the vapor term.

Table 40. Ratios of Measured Evaporation vs. Calibrated KNF Estimates*.

Hour	Rio Blanco	Paraho	Geokinetics
0100	0.699	0.888	0.575
0200	0.687	0.841	0.540
0300	0.795	0.958	0.609
0400	0.776	0.887	0.569
0500	1.268	1.171	0.836
0600	1.571	1.343	1.012
0700	1.803	1.431	1.091
0800	1.795	1.488	1.309
0900	1.824	1.512	1.523
1000	1.359	1.243	1.313
1100	1.110	1.113	1.275
1200	0.898	1.015	1.193
1300	0.754	0.964	1.118
1400	0.672	1.034	1.087
1500	0.680	1.152	1.223
1600	0.674	1.269	1.269
1700	0.681	1.191	1.139
1800	0.620	1.109	1.025
1900	0.531	0.965	0.868
2000	0.488	0.909	0.760
2100	0.535	0.886	0.705
2200	0.555	0.881	0.643
2300	0.627	0.893	0.580
2400	0.689	0.917	0.610

*Calibrations used to calculate these ratios are the ones with no solar radiation lags and with the 0.88 exponent on the vapor pressure term. The evaporation data used was that from the 5-hour running averages. All ratios are averages for the 29-day record.

Table 41. Results of Regressions of Evaporation vs. Climatological Data
for 33 days*

Description of Regression and Equation	R ²
Paraho data w/o any smoothing and no time lags	
E = .00511 + .001511TA	.068
E = .05147 - .000409RH	.052
E = .01177 + .002016U2	.096
E = .02243 + .000106RS	.096
E = -.00459 + .000270TA + .000172RH + .00159U2 + .000083RS	.139
Paraho 3-hr running avg data and no time lags	
E = .00623 + .00145TA	.171
E = .05214 - .00042RH	.151
E = .01442 + .00175U2	.197
E = .02343 + .000095RS	.212
E = .00800 + .000277TA + .000027RH + .00119U2 + .000062RS	.294
Paraho 3-hr running avg data with 1-hr lags on TA and RS	
E = .00915 + .00129TA	.137
E = .02292 + .00010RS	.236
E = .0127 - .000081TA + .000038RH + .00115U2 + .000081RS	.294
Paraho 3-hr running avg data with 2-hr lags on TA and RS	
E = .0122 + .00121TA	.103
E = .0231 + .000098RS	.225
E = .0199 - .000327TA - .000014RH + .00112U2 + .000080RS	.282
Paraho 3-hr running avg data with 3-hr lags on TA and RS	
E = .0149 + .000973TA	.078
E = .0230 + .000099RS	.233
E = .0241 - .000522TA - .000029RH + .00104U2 + .000088RS	.290
Paraho 3-hr running avg data with 4-hr lags on TA and RS	
E = .0202 + .000679TA	.037
E = .0242 + .000086RS	.176
E = .0314 - .000661TA - .000109RH + .00109U2 + .000072RS	.269

Table 41. Results of Regressions of Evaporation vs. Climatological Data
for 33 days* (cont.)

Description of Regression and Equation	R^2
Paraho 5-hr running avg data and no time lags	
$E = .0068 + .001419TA$.261
$E = .0522 - .000423RH$.244
$E = .0169 + .001518U2$.234
$E = .0239 + .000091RS$.308
$E = .0141 + .000317TA - .000032RH + .000868U2 + .000056RS$.399
Paraho 5-hr running avg data with 1-hr lags on TA and RS	
$E = .00866 + .00132TA$.228
$E = .02319 + .000098RS$.359
$E = .01507 + .000085TA + .000010RH + .00803U2 + .000076RS$.410
Paraho 5-hr running avg data with 2-hr lags on TA and RS	
$E = .0122 + .00113TA$.166
$E = .0231 + .000098RS$.363
$E = .0233 - .000288TA - .000034RH + .000768U2 + .000085RS$.407
Paraho 5-hr running avg data with 3-hr lags on TA and RS	
$E = .0165 + .000888TA$.103
$E = .0238 + .000091RS$.308
$E = .0325 - .000516TA - .000121RH + .000761U2 + .000075RS$.379
Paraho 5-hr running avg data with 4-hr lags on TA and RS	
$E = .0208 + .000648TA$.054
$E = .0248 + .000081RS$.245
$E = .0371 - .000600TA - .000171RH + .000786U2 + .000064RS$.360

*All regressions were conducted for Paraho wastewater.

TA - air temperature, °C.

RH - relative humidity expressed as a percentage.

U2 - wind speed at 2 meters, km/h.

RS - solar radiation, J per cm^2/h .

Table 42. Results of Regressions of Evaporation vs. Climatological Data
for 4 days*

Description of Regression and Equation	R ²
Rio Blanco data w/o any lagging of climatic data	
E = -.00369 + .001558TA	.200
E = .03991 - .000317RH	.113
E = .01200 + .001018U2	.119
E = .01706 + .0000676RS	.216
E = -.0056 + .000858TA + .000110RH + .000395U2 + .000041RS	.227
Rio Blanco data with the radiation data lagged 2 hours	
E = .01551 + .00008R4RS	.339
E = -.0186 + .000588TA + .000353RH + .000378UW + .000098RS	.365
Rio Blanco data w/o any lagging of climatic data	
E = .01066 + .000665TA	.057
E = .02324 - .0000036RH	.000
E = .02990 + .000646U2	.018
E = .01750 + .000053RS	.101
E = -.0066 + .00114TA + .000321RH - .000875U2 + .000049RS	.220
Rio Blanco data with the radiation data lagged 2 hours	
E = .01970 + .000032RS	.031
E = -.0102 + .00137TA + .000366RH - .000995U2 + .000039RS	.194
Paraho data w/o any lagging of climatic data	
E = .00574 + .001543TA	.409
E = .05196 - .000449RH	.325
E = .01938 + .001447U2	.156
E = .02475 + .000094RS	.390
E = .0141 + .000646TA - .000056RH + .000482U2 + .000053RS	.471
Paraho data with the radiation data lagged 2 hours	
E = .02325 + .000108RS	.521
E = .00726 + .000536TA + .000100RH + .000386U2 + .000090RS	.530

Table 42. Results of Regressions of Evaporation vs. Climatological Data
for 4 days* (cont.)

Description of Regression and Equation	R^2
Geokinetics data w/o any lagging of climatic data	
$E = .00043 + .001944TA$.499
$E = .05903 - .000575RH$.409
$E = .02243 + .001367U2$.103
$E = .02200 + .000141RS$.681
$E = .0264 + .000301TA - .000163RH - .00038U2 + .000110RS$.712
Geokinetics data with the radiation data lagged 2 hours	
$E = .02267 + .000135RS$.620
$E = .0173 + .000676TA - .000023RH - .000295U2 + .000104RS$.634

*Two sets of days were used. The first Rio Blanco results are for days 176, 199, 223, and 247. All remaining results are for days 178, 205, 230 and 256.

TA = air temperature, °C
 RH = relative humidity, in percent
 U2 = wind speed at 2 meters, km/h
 RS = solar radiation, j per cm²/h

Lagging air temperature one or more hours did not improve any of the results. The relationship between evaporation and solar radiation was best when solar radiation was lagged 1-hour for the 3-hour running averages and two hours for the 5-hour running averages of evaporation data. For the 4-day sample of hourly data (Table 42), the Geokinetics data did not seem to follow this trend. In the case of the Paraho evaporation data, when solar radiation was lagged more than two hours with respect to evaporation the coefficients of determination were decreased.

The most striking results from the regressions of evaporation versus climatological data for the four days of hourly data are the poor results for the Rio Blanco data as compared to the results for the Paraho and Geokinetics data. Two 4-day samples were selected for the Rio Blanco process water, with the results from the second set only slightly better than from the original 4-day sample. Other observations indicate that wind speed at two meters seemed to have little correlation with evaporation, as compared to the relations between evaporation and air temperature, relative humidity, and solar radiation. Lagging solar radiation two hours with respect to evaporation improved the results for the regressions of evaporation versus climatological data for the Paraho and Rio Blanco (when using the second 4-day sample for Rio Blanco) data but decreased the coefficients of determination for the Geokinetics evaporation versus solar radiation.

The coefficients of determination for the multiple linear regressions of evaporation versus air temperature, relative humidity, wind speed at two meters, and solar radiation were nearly the same to slightly higher in magnitude than the coefficients of determination from the calibration of the Kohler-Nordenson-Fox equation.

Calibration of the Kohler-Nordenson-Fox equation for estimating hourly evaporation were completed with the use of the Texas Tech program MERV. The results of the calibration were nearly as good as multiple linear regressions of evaporation versus climatological data. Use of the Kohler-Nordenson-Fox equation would likely be preferred to multiple linear regressions since empirical formulas are generally considered to be more transferable to other locations than are regression equations.

The multiple linear regressions and Kohler-Nordenson-Fox calibrations both considered the effects of lagging air temperature and/or solar radiation with respect to evaporation. No improvements in the results were found from lagging air temperature while lagging solar radiation one or two hours with respect to evaporation generally improved the predictions slightly.

Because of the limitations of the MERV program, calibrations of the Kohler-Nordenson-Fox equation were limited to the use of a sample size of four days of hourly data. It would likely be desirable to modify MERV to allow use of a larger data sample.

The results herein of the Kohler-Nordenson-Fox calibrations and multiple linear regressions for hourly data are at least as good or better than the results of multiple regressions for daily data presented in previous sections of this report.

CHEMICAL COMPOSITION AND RATE OF EMISSIONS FROM OIL SHALE PROCESS WATERS

A significant concern with respect to oil shale process water evaporation ponds is the quantity and composition of organic, inorganic and/or hazardous compound emissions, that may be being released. Research (Hawthorne, 1984) has determined a broad spectrum of compounds that may be being released from oil shale process waters but little is known about the rate at which these compounds are emitted.

Laboratory and field experiments were developed in this research to determine the chemical composition of emissions and their rate of emission from oil shale process waters.

CHEMICAL COMPOSITION OF EMISSIONS

Both laboratory and field experiments were developed to obtain as broad a chemical composition analysis of emissions from oil shale process waters as possible. In addition, a select group of these identified chemical compounds that exhibited high values were characterized in more detail.

Methodology

Analysis of emissions were investigated using two different methods of analysis both in the laboratory and field. One method was to use a Miran 1B ambient air analyzer to measure types of chemical compounds being emitted and the rate of emission of these compounds. The second method was to obtain samples of the process waters and obtain specific gas emission samples from the samples. Specific organic and inorganic emissions of the gas samples were analyzed using inductively coupled plasma (ICP) for trace metals and gas chromatography/mass spectrometry (GC/MS) for a variety of organic compounds.

The laboratory experiments with the Miran 1B ambient air analyzer utilized the same sealed box container used with the chemical composition studies effects on evaporation rates discussed earlier in this report. A sealed hole port into the box was used to extend the sampling device into the box. The Miran 1B would collect (by pumping) an air sample from the sealed box to the analyzer. Each compound analyzed for the Miran 1B required an additional air sample taken from the box.

Chemical Composition of Process Waters

Tables 2, 24 and 25 show results of the chemical analyses performed on the three oil shale process waters studied during 1985 and 1986. Not all chemical compounds found from the analyses are listed in the tables but only those felt to be of significance in defining the range of chemical compounds in process waters. The EPA 624 and 625 analyses resulted in the list of chemical compounds shown in Table 26. Of 103 organic compounds included in the two analyses, Table 26 indicates those that were detectable by the equipment. Table 27 and Figure 6 also give results on the chemical composition of the three process waters.

Chemical Emissions Detected

Laboratory experiments were conducted using the environmentally sealed box which contained mini evaporation pans filled with Geokinetics process water. Field experiments were also conducted on the three process water Class A evaporation pans. The compounds identified by the Miran 1B in the sealed box included acetophenone, acrylonitrile, ammonia, aniline, benzene, butane, creosol, cyclopentane, p-Dichlorobenzene, diethylamine, dimethylacetamide, dimethylamine, ethanolamine, hydrogen cyanide, methylamine, methyl mercaptan, nitrobenzene, phosgene, pyridine and sulfur dioxide. These were the compounds that were over the concentration limit of the Miran 1B. However, nearly every compound analyzed for with the Miran 1B was found in the sealed box.

A number of problems prevented the continued use of the Miran 1B in the laboratory and in the field. First, the Miran 1B contained a battery pack which theoretically provided a discharge time of four hours. This was not a problem in the laboratory where the Miran 1B could be operated with electricity. However, each time the Miran 1B was operated in the field, the battery pack power would completely discharge before one hour of use. Since the time to analyze just one compound requires seven minutes with the Miran 1B, this did not allow for the analysis of more than a few compounds in the field at any one time (recharge time for the battery pack was 14 to 16 hours).

As previously stated, the time to sample for one compound with the Miran 1B was seven minutes. It would, therefore, take more than two hours to analyze for just 20 compounds. During these two hours, many parameters affecting the emissions could change which was another real problem. In the sealed box, the Miran 1B would pump air through the sealed porthole of the box for the collection of each compound analyzed. This means that the volume of air in the sealed box was constantly changing which caused further problems with justifying any use of the Miran 1B and its data. In the field the temperature or wind speed would change frequently. It was extremely difficult to even try to determine emissions and rate of emissions with these continually changing conditions, both in the laboratory and field.

The Miran 1B was cumbersome to use in the field because it required a horizontal position to operate during analysis of the compounds. This means that the instrument could not be carried and analyses performed easily at just any location. It was also difficult to establish a "point source" for the compounds when the wind was blowing.

This instrument (Miran 1B) and approach were abandoned after several attempts. The technique would probably work if only one or two known compounds of interest were to be analyzed. However, it was desired in this research to obtain emissions of as many compounds as possible.

The qualitative analysis using ICP and GC/MS showed that the primary compounds found in the Geokinetics and Paraho process waters are pyridines, including pyridine, dimethyl pyridines and trimethyl pyridines. Some short chain alkanes such as hexane were found, along with ketones such as 2-pentanone, 2-hexanone and cyclohexanone. Aromatics are also prominent groups found in these process waters. Table 43 contains a list of compounds found in these two process waters. This list is not complete because the WRI

Table 43. Compounds Found in Paraho and Geokinetics Process Waters.

Compound	Paraho	Geokinetics
benzene	yes	yes
bromodichloromethane	no	yes
bromoform	no	yes
butane	no	yes
cyclohexanone	no	yes
1, 1-dichloroethane	yes	no
1, 2-dichloroethane	yes	no
1, 2-dichloropropane	no	yes
cis-1, 3-dichloropropene	no	yes
2, 2-dimethyl cyclopentanone	no	yes
2, 3-dimethylpyridine	yes	no
2, 4-dimethylpyridine	yes	no
2, 6-dimethylpyridine	no	yes
2-ethyl-4, 6-dimethylpyridine	yes	no
2-ethyl-6-methylpyridine	yes	no
2-ethyl-5-dimethylpyridine	yes	no
2-ethylpyridine	yes	yes
hexane	yes	no
2-hexanone	no	yes
hexene	no	yes
3-methyl-2-butanone	no	yes
methyl cyclopentane	yes	no
methylene chloride	yes	yes
4-methyl-2-pentanone	no	yes
2-methylpyridine	yes	yes
3-methylpyridine	yes	no
2-pentanone	no	yes
pentene	no	yes
pyridine	yes	yes
toluene	yes	yes
1,1,1-trichloroethane	yes	yes
3,3,5-trimethylcyclohexanone	yes	no
2,3,6-trimethylpyridine	yes	no

laboratory analysis did not look for carboxylic acids or phenols, and many of the peaks on the mass spectrometer were not identified.

CONCENTRATION (RATE) OF SELECTED EMISSIONS BEING RELEASED

Chemical compounds found in process waters generally have high vapor pressures and low water solubilities indicating a potential for high volatilization rates from the process water into the atmosphere (Hawthorne, 1984). Because a disposal practice for process waters is the use of evaporation ponds, the rate of emissions of the volatile compounds from the process water into the atmosphere should be important for human health and other reasons. These rates can be either measured or estimated using mathematical models. All of the models reviewed for estimation purposes, however, require a knowledge of the Henry's law constant (HLC) for each compound. Therefore, in determining emission rates, the Henry's law constants must be either measured or estimated. Henry's law constants for oil shale process waters is a relative unknown.

A study was designed to measure HLC values of selected compounds in two of the three process waters used in this project at three typical environmental temperatures to hopefully allow for estimation of emission rates of these compounds.

Henry's Law

In 1803, William Henry observed that the solubility of a gas in a liquid was directly proportional to its gas phase partial pressure (Lincoff and Gossett, 1984; Prausnitz, 1969). This relationship can be shown mathematically as

$$P = H C_w \quad (31)$$

where P is the partial pressure (atm), C_w is the concentration of an individual gas in water (mol/m^3), and H is the HLC ($\text{atm m}^3/\text{mol}$) (Mackay and Shiu, 1984).

Often a dimensionless HLC is used, and this can be obtained by dividing the H by RT as in the following equation:

$$C_g/C_w = H/RT = K_{aw} \quad (32)$$

where C_g is the concentration in the air (mol/m^3), R is the gas constant ($8.206 \times 10^{-5} \text{ atm m}^3/\text{gmol/K}$), T is the absolute temperature (K), and K_{aw} is the dimensionless HLC (Mackay and Shiu, 1984). The distribution coefficient is often referred to in the literature, and it can be obtained by taking the inverse of the dimensionless HLC.

The HLC for a given system is highly dependent on temperature and moderately dependent on ionic strength (Munz and Roberts, 1986; McAullife, 1971; Gossett, 1987). Each system has unique Henry's law constants since other

components in the gas-solvent system could affect the solubility and vapor pressure of a compound. Yurteri, et al. (1987) measured HLC values for trichloroethylene and toluene in pure water and in a complex mixture of salts and humic materials. They found that the salts and humic substances caused the HLC values in the complex mixture to vary as much as 35 percent from values obtained in pure water. They also found that this matrix effect cannot be modeled by physical or chemical parameters in the water because they did not produce consistent effects.

Experimental Laboratory Methodology

The two process waters studied were Geokinetics and Paraho. An independent laboratory with a gas chromatograph/mass spectrometer (GC/MS) was employed to perform qualitative analyses on these waters. These analyses allowed a number of representative compounds found in either one or both of the waters to be chosen for study (Table 43).

Preliminary tests on the Geokinetics and Paraho waters indicated that these waters were not concentrated enough to allow accurate headspace analysis (described later) at typical environmental temperatures. For this reason, ten organic compounds were chosen for study, and they are shown in Table 44. These compounds were chosen primarily to measure the HLC of different organic compounds which were found in these waters. It was also of interest to determine if any matrix effect would be observed with the process waters on these compounds, so the HLC values for these compounds were also measured in distilled water.

Table 44. Organic Compounds Studied.*

Compound	Purity (%)
benzene	99.9 ⁺
cyclohexanone	99.8 ⁺
2, 6-dimethylphenol	99.8 ⁺
2-hexanone	99 ⁺
1-hexene	99 ⁺
2-pentanone	97
phenol	99 ⁺
pyridine	99.9 ⁺
toluene	99 ⁺
hexane	unknown

* All compounds obtained from Aldrich Chemical Co.

Three different aqueous standard mixtures were prepared to be used in each method in determining Henry's law constants. Table 45 shows the contents of each mixture.

The process waters were initially stored in polyethylene lined drums at 4°C until samples were needed. A recirculating pump was then placed on the drum to stir the water. After 24 hours of recirculating, five gallons of the process water were withdrawn and stored in a Nalgene polyethylene container at 4°C. The reason for this transfer was because it was easier and more convenient to get smaller samples from the five gallon containers, and they could be rolled around gently to stir them before withdrawing samples. The stirring was performed to obtain more uniform and representative samples.

All of the methods used to measure Henry's law constants utilized gas chromatography to quantify the compounds in the gas phase. Headspace concentration of the compounds in equilibrated vessels were measured using a Hewlett Packard 5790A series gas chromatograph equipped with a flame ionized detector

Table 45. Aqueous Standard Mixtures

Mixture No.	Compound	Weight (mg)
1 ^a	benzene	1
	toluene	1
	pyridine	980
2 ^b	1-hexene	14
	2-pentanone	24
	2-hexanone	24
	cyclohexanone	94
3 ^c	phenol	692
	2,6-dimethylphenol	681

^a mixture 1 was diluted to 10 ml with distilled water.

^b mixture 2 was diluted to 12 ml with 6 ml distilled water and 6 ml methanol.

^c mixture 3 was diluted to 10 ml with 5 ml methanol and 5 ml distilled water.

(GC/FID). A Hewlett Packard 3390A integrator was coupled with this system to perform integrations and output the results. A sixty meter SPB-5 wide bore capillary column was used for compound separation. The helium flow through the column was 15 ml/minute and the make-up flow was also 15 ml/minute. The hydrogen and air flows in the FID were 40 and 400 ml/minute, respectively. The injector temperature was 200°C; detector temperature 270°C; and the gas sampling valve temperature 150°C. The gas sampling valve was equipped with a one-milliliter sample loop. The following temperature program was used: 40°C (five minutes), 6°C/minute to 145°C (no hold).

To obtain a gas sample, a 10 ml gas-tight syringe with a push button valve was used to withdraw a 10-ml headspace sample. The needle was inserted through the bottle cap septum, 10 ml withdrawn, and the push-button valve closed before pulling the needle out of the bottle. The 10 ml sample was then injected into the sample loop of the gas sampling valve by quickly opening the syringe valve and depressing the plunger. The 10 ml volume was used to flush the sample loop and inject 1 ml of the sample into the column.

Three methods were used to measure the Henry's law constants of the compounds of interest. A complete review of not only the methods used here but also other available methods that have been performed are contained in Vassar (1988). The three methods chosen were 1) multiple equilibration (McAullife, 1971), 2) modified equilibrium partitioning in closed systems (EPICS) (Gossett, 1987), and 3) fixed volume solvent addition (Ioffe and Vitenberg, 1984). Each of these methods is briefly described below.

The method used for the compounds with K_{aw} values greater than 0.02 was the multiple equilibration technique. Two hundred milliliters (ml) of the water was placed in a 240 ml sample bottle, and 5 microliters of 1-hexene added. One hundred microliters of mixture number 1 was also added to check the accuracy of the method with the benzene and toluene HLC values.

After the sample bottle was stirred, 40 ml of the water placed in a 100 ml gas-tight syringe. Forty milliliters of helium was then added, and the syringe was shaken for 20 seconds. The syringes were then placed in a constant temperature shaker bath and allowed to equilibrate for at least thirty minutes.

A gas sample bottle was then withdrawn from the 100 ml syringe with a 10 ml gas-tight syringe via a 1/3-inch length of Teflon tubing connected between the two syringes. Each syringe had a valve that could be opened or closed to allow or prevent the movement of the gas sample out of the syringe. The 10 ml sample was injected into the gas sampling valve as with the headspace analysis described earlier.

The remaining gas in the 100 ml syringe was dispensed, and another 40 ml of helium drawn into the syringe. (If any liquid happened to be lost when displacing the gas, the amount of helium introduced should equal the amount of liquid left in the syringe to insure a liquid to gas ratio of one.) This procedure was repeated for four equilibrations. A set of four multiple equilibration tests was performed for each water and at each temperature.

The following equation applies to this method (McAullife, 1971):

$$\log C_{g_n} = a n_e + b \quad (33)$$

where $a = -\log(K_{aw}(V_L/V_g) + 1)$

$b = \log(K_{aw} C_o V_L/V_g)$

and $K_{aw} = (10^{-a} - 1) (V_L/V_g)$

with C_{g_n} = the quantity in the gas phase at the n'th equilibration
 C_o = the initial quantity in the system,
 n_e = the equilibration number,
 V_L = the liquid volume (ml),
 and V_G = the gas volume (ml).

If the concentrations are in the linear range of the detector, the peak areas or heights can be used in place of the concentrations.

The modified EPICS technique is used for medium K_{aw} values (greater than 0.02 and less than 3.0). In this method, three bottles contain a relatively large amount of water, and three bottles contain a relatively small amount of water. Two different volumes of water were tested because Gossett (1987) suggests that greater differences between the large and small volumes would produce more precise results. In one set of tests on Geokinetics and Paraho at each temperature, the large volume used was 120 ml and the small volume was 10 ml. In another set of tests on Geokinetics, Paraho and distilled water at each temperature, the large and small volumes used were 200 ml and 5 ml, respectively.

The known volumes were pipetted to the 240 ml sample bottles, the air in the bottles replaced with helium and then sealed with Teflon faced septum screw caps. (The removal of air was required because the capillary column is easily damaged by oxygen.) The bottles were shaken vigorously for 20 seconds and placed in a constant temperature shaker bath.

The process waters were allowed to equilibrate for at least one hour in the shaker bath. Headspace analysis (as described earlier) was then performed to determine the amount of the compound that may already be present in the headspace. The standard mixtures were then added to the bottles with a 100 microliter syringe. The approximate amounts added of each standard are shown in Table 46. The precise amount added was determined gravimetrically by weighing the syringe (to the nearest .00001 gram) directly before and after injection into the sample bottle. After adding the standard mixtures, the bottles were shaken for 20 seconds and equilibrated for at least 1 hour in the constant temperature shaker bath, and headspace analysis followed. The three bottles of high and low water volumes produced nine replicates for statistical analysis.

The equations used for this method are:

$$K_{aw} = (V_{L2} - rV_{L1}) / (rV_{G1} - V_{G2}) \quad (34)$$

and

$$r = ((C_{g1'} - C_{g1}) / (C_{g2'} - C_{g2})) M_2 / M_1$$

Table 46. Volumes of Each Mixture Added to EPICS Bottles, ml.

Mixture No.	High Liquid Volume Bottle	Low Liquid Volume Bottle
1	100	30
2	100	30
3	200	60

where V_L is the volume of the water, V_G is the volume of the gas, C_g is the gas concentration before adding the spike solution (equal to zero for pure water), C_g' is the gas concentration after adding the spike solution and M is the mass added to the water. If the peak areas or heights of the gas concentrations are in the linear range of the detector, they can be used in place of the concentration in the equation. The actual mass of compounds added to the waters need not be known, only their ratio (Gossett, 1987).

The fixed volume solvent addition technique was used for the compounds with K_{aw} values less than 0.02. These compounds included 2-pentanone, 2-hexanone, cyclohexanone, 2,6-dimethylphenol, phenol and pyridine. Vapor containing these compounds was obtained by equilibrating 5 ml of distilled water spiked with the compounds in a 240 ml bottle (bottle #1). Fifty milliliters of the vapor was withdrawn with a syringe from bottle #1 and added to a helium-filled, 240-ml sample bottle capped with a Teflon coated septum screw cap. This bottle was then placed in the constant temperature shaker bath for 30 minutes, after which headspace analysis was performed.

A liquid volume of 2.25 ml was then added to the bottle and the system equilibrated for at least one hour in the constant temperature shaker bath. The precise liquid volume added was determined gravimetrically by weighing the syringe (to the nearest .00001 gram) before and after adding the liquid. After equilibrium had been reached, the headspace was sampled and analyzed. This procedure was carried out in triplicate for each water at each temperature.

The primary requirement for this method is that the gas volume be much greater than the liquid volume. If this condition holds, the following equation applies (Vitenberg et al., 1975)

$$K = (V_G (C_g' - C_g) + V_L C_g') / V_L C_g = 1/K_{aw} \quad (35)$$

(This equation assumes $V_L \ll V_G$.) V_G is the gas volume, V_L is the liquid volume, C_g is the gas concentration before adding the solvent and C_g' is the gas concentration after adding the solvent. Again, if the concentrations are in the linear range of the detector, the peak areas or peak heights may be substituted into the equation in place of concentration.

Experimental Results

At a liquid volume to gas volume ratio of one, the multiple equilibration method worked well for 1-hexene, but not as well for benzene and toluene. The coefficient of variation (CV) values for 1-hexene were all less than 17 percent, while the CV values for benzene and toluene ranged from 10 percent to 45 percent. McAullife (1971) suggests that greater accuracy can be obtained by increasing the liquid volume to gas volume ratio. This change should decrease the CV values for these three compounds and allow them to be accurately determined in the same experiment.

Even though the modified EPICS method is only valid for benzene and toluene in this study because it only performs well for medium values of Henry's law constants, it was performed for all of the compounds used. As Gossett (1987) and Yurteri et al. (1987) predicted, this method had extremely high CV values at both the low and high HLC values. These CV values ranged from 4 percent for benzene and toluene to greater than 100 percent for most of the compounds with either extremely low HLC values or extremely high HLC values.

The two independent tests performed with different water ratios proved that the larger ratio does produce more precise results, as can be seen in Table 47. There was a noticeable decrease in the CV values for the higher ratios of liquid volumes.

The fixed volume solvent addition method worked well for 2-pentanone and 2-hexanone, and results were obtained for cyclohexanone and 2,6-dimethylphenol. It should have also worked for pyridine and phenol. However, these compounds resulted in some problems. Both phenol and pyridine had poor detector response factors. It would take very little pyridine to overload the detector, so its peak areas were not very reliable. Phenol was very difficult to obtain reliable HLC values, and the primary reason was thought to be due to adsorption to the sample bottle. The adsorption should therefore be measured and accounted for in the HLC calculation (Ioffe and Vitenberg, 1984). Teflon bottles could also be used to decrease the amount of adsorption of the polar compounds like phenol onto the bottle.

The HLC values for cyclohexanone and 2,6-dimethylphenol were difficult to obtain at the 10°C temperature because they were so small. The K_{aw} values are in the range of 0.0001, so they would require a large amount of the compound to be in the vapor initially in order to measure the HLC. It was very difficult to obtain the correct initial concentration for these two compounds because the addition of too much of the compound would bring it out of the linear range of the detector, and not enough initial concentration would bring it out of the detection range when the solvent was added. The range between the maximum allowed and the minimum required was very narrow for these two compounds at 10°C.

Since the HLC values were only required at three temperatures to obtain the temperature regression coefficients, the HLC values for these two compounds were measured at 49°C instead of 10°C to obtain the third temperature value. The temperature coefficients were then calculated, and the values at 10°C determined from them.

Table 47. Comparison of the Percent Coefficient of Variation with Different Liquid Volume Ratios for the Modified EPICS Method.

Compound	Percent Coefficient of Variation					
	10°C		25°C		40°C	
	#1*	#2**	#1	#2	#1	#2
(Geokinetics-17)						
1-hexene	157.4	27.2	185.9	72.7	48.4	--
benzene	45.9	5.3	8.1	7.0	12.1	7.1
2-pentanone	--	27.4	14.8	25.3	26.6	25.2
toluene	3.0	4.6	42.2	6.6	16.4	9.2
2-hexanone	90.1	31.5	10.5	19.0	17.0	21.4
cyclohexanone	12.1	57.0	50.0	40.1	79.1	59.9
2, 6-dimethylphenol	--	80.7	--	69.5	80.5	--
(Paraho 75/76)						
1-hexene	61.0	121.2	45.5	13.8	38.5	--
benzene	4.5	5.0	5.5	6.1	7.9	8.4
2-pentanone	--	32.2	115.6	60.9	28.6	16.5
toluene	8.3	8.3	26.7	5.9	10.0	7.9
2-hexanone	--	62.8	92.3	28.2	25.2	11.0
cyclohexanone	--	45.7	70.1	34.5	45.3	36.7
2,6-dimethylphenol	--	72.3	48.4	83.9	97.2	87.0

*Coefficient of Variation = 100% (standard deviation/mean)

*Vw1 = 120 ml

Vw2 = 10 ml

**Vw1 = 200 ml

Vw2 = 5 ml

The measured HLC values for distilled water, Geokinetics, and Paraho are contained in Table 48. The relatively high CV values are due to the fact that for most of the compounds only three or four observations were obtained for the mean value. If more observations were measured, the CV values should decrease. Table 49 contains literature values of not only most of the compounds studied here, but also some other compounds found in the process waters.

The temperature effect on HLC can be expressed by the following van't Hoff-type relationship (Kavanaugh and Trussell, 1980)

$$\ln(H_c) = - H/RT + K \quad (36)$$

where H is the change in enthalpy due to dissolution of the component in water (kcal/kmol); R is the universal gas constant, 1.987 kcal/kmol/K; T is the absolute temperature (K); and K is a constant. This relationship produces an estimate of the form (Nicholson, et al. 1984)

$$H_c \text{ (m}^3 \text{ atm/gmol)} = \exp(A - B/T) \quad (37)$$

where T is the absolute temperature (°K) and A and B are constants. The HLC values were measured at 283, 298 and 313° Kelvin (10, 25 and 40°C), and a linear regression of $\ln(H_c)$ versus $1/T$ performed to determine the linear coefficients A and B.

The temperature regressions (Table 50) show that the measured values do model the van't Hoff-type equation well. The R^2 values are all above 0.90, and the majority of them are above 0.95. These R^2 values and the temperature regressions are significant between 10°C and 40°C, so they would also be valid for evaporation ponds because the pond temperatures are typically within this range. No temperature regressions for the compounds studied here were found in the literature, so no comparisons could be made with the A and B coefficients determined.

An analysis of variance was performed on the raw data to determine whether the different waters or temperatures had significant effects on the HLC values. Analysis of the whole model which included each compound for each water and at each temperature showed that there was a 99.99 percent probability that 1) the type of water, 2) temperature, 3) compound and 4) temperature-compound interactions all had significant effects on the HLC values.

The significance of the water composition at each temperature was also analyzed with the results shown in Table 51. The p-values, which indicate the probability of making a type-I error when the null hypothesis is rejected, indicate that the water and water-compound interactions were always significant effects on the Henry's law constant at each temperature.

As indicated earlier, Yurteri et al. (1987) found that water composition, namely salts, surfactants and humic material, did affect the HLC values, so these results were expected. However, Hawthorne et al. (1985) only detected

Table 48. Measured Henry's Law Constant Values ($\text{m}^3 \text{ atm/gmol}$).

Compound	Temp	Distilled ^a		Geokinetics ^b		Paraho	
		HLC	CV% ^c	HLC	CV%	HLC	CV%
1-hexene	10	1.33E-1	8.2	1.26E-1	9.0	1.24E-1	7.9
	25	2.02E-1	16.1	2.36E-1	12.3	1.70E-1	10.2
	40	3.89E-1	8.0	2.76E-1	11.5	2.54E-1	16.1
benzene	10	3.73E-3	5.1	3.52E-3	5.3	3.32E-3	4.9
	25	6.24E-3	7.1	6.34E-3	7.0	5.04E-3	6.8
	40	1.10E-2	5.8	9.60E-3	7.1	9.83E-3	8.4
toluene	10	2.94E-3	4.9	3.44E-3	4.6	3.10E-3	8.8
	25	6.68E-3	9.3	7.59E-3	6.6	4.64E-3	20.0
	40	1.62E-2	8.3	1.32E-2	9.2	1.17E-2	7.9
2-pentanone	10	2.25E-5	18.2	3.18E-5	3.2	2.16E-5	11.7
	25	7.23E-5	3.1	1.01E-4	8.0	7.42E-5	0.36
	40	2.13E-4	9.8	2.92E-4	11.4	1.78E-4	12.8
2-hexanone	10	2.24E-5	10.9	3.63E-5	23.8	2.72E-5	10.8
	25	9.86E-5	20.3	1.22E-4	5.8	8.07E-5	11.8
	40	2.89E-4	11.3	4.37E-4	12.5	2.25E-4	15.7
cyclohexanone	10 ^d	3.69E-6	--	4.17E-6	--	3.24E-6	--
	25	1.22E-5	20.9	1.49E-5	22.2	1.12E-5	3.8
	40	2.81E-5	8.3	4.14E-5	7.4	2.17E-5	13.4
	49	6.36E-5	--	xx	xx	xx	xx
2,6-dimethyl-phenol	10 ^d	1.17E-6	--	2.89E-6	xx	1.75E-6	--
	25	5.04E-6	36.5	5.73E-6	30.1	6.53E-6	20.4
	40	1.49E-5	--	3.22E-5	14.0	2.11E-5	--
	49	3.81E-5	--	xx	xx	xx	xx

^a distilled water

^b Geokinetics-17 retort water

^c CV% = (standard deviation/mean) *100%

^d obtained from $H_c = (A - B/T)$: refer to Table 5 for A and B (distilled water only)

-- two or less observations

xx no values observed

Table 49. Henry's Law Constant Values ($\text{m}^3 \text{ atm/gmol}$).

Compound	H_c^*	Solvent	Temp (C)
benzene	5.5E-3	water	25
	4.39E-3	water	20
	4.30E-3	water	25
toluene	6.6E-3	water	25
	5.18E-3	water	20
	6.1E-3	water	25
pyridine	1.2E-5	water	25
	1.3E-5	water	25
	1.0E-5	retort water	25
	1.3E-5	gas cond.	25
2-methylpyridine	1.2E-5	retort water	25
2,4-dimethylpyridine	7.2E-6	retort water	25
2,6-dimethylpyridine	1.5E-5	water	25
	1.2E-5	retort water	25
	1.4E-5	gas cond.	25
2,4,6-trimethylpyridine	1.0E-5	retort water	25
	1.4E-5	gas cond.	25
2,6-dimethylphenol	7.6E-6	water	25
	6.7E-6	water	25
	1.2E-5	retort water	25
	1.0E-5	gas cond.	25
n-hexane	1.198	water	25
1-hexene	1.645	water	25
	4.05E-1	water	25
2-pentanone	5.8E-5	water	25
	3.16E-5	water	20
	7.8E-5	retort water	25
	8.4E-5	gas cond.	25
cyclohexanone	1.2E-5	water	25
	1.0E-5	retort water	25
	8.6E-6	gas cond.	25
butanone	5.9E-5	retort water	25
cyclopentanone	9.1E-6	retort water	25
pyrrole	1.8E-5	retort water	25
propionitrile	4.7E-5	retort water	25
butyronitrile	6.2E-5	retort water	25

* Sources are indicated in Vassar (1988).

Table 50. Temperature Coefficients ($H_c = \exp(A - B/T)$).

Compound	A	B	R^2
(Distilled Water)			
1-hexene	9.08	3154	.976
benzene	5.28	3081	.999
toluene	11.93	5031	.997
2-pentanone	15.02	7299	.990
2-hexanone	20.45	8840	.975
cyclohexanone	10.22	6433	.975
2,6-dimethylphenol	4.35	7927	.985
(Geokinetics-17)			
1-hexene	6.25	2337	.910
benzene	4.86	2968	.995
toluene	7.83	3800	.998
2-pentanone	15.40	7310	.987
2-hexanone	13.94	6832	.992
cyclohexanone	12.10	6929	.999
2,6-dimethylphenol	12.76	7278	.961
(Paraho 75/76)	5.35		
1-hexene	6.40	2111	.990
benzene	7.88	3452	.999
toluene	13.59	3892	.935
2-pentanone	10.21	6894	.988
2-hexanone	15.77	7473	.969
cyclohexanone	10.21	6468	.973
2,6-dimethylphenol	17.22	8661	.974

$H_c = m^3 \text{ atm/g mole}$
 $T = \text{Kelvin}$

Table 51. Analysis of Variance Results for Each Temperature.

Factor	p - values [*]		
	10°C	25°C	40°C
Water	.0001	.0000	.0000
Compound	.0000	.0000	.0000
Water-Compound	.0000	.0000	.0000

* Significant at $\alpha = 0.05$ with a 99.99 percent probability.

differences between the distilled water HLC values and the process water HLC values for 2,6-dimethylphenol. They only measured the HLC at 25°C, though, so they could not perform any statistical analysis on the data to detect whether or not any significant differences between the waters existed.

Discussion of Results

Since the HLC values are not only extremely dependent upon temperature, but also on the composition of the water, they should be measured for each type of process water at expected temperatures so that accurate values can be obtained. The methods studied here can be used for the range of HLC values indicated if the process waters are spiked with the compounds. If it is desired not to spike the waters, some other method of concentrating the headspace will have to be used. One such method would be the use of a purge and trap system. This concentrates the gas sample before injecting it into the GC.

With all the methods available (Vassar, 1988), a number of compounds can be studied, and the HLC values measured in each process water. In the future, more compounds than the ones studied in this report, including inorganics, should be measured and applied to obtain emission estimates from Henry's law so that the environmental impact of oil shale process water evaporation ponds can be determined from an emissions standpoint. The procedure for estimating the rate of emissions is in Vassar (1988). No attempt to estimate measured rates of emission were performed in this study.

The emissions of some of the volatile organic compounds studied in this report could pose a threat, not only to personnel working near the retort facilities and evaporation ponds, but also to plants and animals near the facilities and ponds. The degree of harm produced by these compounds to the environment (their emission rate) is dependent on their concentrations in the water, on their HLC values in the particular process water, on the depth of the pond, and on climatological parameters such as wind and temperature.

The complex nature of the process waters will also affect the emission rates because the compounds could react with suspended solids, emulsions and other contaminants. The emission rates from process waters should therefore be estimated and measured to determine if the dissolved solids and the matrix effect can be modeled and incorporated into the estimates. If the emissions are both measured and estimated, the accuracy of the estimates can be determined and new models developed if they are required. This would enable the emissions to be incorporated into the evaporation pond design so that a balance could be obtained between limiting emissions and promoting evaporation.

Finally, the use of Henry's Law Constant with Equations (22), (23) and (24) will give estimates of the mass flux into the atmosphere of individual compounds with time. An example for two of the eight compounds for which HLC values were determined are given below for illustrative purposes only to indicate the effect of volatile organic compounds from process water evaporation ponds into the environment. The values obtained are questionable as being representative since major assumptions are made for several of the quantities in the equations which are not completely validated as the correct

values that apply to these specific compounds in oil shale process waters of the type studied in this research. Hawthorne (1984) gives details on the calculations that are required to obtain the values needed in Equations (22) and (23) for oil shale process waters.

The two compounds that are used for illustrative purposes are 2,6-dimethylphenol and 2-pentanone at 25°C for Geokinetics process water. Hawthorne (1984) gives values of k_G and k_L for these compounds for half-life values of eight days for 2,6-dimethylphenol and three days for 2-pentanone using a pond depth of 1 meter and a windspeed of 3.6 m/s. For 2,6-dimethylphenol, the values of k_G and k_L are assumed to be 3.3×10^{-3} m/s and 3.7×10^{-6} m/s, respectively. For 2-pentanone, the values of k_G and k_L are assumed to be 3.5×10^{-3} m/s and 3.9×10^{-6} m/s, respectively. Using the appropriate HLC value in Table 48 and a gas constant R of 8.21×10^{-5} atm m³ mol⁻¹ °K⁻¹, the values of K_{ol} are calculated by Equation (23) to be 6.4×10^{-7} m/s and 3.1×10^{-6} m/s for 2,6-dimethylphenol and 2-pentanone, respectively. Hawthorne (1984) obtained values of 1.1×10^{-6} m/s and 2.9×10^{-6} m/s for 2,6-dimethylphenol and 2-pentanone, respectively using literature HLC values at 0°C. A significant difference can be seen between the K_{ol} values for 2,6-dimethylphenol. Substitution of these results, assuming approximately one half of one percent by weight of each compound in the process water, for values for 2,6-dimethylphenol of 0.20 g mol/l and 0.5 mm of Hg for C_w and P , respectively and for 2-pentanone of 0.25 g mol/l and 15 mm of Hg for C_w and P , respectively, the emission rates obtained from Equation (22) are 5.43×10^{-5} g mol/m² s and 1.70×10^{-4} g mol/m² s for 2,6-dimethylphenol and for 2-pentanone, respectively. These values indicate that approximately 43 pounds of 2,6-dimethylphenol and 131 pounds of 2-pentanone would be released into the atmosphere from a 1 acre evaporation pond on a daily basis. The amounts are not high but if each volatile compound in oil shale process waters produce somewhat similar amounts then the total amount being emitted for all volatile compounds from evaporation ponds could possibly be significant and of concern to the environment and human health.

FEASIBILITY OF USING EVAPORATION FOR THE DISPOSAL OF OIL SHALE PROCESS WATERS

Stochastically generated climatological data associated with a selected evaporation model is used to evaluate the feasibility of evaporation ponds for the disposal of oil shale process waters. An example using data at Laramie, Wyoming is presented for what might be considered a typical 50,000 barrel/day oil shale operation producing oil shale process waters.

SELECTION OF EVAPORATION MODEL

In a previous section of this report on evaporation models, results showed that evaporation can be predicted on a daily basis with reasonable accuracy for oil shale process waters using the calibrated Penman, KNF, Haass or statistically developed regression models for all waters combined (Equation 30). No definite findings were developed, however, indicating significant differences between these models in predicting evaporation of oil shale process water. The KNF model was thus selected for use in assessing the feasibility of using evaporation ponds for the disposal of oil shale process waters. The primary reason that the KNF model was selected over the other models was because of existing available data sets in units that could be used directly by the model.

GUIDELINES FOR EVAPORATION POND DESIGN

Evaporation from a pond or any other free surface can be predicted on a daily basis with a knowledge of daily climatological parameters. Extending the prediction of evaporation to an annual value can be accomplished by summation of predicted daily evaporation values. Ultimately, the prediction of evaporation over any time period can be accurately estimated by summing the daily predictions for evaporation as long as the necessary climatological parameters are known for every day of the time period.

If an evaporation pond for oil shale process water is to be designed for 20 years, then a 20-year sample of daily climatological values could be used to determine the total amount of evaporation that would occur during the life of the pond and this data could be used to determine the required size of the ponds. If the required climatological data had been collected over the 20 years prior to the design of an evaporation pond, this would be an excellent set of data. The available record would be able to predict deterministically, within the accuracy of any given model, the amount of evaporation that would have occurred during the last 20 years. The next 20 years, however, may not be the same as the 20 years immediately preceding the design of such a structure. In fact, the next 20 years into the future may be completely different.

A historical sample of data of almost any kind is merely a single set within an entire population of possible occurrences. In the case of pond design, a 20-year historical sample may be considered one set within a population of many possible 20-year sets. For this reason, the design of projects, such as evaporation ponds, that are designed for use in the future must employ some form of stochastic model, in which the design is based on estimates of probable future occurrences. In this sense, using a historical sample to design a project for use in the future is, in fact, a stochastic model, and

although it may be a very good model, it is a very simplistic one in that it only considers one possible future occurrence. By developing processes which create other possible occurrences, a more accurate model of future conditions can be obtained that will lead to a better engineered structure.

The design of engineered structures or anything else that must interact with the forces of nature at some time in the future is not an exact science. The natural world consists of many phenomena which can be measured, counted or otherwise determined once they have occurred. Values of temperature, precipitation, streamflow, and others can easily be measured on a daily, weekly, events. A succession of such values would be a time series of events. Moreover statistical analysis can identify patterns and trends within such sets of data. Still with all this information, predicting what will happen in the future, based on what has happened in the past cannot be completely deterministic (Haan, et al., 1982). Rather, stochastic models that determine many estimated occurrences must be used.

The development of a stochastic model begins with an existing sample or "set" of data. Two assumptions must be made of the sample of data that is available.

1. The statistics of the known sample are representative of the entire population (the mean and variance of the sample are the same as the mean and variance of the entire population).
2. The factors which created the characteristics of the known sample do not change with time (in streamflow, for example, the addition of a dam, or some diversionary inlet or outlet would change the characteristics of a sample).

A stochastic model depends heavily on the two assumptions of stationarity and representativeness (Haan, 1977), and is in fact a probabilistic model having parameters that must be obtained from some observed data. When developing data, a model should essentially preserve the mean and variance of the original data. For this reason generated data cannot improve a bad original sample of data but only provide other possibilities within the framework of the existing sample (Haan, 1977).

When new stochastic data sets are generated, a random component is used to give equal probabilities to all possible occurrences. If the data generated were completely independent from one occurrence to the next, the equation for generating the new data may have the form (Haan, 1977; Viessman, 1977):

$$X_i = X_m + ks \quad (38)$$

where:

X_i - the new value generated

X_m - the mean of the original sample

- s - the standard deviation of the original sample
- k - a function of the random component and the curve of the distribution of the original sample.

In this equation, k is determined by generating a random number (Nr) between zero and one. The random number then represents the area under the curve of the distribution of the known sample. The value k can be determined from distribution tables or mathematical approximations to distribution curves. As an example of the value of k, if the original sample was determined to have a normal distribution, then if:

Nr = 0.50 the value of k = 0.0,

Nr = 0.16 the value of k = -1.0, and if

Nr = 0.84 the value of k = 1.0.

Equation (38) would generate new values based entirely on a random basis within a possible set. In nature, however, many series are not completely random. Rather, many climatological or hydrological parameters seem to show some dependence from one event to the next. This is called persistence, and it is commonly seen in events such as streamflow where high flows are followed by high flows, and in parameters such as temperature when two or three days in a row may be similar because of a particular weather pattern. Stochastic models need to incorporate this persistence into generated data. The markov process or model is one method of preserving persistence in stochastic data sets.

Database Development

Several markov models, or auto regressive models, exist which can be used to generate new data while maintaining the persistence of an existing data set. The simplest of these is the first order markov process. This model has the form:

$$X_i = X_m + r(X_{i-1} - X_m) + ks(1 - r^2)^{0.5} \quad (39)$$

where all the values are the same as in equation (38). The new values X_{i-1} and r, respectively, represent the previous generated value and the auto correlation coefficient of values in the original sample for one time lag. In this equation each new value is generated using the statistics of the entire original sample and is also correlated to the previous sample generated.

Often, the original sample has a trend or periodicity that should be maintained. An example of this would be the variation in temperature on an annual basis. A model which may account for this is the multi-period markov process (Haan, 1977; Viessman, 1977). In this model the original sample is broken down into several periods such as weeks or months. For each period, a

mean and standard deviation can then be computed from the original sample. The equation for a first-order multi-period model has the form:

$$X_{i,j} = X_{mj} + r_j(s_j/s_{j-1})(X_{i-1,j-1} - X_{mj-1}) + ks_j(1 - r_j^2)^{0.5} \quad (40)$$

where the i subscripts in the equation represent successive values for X while the j subscripts represent the successive periods of the model. By using this equation the trend of a set of data can be discretized and incorporated into the stochastic model that is used to predict future events.

The concept of equations (39) and (40) is that the new value that is predicted has some relationship to the value that immediately precedes it. This method of correlation can easily be extended to values of two or more lags using both single period and multi-period models. These are called second, third, or higher order markov models, or higher order auto-regressive models. The only addition is that multiple regression rather than simple regression must be used to determine the relationships between a value and its preceding values for the required number of time increments or lags (Haan, 1977; Haan, et al., 1982).

Finally, markov modeling is often used to examine the same process at different locations, such as streamflow at two different points on a river or on two different rivers. If these two or more events are independent of each other, then the process of generating new data for the two breaks down to two independent models. If, on the other hand, a relationship exists between the two then a multisite markov model must be employed that will preserve this relationship. A multisite model would require both auto correlations of values, as well as cross correlations between the two non-independent factors for the required number of lags.

This form of modeling may be easily simplified into many forms, one simple method would be to develop two models and apply the same random number to each at the same time. Another method might be to simply predict one new value and correlate the other new value to the generated value. Finally, it may be easiest to modify the model somehow to achieve independence. For example, if the streamflow of two adjacent watersheds is not independent, a new model might be developed that considered precipitation as the random event, rather than streamflow. Once an independent precipitation event was generated it could be applied to both watersheds deterministically to generate the two new streamflow values (Haan, 1977).

For the prediction of evaporation for a set period of time into the future, a computer model that uses a markov model was developed (Richard, 1988). For each climatological factor involved in the prediction of evaporation (temperature, solar radiation, relative humidity, and wind speed), an independent first order markov model was developed.

First, an original sample of 20 years of data for the period 1966 to 1985 was collected. For each year a period of 26 weeks (182 days) beginning on May

1 of each year was chosen as the sample size. This sample was the best available sample of climatological data for the Laramie area. However, there were some missing data points. The initial step in modeling this set of data was to fill in the missing data points. Using the original sample, weekly statistics were computed. Then all missing data points were filled with the use of a random generating equation with the same form as equation (38) using the statistics for the week that the missing day was included.

The statistical properties of this newly filled data set were compared to the values obtained prior to filling in the missing values. It was determined that the process of filling in the missing points essentially preserved the mean of the sample, but may have biased the variance. For this reason, the markov model chosen for generating new sets of data was a modification of the multi-period model. This equation had the same form as the previous equation (39) but excluded the factor s_j/s_{j-1} . Also, it was decided that the process of filling missing data points randomly may have biased the time lag correlations for some periods, so a single lag correlation was used for each set. This was found by lagging the entire 20-year data set by one day.

The model employed 182 daily periods per year beginning with May 1 as day number one of every year within the 20-year set. Each daily period had its own mean and standard deviation. The model used the mixed congruent method to generate a nine digit random number. Then, the last three digits of every random number were converted to a number between .001 and .999. Using a normal distribution approximation, each random digit was converted to a k value for generating a new data point.

New values for each of the climatological factors were generated independently for every day. A 22-year set of data was generated and the first two years of generated data (364 daily values) for every variable were thrown out to eliminate any initial bias in the generating models. After a new 20-year set of data had been calculated, the statistics on the new set were calculated for comparison to the original values. These comparisons can be found in Richard (1988). The model was used to generate 1000 possible 20-year sets of data for analysis.

The model also contained several separate subroutines. The first of these was a subroutine to develop possible weekly precipitation values. This subroutine had its own unique six digit, mixed congruent random number generating sequence and used the same form of markov equation as was used in modeling the other climatological factors. Whenever this routine generated a negative number the actual precipitation was considered to be zero, but the negative value was used to generate the succeeding value in the time series. Fifty-two weekly precipitation values were calculated for each year beginning with May 1 of every year. Once again, the first two years of every set generated was eliminated to remove any initial bias.

The next step in the model was to determine the daily evaporation using the previously generated climatological data. The potential evaporation was computed using the KNF equation. The computed daily values were then summed to 26 values of weekly evaporation per year.

For each year in a set, 26-weekly evaporation values and 52-weekly precipitation values constituted one year. During the 26 weeks from October through April, evaporation was assumed to be zero. This was considered a conservative factor in the model. These annual values were then summed to determine the total precipitation and evaporation from a pond system during a 20-year period. The difference of total precipitation from total evaporation was considered to be the total allowable input of oil shale process water to the system in depth per unit area. This total volume of input was assumed to be entering the system at a constant rate, so a weekly input to the system was the total input divided by 1040.

Risk Assessment

In order to determine the pond volume, two factors were calculated; the maximum depth in the pond at any time and the area of the pond. The area of any evaporation pond for oil shale process waters will depend on the actual volume of process water produced. The total volume produced divided by the allowable input in depth per unit area can be used to determine the pond area. The required depth, on the other hand, can be determined using mass balance techniques. These two dimensions can be considered concurrently or independently, with the design considered more conservative if the two are treated independently of each other. For the purpose of this report, the depth and area dimensions of a pond were considered independent.

A statistical average of the 1000 generated values of total allowable inflow to a pond was determined to be 198.5 inches, with the average evaporation and precipitation being 495.9 and 297.4 inches, respectively. Using this average value of inflow would mean an annual inflow to the pond of 9.93 inches to the pond or 0.83 ft^3 of water per square foot of pond area. By comparison, the lowest total input to the system was 131.0 inches which reduces to an annual input of only $0.55 \text{ ft}^3/\text{ft}^2$. From this, the most conservative estimate for pond area would be obtained using a design input of 0.55 cubic feet of water per year for every square foot of pond area.

The maximum depth of water in a theoretical evaporation pond was determined using a weekly mass balance on a unit area of the pond. The computation of pond depth began on May 1 of year one by assuming an initial depth in the pond of the total precipitation plus the total inflow divided by 40. From this starting point, a new depth was calculated at the end of every week. The maximum depth in the pond during a 20-year set was the criteria used to compare sets. The results of the three sets with the highest pond depths have been plotted for visual comparison. Figures 14 through 16 show the three most critical sets in decreasing order.

The analysis of the 1000 sets of possible 20-year events indicate that a conservatively designed pond would be able to safely contain a water depth of 64 inches of water (not including freeboard), while accommodating an inflow of $0.55 \text{ ft}^3/\text{ft}^2$ annually. This design is conservative. Yet, even these specifications for pond dimensions cannot completely size a pond without some knowledge of the anticipated inflow volumes. Potential inflow volumes of oil shale process waters may vary depending on several factors in the actual processing of oil shale.

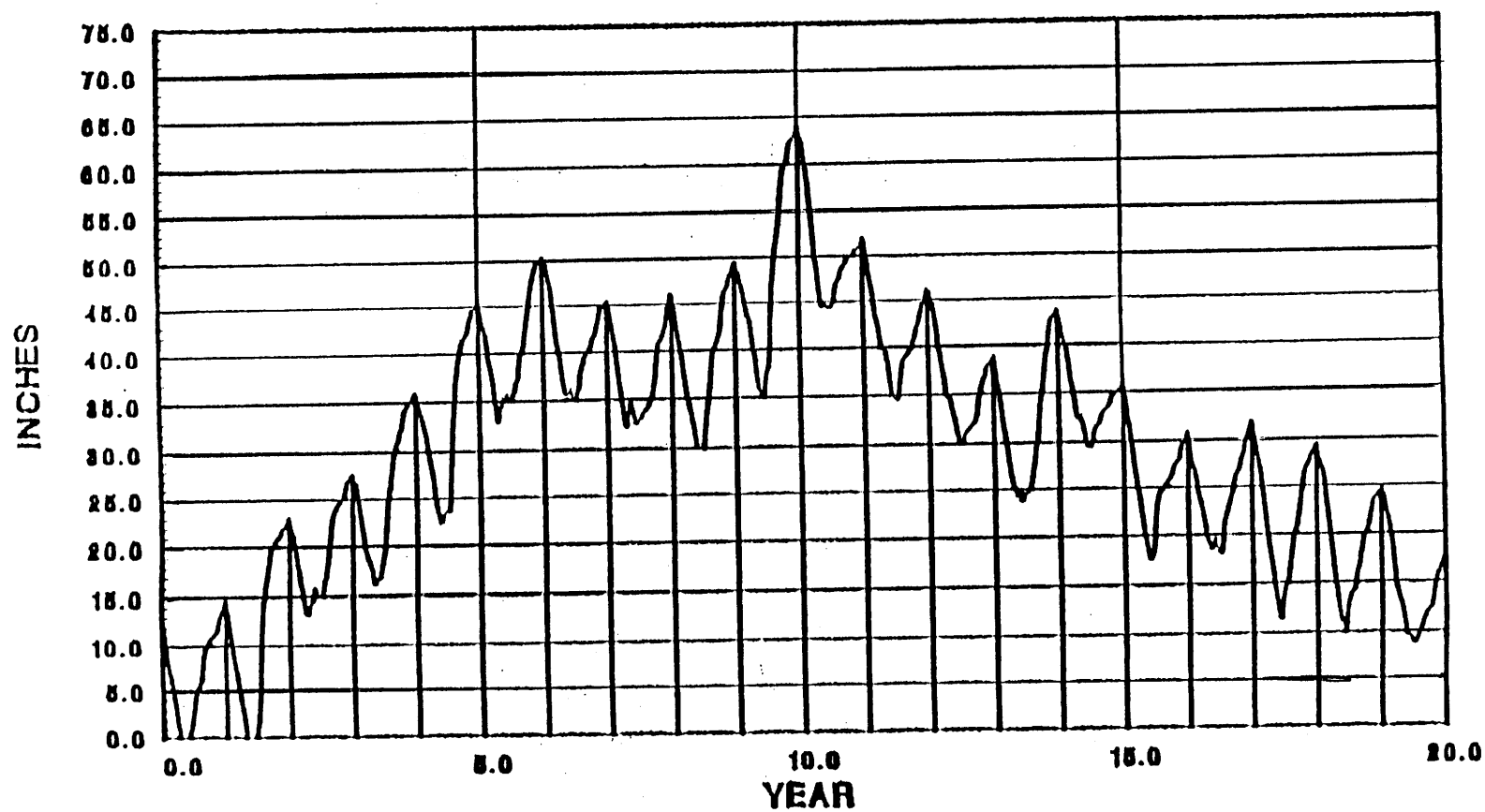


Figure 14. Variation in Pond Depth: Set #1.

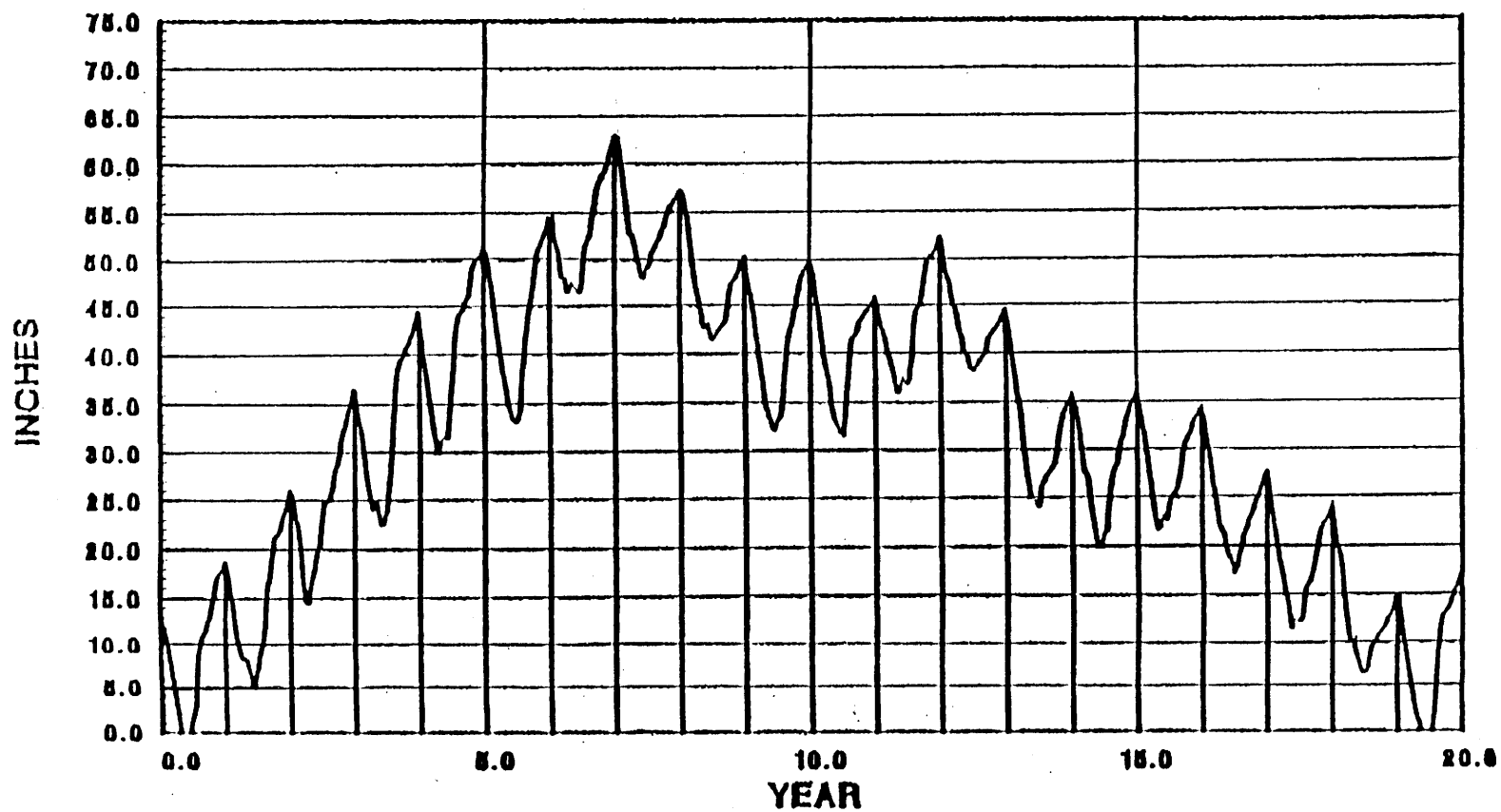


Figure 15. Variation in Pond Depth: Set #2.

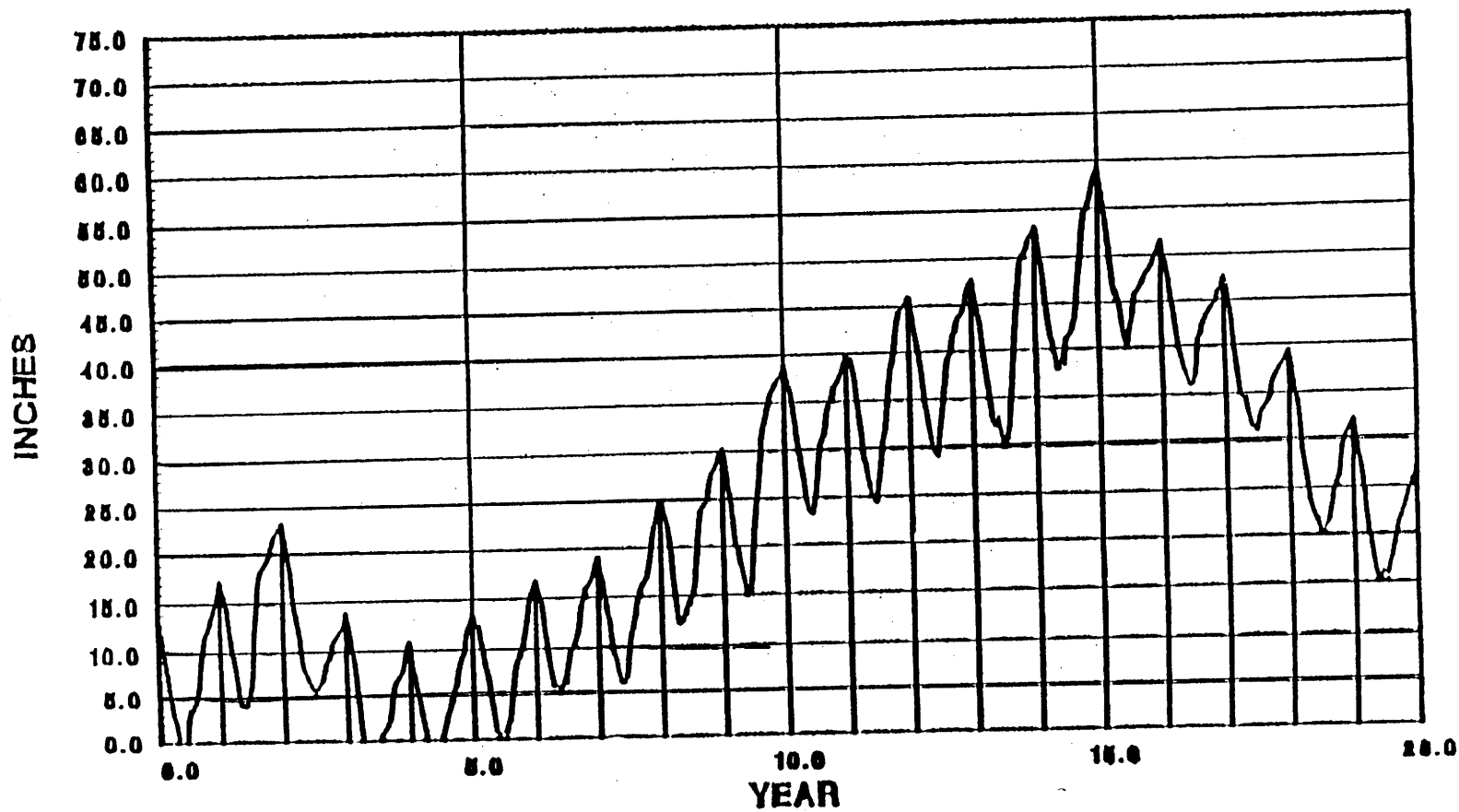


Figure 16. Variation in Pond Depth: Set #3.

The methodology or guidelines described here for the development of many different possible specific period data sets of climatological variables to be used in the KNF evaporation model to determine the worst case scenario over the specified time period chosen for the life of the evaporation pond indicates the environmentally safe design situation to reduce the risk of overtopping the evaporation pond to an acceptable level. A decision would have to be made on the number of data sets analyzed to reduce the risk of overtopping to the acceptable level specified by the regulatory agency responsible for compliance.

Example

When sizing an evaporation pond for oil shale process waters, a stochastic model is one of the best ways to estimate the losses from the system through evaporation. The inflows to the pond, on the other hand, should be somewhat more deterministic. The inflow of process water to an evaporation pond will not be the same from one processing location to the next, but at any given site, for a given process the production of process water ought to be accurately determined or predicted.

The volume of oil shale process waters that may be produced by industry vary widely. Fox (1980) and Nowacki (1981) indicate that the range of produced oil shale process waters will generally be between 0.22 barrels of process water per barrel of oil produced to 2.3 barrels per barrel of oil produced. The lower end of the range for produced waters is generally characteristic of above ground retorting operations while the upper end of the range could be typical of in situ retorts with significant groundwater intrusion. A reasonably sized oil shale operation can be assumed to produce at least 50,000 barrels of oil per day which means that anywhere from 11,000 barrels/day (0.22 barrels/day) to 115,000 barrels/day (2.3 barrels/day) of process water would be produced as a product which must be properly disposed. This amount of process water translates to between 518 and 5,410 acre-feet/year of produced water for disposal.

It was shown previously by using climatological data for Laramie, Wyoming and the stochastic analysis for development of 20-year data sets that a conservatively designed evaporation pond would be able to safely contain a water depth of 64 inches of water without addition of freeboard (need at least a six foot deep pond with freeboard) while accommodating an inflow of 0.55 ft³/ft² annually. This means that the water surface area needed for evaporation ponds is between 940 (518/0.55) and 9840 acres. Since there are 640 acres in a square mile, even the smallest area needed by an oil shale operation for process water disposal for an above ground retorting process producing 0.22 barrels of process water per barrel of oil would be almost 1.5 square miles. This example indicates that the utilization of evaporation ponds as a means of process water disposal in the western United States is highly questionable because of the land area needed for disposal that would require lining for protection of the land alone without any consideration given to gaseous emissions that may be released to the atmosphere from the process water in the ponds by the evaporation process.

The stochastic model developed has given what would seem to be reasonable results. Although the model is straight forward, its long-term averages show

very good agreement with established values. The total 20-year average evaporation of 495.9 inches, as previously stated, is equivalent to an annual evaporation from the model of 24.8 inches which is very close to the estimated annual average of 20 to 22 inches for the Laramie area (Martner, 1982). Similarly, the total 20-year precipitation of 297.4 inches reduces to an average annual precipitation from the model of 14.9 inches which is well within the range of 10 to 16 inches of rain for Laramie (Martner, 1982).

The assumptions made in the development of the model, as stated previously, did not seem to distort the generated data in any way. Also, the use of a normal distribution on all of the generated variables, for simplicity sake, did not seem to bias the results. Comparisons of the statistics of generated data sets to the original parameters of the model indicated that the characteristics of the original sample were essentially preserved.

The results of this model seem well within the range of reality. In fact, the estimates of pond depth and volume seem rather conservative. Clearly these results would be usable in the actual sizing of an evaporation pond in the Laramie area.

DISCUSSION AND CONCLUSIONS

This section of the report summarizes the results which were developed to meet the specific purposes and objectives of this research study on oil shale process water evaporation. Several conclusions are summarized along with some recommendations for possible future research.

DISCUSSION OF RESULTS

The two major purposes of this research program were: (1) to study chemical, microclimatological, and interactive effects on the evaporation of low-quality oil shale retort wastewaters, and to develop more applicable evaporation models and evaporation design criteria for the disposal of oil shale process waters and (2) to analyze the processes associated with the release of potentially toxic emissions from these low-quality effluents. These purposes were accomplished by the research through the major objectives outlined in Table 1. An extensive literature was studied in the process of accomplishing this research and has been enumerated.

Three oil shale process waters were used in a combined field and laboratory study effort. Two waters were from modified in situ retorting methods, and one from a surface retorting method. The field studies were designed to continuously monitor microclimatological conditions and evaporation using Class A evaporation pans. Freshwater evaporation was monitored as a control. The process waters were routinely monitored for concentrations of organic and inorganic constituents. These data were used to identify significant effects acting on the evaporation of these waters under confounded field conditions. Laboratory studies were designed to isolate and describe significant climatic, chemical, and interactive effects on evaporation rates under controlled conditions.

Separate laboratory studies were also conducted to evaluate the processes associated with the release of toxic emissions during evaporation of these process waters. In these chemically complex waters, this is a very confounded problem. It was beyond the scope of this project to completely define the emission process and interacting processes of even the major organic species. Laboratory studies were designed, however, to study significant effects on the Henry's Law Constant (HLC) of eight major organic compounds in two of the oil shale process waters and in distilled water. HLC is a required component in most models used to estimate the emission rate or flux of a given compound from a liquid to a gaseous phase. An example of estimating the emission rates of two of the eight organic compounds using the HLC values for those compounds was performed. It indicates that emissions from oil shale process waters could be significant.

For much of this study, Class A evaporation pans were used because they are the standard measurement for evaporation. Many studies have related evaporation from Class A pans to the evaporation of reservoirs and impoundments. A major disadvantage of this pan is its large size (4 ft. dia. x 10 in. deep). This size of evaporator was not practical for the laboratory studies designed for this program. A side-study, therefore, was conducted to design a mini pan for evaporation which could show correlations to the measurements of a standard Class A evaporation pan. This was accomplished and the results are reported in Appendix A.

Field data obtained during 1985 were used to indicate the significant meteorological parameters affecting evaporation rate of the different process waters and fresh water. The results indicated that ambient air temperature, water temperature, wind speed (at the water surface), radiation intensity and barometric pressure were the significant meteorological parameters affecting evaporation rate. An environmental chamber laboratory study was then developed to analyze the interactive effects of ambient air temperature, wind speed and relative humidity on evaporation rate. No significant differences were found between the evaporation rate of process waters and fresh water in the laboratory. Significant interactive effects were found between air temperature and relative humidity, air temperature and wind speed and relative humidity and wind speed. These results were expected.

Field data obtained during the summers of 1985 through 1987 were used to identify the significant chemical parameters affecting evaporation rate of the oil shale process waters and fresh water. Six of the chemical parameters measured were found to significantly affect evaporation rate. These six chemical parameters were alkalinity, chloride concentration, sulfate concentration, TDS, TOC and pH. From both field and extensive laboratory studies on chemical concentration of process waters, no significant effect on evaporation rate was found with increasing chemical concentration based on a doubling of the TDS and TOC concentrations observed during a field season. This result was surprising and it is believed that color and increasing chemical concentration result in increased heating and molecular activity of the oil shale process waters in such a manner that no discernable effect could be measured with respect to evaporation rate or amount.

The results of the analysis of climatological and chemical parameter effects on evaporation rate were used to analyze existing evaporation models and develop a model for oil shale process waters which included the significant climatological and chemical parameters found in this study. The developed model for all waters combined utilized all the significant chemical parameters (six) stated above. The climatological variables generally indicated higher levels of significance in the prediction of evaporation rate than did the chemical parameters. Multicollinearity may exist between some of the parameters. High multicollinearity can result in some regression coefficients of the model being adversely affected. It is probable that some multicollinearity exists between chemical parameters resulting in inaccurate regression coefficients for those parameters. The resultant model developed for all the waters combined had a coefficient of correlation of 0.79 which indicates that it does a reasonably good job of estimating evaporation rate of oil shale process waters.

Ten established evaporation models and the developed statistical evaporation model for all waters combined (Equation 30) were compared for accuracy in predicting the daily evaporation from the process waters and from fresh water. Comparison and analyses performed were based on 160 days of evaporation data measured in 1985 and 1986. Regression analysis was used and determinations were made based on correlation coefficients and coefficients of determinations between the measured daily values and estimated daily values.

Results indicated that three established models and the developed statistical model (Equation 30) showed good correlation with measured daily values. The three established models were the Kohler-Nordenson-Fox (KNF), the

Priestly-Taylor (PT), and the Penman Combination Equation (Pm1). The developed statistical model (Equation 30) showed the best correlations with measured daily values. The major difference in the developed model (Equation 30) and the established models are the inclusion of chemical parameters. If these chemical parameters cannot be measured, estimates of evaporation on a daily basis from oil shale process waters can be obtained by use of one of the three established models after calibration for that location.

An unexpected conclusion was made from these data. All three established models identified, and the developed model (Equation 30) used solar intensity as a factor or variable in estimating evaporation. The models tested which simplified this parameter through the use of coefficients, or simply eliminated this parameter, were not as effective as the four identified models in estimating process water evaporation. It was concluded, therefore, that solar radiant flux is an important factor when estimating evaporation from process waters.

An evaluation of the KNF equation on a diurnal (hourly) basis was also performed for a 33-day period. The estimates using the sum of hourly KNF estimates were higher than the measured values by 10 to 15 percent. Therefore, the KNF equation was calibrated for diurnal variations. The results of the calibration were nearly as good as the developed regression models of evaporation versus climatological and chemical data (Tables 41 and 42). Use of the KNF equation is preferred to the developed regression models (Tables 41 and 42) since empirical formulas are generally considered to be more transferable to other locations than are regression models.

Because chemical data cannot be projected for future oil shale process waters, the KNF equation was used to estimate evaporation on 1000 sets of 20-year climatological data produced by stochastic modeling. Results indicated that a conservatively designed pond would be able to safely contain a water depth of 64₃ inches (not including freeboard), while accommodating an inflow of 0.55 ft³/ft² annually. The inflow volume of process water was then estimated using published data. These data indicate that between 0.22 to 2.3 barrels of process water could be produced per barrel of oil, depending on the exact process utilized. For a theoretical 50,000 barrel/day operation, these numbers translate to 11,000-115,000 barrels of processed water produced per day, or 518 to 5410 acre-feet/yr. Using the developed inflow figure of 0.55 ft³/ft², the pond size required for this theoretical operation would be between 940 and 9840 acres.

These results demonstrate the importance of making accurate evaporation estimates for these waters and the scope of the disposal problem. Obviously, similar modeling efforts will have to be repeated in the future. However, two major conclusions can be made from this analysis. Evaporation pond design will have to maintain fairly shallow depths (64 inches) in order to optimize free water evaporation, and that extremely large areas (1,000-10,000 acres) will have to be used if this management technique (evaporation ponds) is employed. These data further conclude, or suggest, that the volume of these waters that could potentially be produced may be an important factor in determining the retorting process used for production (i.e., the production of process water may have to be minimized) or that the utilization of evaporation ponds as a means of process water disposal in the western United States is highly questionable.

The analysis of processes associated with the release of potentially toxic emissions from oil shale process waters were investigated in the laboratory and field. Gas emission samples from the process waters were collected and analyzed in the laboratory. Primary compounds found from the analyses of the gas samples indicate that potentially toxic emissions are in the samples. The rate of emission of these volatile compounds from the process water into the atmosphere is important. These rates can be either measured (difficult) or estimated using mathematical models which required a knowledge of the Henry's Law constant of each compound.

Henry's Law constants were measured for eight major organic compounds across three temperatures for two oil shale process waters and in distilled water in which the compound was inoculated. The process waters used were Geokinetics and Paraho. The eight compounds studied were chosen because of several factors, including the results of GC/MS analysis of the process waters (EPA 624; EPA 625), the range of previously measured HLC values, and their environmental importance. The compounds studied were: 1-hexene, n-hexane (n-hexane or one of its isomers), benzene, toluene, 2-pentanone, 2-hexanone, cyclohexanone, and 2,6 dimethylphenol. Temperatures analyzed were 10°C, 25°C and 40°C.

Analysis of variance results of the entire experimental model indicated that the type of waters, the water temperature, the compound, and a temperature-compound interaction all had significant effects on the HLC values. Further ANOVA tests analyzed the significance of the water composition at each temperature. These results indicate that the water type and water-compound interactions always produced significant effects on the HLC at each temperature analyzed. In general, these results show that a strong matrix effect exists on the HLC that is dependent on the specific chemical characteristics of the individual water.

Regression analyses were used to further describe the temperature effects on the compounds. Analysis of the regression coefficients also showed that the temperature effect on HLC values are significantly different between process waters and distilled water. The observed differences between the slopes (regression coefficients) for each water and each compound show that the waters affect the HLC of each compound differently. This is further evidence of a very strong matrix effect.

The major conclusion drawn from these data, therefore, is that in order for the emission rates of a given compound to be accurately estimated, the HLC must be known for each specific water and at each expected water temperature. The example presented on two of the eight compounds for which the HLC values were obtained indicate that emissions from oil shale process waters could be significant.

CONCLUSIONS AND RECOMMENDATIONS

Major conclusions of this study are:

1. When considered as a complete model, five climatological parameters and six chemical parameters produce significant effects on process water evaporation. Climatological parameters are: ambient temperature, water temperature, wind speed (measured at the water surface),

radiation intensity, and barometric pressure. The chemical parameters are alkalinity, chloride concentration, sulfate concentration, total dissolved solids (TDS), total organic carbon (TOC), and pH; however, these results may be strongly affected by multicollinearity.

2. Under controlled climatic conditions, process water evaporation on a large scale was not significantly changed with increasing chemical concentrations over the range of concentrations studied.
3. Under controlled chemical conditions, process water evaporation was significantly affected by ambient temperature, relative humidity, wind speed, a temperature-wind speed interaction, and a relative humidity-wind speed interaction. No significant differences existed between process water and fresh tap water under the conditions studied.
4. Solar radiant flux is a critical parameter in selecting an evaporation model to estimate oil shale process water evaporation.
5. The statistical model (Equation 30) developed for this study showed the best results in estimating oil shale process water evaporation; however, three existing established models (KNF, Priestly-Taylor and Penman combination) were also relatively accurate.
6. The calibrated Kohler-Nordenson-Fox evaporation equation for hourly data is at least as good as the developed statistical models (Tables 41 and 42) for evaluating diurnal evaporation rate.
7. Key impoundment design parameters were found to be the pond depth and the total allowable input. Even under conservative estimates, extremely large areas (1000+ acres) will have to be used for disposal of oil shale process waters by evaporation.
8. In order to accurately estimate emission rates from oil shale process waters for a given compound, the Henry's Law constant must be known for each specific water and at each expected water temperature.

Recommendations for future studies should include:

1. Comparison of the established and developed models of this study need to be analyzed on a broad range of evaporation data from different locations in the western United States.
2. Refinement in the stochastic procedures utilized to size evaporation pond impoundments and the statistical distribution to be used (normal or some other distribution).
3. More compounds found from the gas emission analyses studied in this report, including inorganics, should be measured for HLC and other constants such as partial pressure so that accurate estimates of emission rates from evaporation ponds can be made. This report only

indicated that emissions from evaporation ponds could be significant and as such could be an environmentally important consideration for the oil shale industry.

4. Emission rates from oil shale process waters should be estimated and measured to determine if dissolved solid and matrix effects can be modeled.

GLOSSARY

(Acronyms and Abbreviations)

<u>Term</u>	<u>Description</u>
A1,A2,A3,A4,A5	Emperical coefficients
Al	Aluminum
α	Albedo
ALK	Alkalinity of a water
ANOVA	Statistical analysis of variance
B	Bowen's Ratio, or radiant heat transfer to the sky
BMDP	Computer statistical package
BMDP9R	Computer statistical package using regression analysis
Ca	Calcium
Cg	Concentration in the vapor phase
C_{g_n}	Vapor phase concentration at the n'th equilibration
CL	Chlorine
CO	Carbon monoxide
C_o	Initial quantity in the system for multiple equilibration method
COD	Chemical oxygen demand
CO ₂	Carbon dioxide
c_p	Specific heat of water
CV	Coefficient of variation
C_w	Concentration in the liquid phase
DELTA or Δ	Slope of the saturation vapor pressure versus temperature curve
DOE	Department of Energy
e	Vapor pressure

GLOSSARY

(Acronyms and Abbreviations)
(Continued)

<u>Term</u>	<u>Description</u>
E	Evaporation
e_a	Actual vapor pressure
EA	Aerodynamic function
E_a	Evaporation given by the aerodynamic equation
EF	Fresh water evaporation
EG	Geokinetics process water evaporation
EP	Paraho process water evaporation
E_p	Pan evaporation
EPA	Environmental Protection Agency
EPICS	Equilibrium partitioning in closed systems
ER	Rio Blanco process water evaporation
ES	Saturation vapor pressure
e_s	Saturation vapor pressure (using T_s)
e_{sa}	Saturation vapor pressure (using mean T_a)
EVAP	Evaporation
$f(u)$	Empirical function of windspeed
G	Soil heat flux
GAMMAP	Psychrometric constant
GC	Gas chromatography
GC/FID	Gas chromatography/flame ionized detector analysis
GC/MS	Gas chromatography/mass spectrometry analysis
H	Sensible heat
HARB	Harbeck evaporation formula

GLOSSARY

(Acronyms and Abbreviations)
(Continued)

<u>Term</u>	<u>Description</u>
Hc	Henry's Law Constant, atm m ³ /gmole
HCO ₃	Bicarbonate
H ₂ S	Hydrogen sulfide gas
HLC	Henry's Law Constant
I	Inflow
ICP	Inductively coupled plasma analysis
k	Coefficient of a probability distribution, Henry's Law Constant (units of pressure)
K	Distribution coefficient, potassium, sensible heat transfer
k _G	Gas phase mass transfer coefficient
K _h	Coefficient of turbulent heat transfer in air
k _L	Liquid phase mass transfer coefficient
K _p	Pan coefficient
K _w	Coefficient of turbulent vapor transfer in air
Kaw	Dimensionless Henry's Law Constant
Kol	Overall mass transfer coefficient
KNF	Kohler-Nordenson-Fox evaporation formula
L or L _v	Latent heat of vaporization
Lat	Latitude
LIN	Linacre evaporation formula
ly/day	langleys (energy term) per day
M	Mass added

GLOSSARY

(Acronyms and Abbreviations)
(Continued)

<u>Term</u>	<u>Description</u>
MERV	Computer program for analyzing linear and nonlinear functions
MEY	Meyer evaporation formula
Mg	Magnesium
MINITAB	Computer statistical package
N	Mass flux
Na	Sodium
Nat. Aca. of Sci.	National Academy of Science
n_e	equilibration number
NH_3^-	Ammonia gas
NO_2	Nitrogen dioxide
NO_x	Nitric oxide compounds
Nr	Random number
NSCORES	Normal score plots
O	Outflow
P	Atmospheric pressure, partial pressure
ρ	Air density
pH	Measure of hydrogen concentration = $-\log[\text{H}^+]$ (buffering capacity)
PM1	Penman combination equation
PM2	Penman mass transfer equation
P_r	Precipitation
PT	Preistly-Taylor evaporation formula

GLOSSARY

(Acronyms and Abbreviations)
(Continued)

<u>Term</u>	<u>Description</u>
S_p	Seepage
ΔS	Change in storage
T	Temperature
T_a	Air temperature
T_b	Bottom pan or water temperature
$t_{1/2}$	Half life
TD	Dew point temperature
TDS	Total dissolved solids
T_e	Temperature of evaporated water
TKN	Total Kjeldahl nitrogen
TOC	Total organic carbon
T_s	Surface water temperature
UP	Wind run at pan height
USGS	United States Geological Survey
V_G	Gas volume
V_L	Liquid volume
WATEQ	Computer program for determining the major water equivalent amounts of different ions in solution
W_g	Ground wind speed
WRI	Western Research Institute
X1	Air temperature
X2	Relative humidity
X3	Wind run at two meters

GLOSSARY

(Acronyms and Abbreviations)
(Continued)

<u>Term</u>	<u>Description</u>
X4	Solar radiation
X _i	Generated value
X _m	Mean of data sample
γ	Psychrometric constant
Γ	Dry adiabatic lapse rate
Z	Pond depth

PROJECT PUBLICATIONS

- Eyre, S.M. 1987. Comparison of Evaporation Models for Oil Shale Retort Waters. M.S. Thesis, Department of Civil Engineering, University of Wyoming, Laramie, Wyoming. 103 p.
- Haass, M.J. 1985. Evaporation of Oil Shale Wastewater. M.S. Thesis, Department of Civil Engineering, University of Wyoming, Laramie, Wyoming. 94 p.
- Hasfurther, V.R. and M.J. Haass. September 1986. State-of-the-Art Evaporation Technology. DOE/LC/11049-2205.
- Hasfurther, V.R., M.J. Haass and L.O. Pochop. 1985. Oil Shale Process Water Evaporation. In Proc. 1st Annual Oil Shale Tar Sands Contractors Meeting. Morgantown, West Virginia. DOE/METC-85/6026.
- Hasfurther, V.R., M.J. Haass and T.L. Reeves. 1986. Oil Shale Process Water Evaporation. P. 190-198. In Proc. 19th Annual Western Oil Shale Symposium. Golden, Colorado: Colorado School of Mines Press.
- Hasfurther, V.R., L.O. Pochop and T.L. Reeves. 1988. Evaporation Process Analysis and Emissions from Oil Shale Retort Waters. In Proc. of the 3rd Annual Oil Shale, Tar Sand, and Mild Gasification Contractors Review Meeting. Edited by Theodore C. Bartke, Morgantown, West Virginia. DOE/METC-88/6098.
- Koontz, P.D. 1986. Chemical Characterization of Oil Shale Retort Waters for Predicting Evaporation Rates. M.S. Thesis, Department of Civil Engineering, University of Wyoming, Laramie, Wyoming. 108 p.
- Richard, D.E. 1988. A Stochastic Model for the Design of Evaporation Ponds for Oil Shale Retort Waters. M.S. Thesis, Department of Civil Engineering, University of Wyoming, Laramie, Wyoming. 112 p.
- Vassar, A.C. 1988. Determination of Henry's Law Constants for Selected Organic Compounds in Oil Shale Retort Waters. M.S. Thesis, Department of Civil Engineering, University of Wyoming, Laramie, Wyoming. 73 p.
- Vassar, A., L.O. Pochop and V.R. Hasfurther. 1987. Design and Testing of a Mini Class A Evaporation Pan. Topical Report DOE/LC/11049-2352 (DE87006487).

REFERENCES

- Bartholic, J.F., L.N. Namken and C.L. Wiegand. 1970. Combination Equations Used to Calculate Evaporation and Potential Evaporation. U.S. Department of Agriculture. Report ARS 41-170.
- Beard, J.T. and J.L. Gainer. 1970. Influence of Solar Radiation Reflectance on Water Evaporation. Journal of Geophysical Research 75 (27): 5155-5163.
- Cohen, Y., W. Cocchio and D. Mackay. 1978. Laboratory Study of Liquid-Phase Controlled Volatilization Rates in Presence of Wind Waves. Environ. Sci. Technol. 12: 553-558.
- Dilling, W.L. 1977. Interphase Transfer Processes. II. Evaporation Rates of Chloro Methanes, Ethanes, Ethylenes, Propanes, and Propylenes from Dilute Aqueous Solutions. Comparison with Theoretical Predictions. Environ. Sci. Technol. 11: 405-409.
- Dobson, K.R., M. Stephenson, P.F. Greenfield and P.R.F. Bell. 1985. Identification and Treatability of Organics in Oil Shale Retort Water. Water Research 19: 849-856.
- Doskey, P.V. and A.W. Andren. 1981. Modeling the Flux of Atmospheric Polychlorinated Biphenyls Across the Air/Water Interface. Environ. Sci. Technol. 15: 705-711.
- Dunne, T. and L.B. Leopold. 1978. Water in Environmental Planning. New York: W.H. Freeman and Company.
- Eklund, B.M., W.D. Balfour and C.E. Schmidt. 1985. Measurement of Fugitive Volatile Organic Emission Rates. Environmental Progress 4: 199-202.
- Eyre, S. 1987. Comparison of Evaporation Models for Oil Shale Retort Waters. M.S. Thesis, Department of Civil Engineering, University of Wyoming, Laramie, Wyoming.
- Fox, J.P. et al. 1980. Potential Uses of Spent Shale in the Treatment of Oil Shale Retort Waters. In Thirteenth Oil Shale Symposium Proceedings, Colorado School of Mines, Golden, Colorado.
- Fox, J.P., D.S. Farrier and R.E. Poulson. 1978. Chemical Characterization and Analytical Considerations for an In Situ Oil Shale Process Water. Department of Energy, Laramie Energy Technology Center. LETC/RI-78/7.
- Garstka, W.V. 1978. Water Resources and the National Welfare. Fort Collins, Colorado: Water Resources Publications.
- Gossett, J. 1987. Measurement of Henry's Law Constants for C₁ and C₂ Chlorinated Hydrocarbons. Environ. Sci. Technol. 21: 202-208.

- Gowda, T.P.H. and J.D. Lock. 1985. Volatilization Rates of Organic Chemicals of Public Health Concern. Journal American Society of Civil Engineers, EED, 111: 755-776.
- Haan, C.T. 1977. Statistical Methods in Hydrology. Ames, Iowa: Iowa State University Press.
- Haan, C.T. et al. (eds.). 1982. Hydrologic Modeling of Small Watersheds. St. Joseph, Michigan: American Society of Agricultural Engineers.
- Harbeck, G.E., Jr. 1962. A Practical Field Technique for Measuring Reservoir Evaporation Utilizing Mass-Transfer Theory. U.S. Geological Survey. Professional Paper 272-E.
- Haass, M.J. 1985. Evaporation of Oil Shale Wastewater. M.S. Thesis, Department of Civil Engineering, University of Wyoming, Laramie, Wyoming.
- Hasfurther, V.R. and M.J. Haass. September 1986. State-of-the-Art Evaporation Technology. DOE/LC/11049-2205.
- Hawthorne, S.B. 1984. The Emission of Organic Compounds from Shale Oil Wastewaters. Ph.D. Thesis, University of Colorado, Boulder, Colorado.
- Hawthorne, S.B., R.E. Sievers and R.M. Barkley. 1985. Environmental Science and Technology 19: 992-997.
- Ioffe, B.V. and A.G. Vitenberg. 1984. Head Space Analysis and Related Methods in Gas Chromatography. New York: John Wiley and Sons.
- Kavanaugh, M.C. and R.R. Trussell. 1980. Design of Aeration Towers to Strip Volatile Contaminants from Drinking Water. Journal AWWA 684-692.
- Keith, L.H. (ed.). 1982. Energy and Environmental Chemistry. Vol. 1, Fossil Fuels. Ann Arbor, Michigan: Ann Arbor Science.
- Kohler, M.A. 1954. Lake and Pan Evaporation. U.S. Geological Survey. Professional Paper 269.
- Kohler, M.A. et al. 1958. Pan and Lake Evaporation. U.S. Geological Survey. Professional Paper 298.
- Koontz, P.D. 1986. Chemical Characterization of Oil Shale Retort Waters for Predicting Evaporation Rates. M.S. Thesis, Department of Civil Engineering, University of Wyoming, Laramie, Wyoming.
- Lincoff, A.H. and J.M. Gossett. 1984. The Determination of Henry's Constant for Volatile Organics by Equilibrium Partitioning in Closed Systems. In Gas Transfer at Water Surfaces, W. Brutsaert, G.H. Jirka, eds. Boston, MA: D. Reidel.
- Linsley, R.K., Jr., M.A. Kohler and J.L.H. Paulhus. 1958. Hydrology for Engineers. First edition, New York: McGraw-Hill, Inc.

- Linsley, R.K., Jr., M.A. Kohler and J.L.H. Paulhus. 1975. Hydrology for Engineers. Second edition, New York: McGraw-Hill, Inc.
- Liss, P.S. and P.G. Slater. 1974. Flux of Gases Across the Air-Sea Interface. Nature 247: 181.
- Mackay, D. and P.J. Leinonen. 1975. Rate of Evaporation of Low-Solubility Contaminants from Water Bodies to Atmosphere. Environ. Sci. Technol. 9: 1178-1180.
- MacKay, D. and S. Paterson. 1986. Model Describing the Rates of Transfer Process of Organic Chemicals Between Atmosphere and Water. Environ. Sci. Technol. 20: 810-816.
- Mackay, D. and W.Y. Shiu. 1981. A Critical Review of Henry's Law Constants for Chemicals of Environmental Interest. J. Phys. Chem. Ref. Data 10 (4): 1175-1199.
- Mackay, D. and W.Y. Shiu. 1984. Physical-Chemical Phenomena and Molecular Properties. In Gas Transfer at Water Surfaces, W. Brutsaert, G.H. Jirka, eds. Boston, MA: D. Reidel.
- Mackay, D. and A.T.K. Yeun. 1983. Mass Transfer Coefficient Correlations for Volatilization of Organic Solutes from Water. Environ. Sci. Technol. 17: 211-217.
- Martner, B.E. 1982. Wyoming Climate Atlas. Lincoln, Nebraska: University of Nebraska Press.
- McAulliffe, C. 1971. GC Determination of Solutes by Multiple Phase Equilibration. Chem. Tech. 1: 46-51.
- McKell, C.M. et al. (eds.). 1984. Paradoxes of Western Energy Development. American Association for the Advancement of Science Symposium #94. Boulder, Colorado: Western Press.
- Morton, F.I. 1965. Potential Evaporation and River Basin Evaporation. Journal of the Hydraulics Division, ASCE, 91 (HY6): 67-97.
- Munz, C. and P.V. Roberts. 1986. Effects of Solute Concentration and Cosolvents on the Aqueous Activity Coefficient of Halogenated Hydrocarbons. Environ. Sci. Technol. 20: 830-836.
- National Academy of Sciences. 1980. Surface Mining of Non Coal Minerals, Appendix II: Mining and Processing of Oil Shale and Tar Sands. Washington, D.C.: National Academy of Sciences.
- Nicholson, B.C., B. Maguire and D. Bursill. 1984. Henry's Law Constants for the Trihalomethanes: Effects of Water Composition and Temperature. Environ. Sci. Technol. 18: 518-521.
- Nordenson, T.J. 1963. Appraisal of Seasonal Variation in Pan Coefficients. International Association of Scientific Hydrology, General Assembly of Berkeley, Committee for Evaporation. Publication No. 62.

- Nowacki, P. (ed.). 1981. Oil Shale Technical Data Handbook. Park Ridge, New Jersey: Noyes Data Corp.
- Painter, D.E. 1974. Air Pollution Technology. Reston, VA: Reston Publishing, Inc.
- Peck, E.L. and D.J. Pfankuch. 1963. Evaporation Rates in Mountainous Terrain. International Association of Scientific Hydrology, General Assembly of Berkeley, Committee for Evaporation. Publication No. 62.
- Prausnitz, J.M. 1969. Molecular Thermodynamics of Fluid-Phase Equilibria. Englewood Cliffs, NJ: Prentice-Hall.
- Rathbun, R.E. and D.Y. Tai. 1982. Volatilization of Ketones from Water. Water, Air and Soil Poll. 17: 286.
- Rathbun, R.E. and D.Y. Tai. 1986. Gas-Film Coefficients for the Volatilization of Ethylene Dibromide from Water. Environ. Sci. Technol. 20: 949-952.
- Richard, D.E. 1988. A Stochastic Model for the Design of Evaporation Ponds for Oil Shale Retort Waters. M.S. Thesis, Department of Civil Engineering, University of Wyoming, Laramie, Wyoming.
- Rideal, E.K. 1925. On the Influence of Thin Surface Films on the Evaporation of Water. Journal of Physical Chemistry 29: 1585-1588.
- Russell, P.L. 1980. History of Western Oil Shale. 1980. East Brunswick, New Jersey: The Center for Professional Advancement.
- Salhotra, A.M., E.E. Adams and D.R.F. Harleman. 1985. Effect of Salinity and Ionic Composition on Evaporation: Analysis of Dead Sea Evaporation Pans. Water Resources Research 21 (9): 1336-1344.
- Singh, V.P. (ed.). 1981. Modeling Components of Hydrologic Cycle. In Proceedings of the International Symposium on Runoff Modeling. Littleton, Colorado. Water Resources Publications.
- Smith, J.H., D.C. Bomberger, Jr. and D.L. Haynes. 1980. Prediction of the Volatilization Rates of High-Volatility Chemicals from Natural Water Bodies. Environ. Sci. Technol. 14: 1332-1337.
- Smith, J.H., D. Mackay and C.W.K. Ng. 1983. Volatilization of Pesticides from Water. In Residue Reviews, F.A. Gunther and J.D. Gunther, eds. pp. 73-88. New York: Springer-Verlag.
- Stewart, J.B. 1983. A Discussion of the Relationships Between the Principal Forms of the Combination Equation for Estimating Crop Evaporation. Agricultural Meteorology 30: 111-127.
- Stuber, H.A. and J.A. Leenheer. 1978. Inorganic Sulfur Species in Waste Waters from In Situ Oil Shale Processing. J. Envir. Sci. Health A13 (9): 633-675.

- U.S. Environmental Protection Agency. 1977. Preliminary Assessment of the Environmental Impacts From Oil Shale Development. USEPA 600/7-77-069.
- Van Bavel, C.H.M. 1966. Potential Evaporation: The Combination Concept and Its Experimental Verification. Water Resources Research 2 (3): 455-467.
- Vassar, A.C. 1988. Determination of Henry's Law Constants for Selected Organic Compounds in Oil Shale Retort Waters. M.S. Thesis, Department of Civil Engineering, University of Wyoming, Laramie, Wyoming.
- Vassar, A., L. Pochop and V. Hasfurther. 1987. Design and Testing of a Mini Class A Evaporation Pan. Topical Report DOE/LC/11049-2352 (DE87006487).
- Viessman, W., Jr., J.W. Knapp, G.L. Lewis and T.E. Harbaugh. 1977. Introduction to Hydrology. New York: Harper and Row Publishers, Inc.
- Warnaka, K.E. 1985. Variability of Evaporation Estimates. M.S. Thesis, Department of Agricultural Engineering, University of Wyoming, Laramie, Wyoming.
- Welles, C. 1970. The Elusive Bonanza: The Story of Oil Shale, America's Richest and Most Neglected Natural Resource. New York: E.P. Dutton and Company, Inc.
- Yurteri, C., D.F. Ryan, J.J. Callow and M.D. Gurol. 1987. The Effect of Chemical Composition of Water on Henry's Law Constant. Journal WPCF 59 (11): 950-956.

APPENDIX A
MINI-EVAPORATION PAN

DEVELOPMENT OF A MINI-EVAPORATION PAN

Many methods have been used to estimate potential evaporation from ponds or reservoirs. The most widely used method is the Class A evaporation pan. This pan is usually constructed of galvanized metal or stainless steel. It is 4 feet in diameter by 10 inches deep, and the water level is typically maintained at an 8 inch depth (Hounam, 1973). The Class A pan holds sixty-three gallons of water, with 1 inch of evaporation being equivalent to 7.8 gallons of water.

The large size of the Class A pan prevents it from being used economically in many evaporation studies, especially when replications are desired due to the volume of water required. For this reason an insulated mini-evaporation pan was designed to evaporate at the same rate as the Class A pan, yet require less water. This is very important in arid areas away from a source of water.

The mini-evaporation pan holds 4.2 gallons of water when the water level is 1.5 inches from the top of the pan. One inch of evaporation from the minipan is equivalent to 0.5 gallons of water. The minipan, therefore, requires 1/16 the amount of water of a Class A pan.

Automation of a minipan would be desirable in remote locations. This appendix details the design and testing of an automation device for minipans and the field tests conducted on the minipans and automation device.

The details of the initial design and testing of a mini Class A evaporation pan are contained in a DOE publication (DOE/LC/11049-2352) by Vassar, et al., in March 1987. From the design and testing with two months of data obtained during the summer of 1985, a 1 foot diameter by 10 inch deep pan with 1 inch of polyurethane foam insulation surrounding it (Figure A-1) provided evaporation at a rate very similar to the Class A pan (mean evaporation was only 3.1 percent different from that of a Class A pan and its daily water temperature cycles were comparable with that of the Class A pan).

METHODOLOGY

Class A evaporation pans are usually automated with some type of float system attached to a water storage tank, by using electronic sensors of water depth to control the flow of water into the Class A pan, or using pressure transducers. In a mini Class A evaporation pan, several of the above types of automation devices are either too large (bulky) or difficult to utilize in remote areas. The size of a float device must not be very large in relation to the surface area of the minipan.

The design chosen for automation of the minipans utilizes a ping pong ball filled with spray foam insulation as a float, a mercury switch attached to the float system with the switch controlling a solenoid valve

MINI CLASS A EVAPORATION PAN

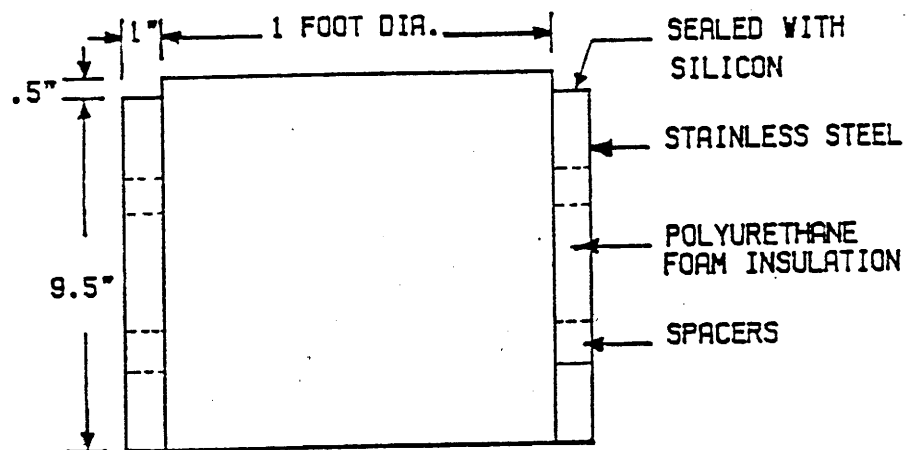


Figure A-1. Schematic of Mini Class A Pan.

attached to a pipe from a water storage tank. As the water level in the minipan decreases due to evaporation, the float and the mercury switch makes contact to open the solenoid valve, allowing water to flow into the pan from the storage tank until the mercury switch is again tripped by the rising float.

The storage tank is a 3 foot high by 4 inch diameter PVC pipe. One inch of evaporation in the pan is equivalent to a 9 inch drop in the storage tank allowing for precise measurements of evaporation in the storage tank utilizing a float and F-1 recorder.

The solenoid valve is operated by a 12 volt car battery. When opened, it uses 0.5 amps so the batter will remain charged for long periods.

FIELD EXPERIMENTATION

The test site was located northwest of Laramie, Wyoming at the same location as the field experimentation site for the oil shale process water evaporation study. Data from a fresh water Class A evaporation pan was available for comparison with the minipans.

Four minipans with different thicknesses of polyurethane foam insulation were tested. These were the four minipans tested in the original study in 1985 (Vassar, et al., 1987). These four minipans will be referenced throughout the rest of this report as follows:

- Pan 1 - Zero Insulation
- Pan 2 - 0.25 inches Insulation
- Pan 3 - 0.25 inches Insulation

The minipans were placed on a wooden platform constructed of 1 inch by 4 inch boards spaced 1 inch apart. Each minipan was filled with fresh water and operation was initiated in June 1987.

Initially only Pan 3 was automated so that it could be tested and compared with the other pans. On July 10, 1987, Pans 1 and 4 were also automated.

The evaporation from the minipans that were not automated and from the Class A pan was measured daily with a hook gage in accordance with Class A pan measurement instructions. The water level was measured, brought to 1.5 inches from the pan rim, and measured again. The required depth of 1.5 inches from the pan rim for the minipans was established by the previous tests conducted on the pans (Vassar et al., 1987).

The evaporation from the automated pans was determined daily by measuring the depth of water in the storage tank with a measuring tape and continuously recorded with the F-1 recorder. The water level in the automated pans was maintained between 1.5 and 2 inches from the pan rim. The hook gage was used to measure this depth each day to determine the ability of the float-switch mechanism to keep the water depth within the range set for the switch (approximately 0.05 inches).

RESULTS AND DISCUSSION

Testing of the minipans occurred between June 5 and August 19, 1987. Rain occurred on 13 days during this period and those particular days were not included in the analyses. The results of the 1985 tests are summarized with the results from this study so that similarities and differences can be indicated and discussed.

Statistical tests of results from measurements on the minipans versus one Class A pan for each study are shown in Table A-1. A paired t-test was used to compare the mean differences. In the 1985 study, Pans 1 and 2 were significantly different from the Class A pan at the 0.05 level. In the present study, Pans 1, 2 and 3 were all significantly different from the Class A pan at the 0.05 level. Pan 4 was not significantly different from the class A pan for either year.

The analysis of variance in 1985 produced F-ratios which showed no significant difference in variance between evaporation from the Class A pan and any of the minipans at the 0.05 level. The same test in the present study produced F-ratios which showed that Pan 1 had a significantly different variance from the Class A pan, but the other three pans were not significantly different from the Class A pan.

In 1985, the percent differences of Pans 1, 2, 3 and 4 from that of the Class A pan were 23.8, 5.6, 5.3 and 3.1, respectively. In 1987, the percent differences for Pans 1, 2 and 3 were higher at 34.7, 17.7 and 12.9, respectively, while Pan 4 had a 3.5 percent difference from the Class A pan.

The evaporation data obtained for each year are presented in Table A-2 and Table A-3. The average differences between the minipans and the Class A pan were approximately the same for each study.

The means and standard deviations of the water levels in the automated pans are shown in Table A-4. The water levels are the hook gage readings taken from the top of the pans.

The statistical comparisons for both studies indicate that Pan 4 with 1 inch of foam insulation is the best prototype of the Class A pan. In the previous 1985 study, the 0.25 inch insulated pans were on the borderline for being similar to the Class A pan. The present study, however, shows that 0.25 inches of foam insulation is not enough to produce evaporation measurements similar to the Class A pan.

The percent differences of evaporation between Pans 1, 2 and 3 and the Class A pan were higher in the present study than those from the previous study. However, the differences between Pan 4 and the Class A pan remained between 3 and 4 percent for both studies.

The small standard deviations of the water level measurements indicate that the automation system was able to provide accurate water level readings consistent with conventional hook gage measurements. When the pans were automated, the evaporation measurements actually were more

Table A-1: Statistical Comparison of Mean Evaporation.

Year	Mini Pan #	Insulation (inches)	Mean Evap. (in./day)	Percent* Diff.	T Value	F Ratio
1985	1	0.0	.401	+23.8	-7.95**	1.21
	2	0.25	.342	+5.6	-2.50**	1.08
	3	0.25	.341	+5.3	-1.98	1.03
	4	1.00	.334	+3.1	-1.00	1.12
1987	1	0.00	.427	+34.7	-13.92**	1.83**
	2	0.25	.373	+17.7	-14.15**	1.24
	3	0.25	.358	+12.9	-5.02**	1.38
	4	1.00	.328	+3.5	-1.63	1.23

* Percent difference was
 $(\text{minipan avg.} - \text{Class A pan avg.}) / \text{Class A pan avg.}$

** Significant at = 0.05

In 1985, Class A pan evaporation averaged 0.324 inches/day.

In 1987, Class A pan evaporation averaged 0.317 inches/day.

Table A-2: Evaporation Rates and Comparison Between Class A and Minipans.*

Date (1985)	4 foot evap.	#1 evap.	diff.	#2 evap.	diff.	#3 evap.	diff.	#4 evap	diff.
7/2	0.38	0.47	-0.09	0.38	0.00	0.28	0.10	0.39	-0.01
7/3	0.38	0.53	-0.15	0.45	-0.07	0.42	-0.04	0.47	-0.09
7/16	0.33	0.40	-0.07	0.35	-0.02	0.34	-0.01	0.34	-0.01
7/17	0.18	0.24	-0.06	0.21	-0.03	0.22	-0.04	0.20	-0.02
7/24	0.18	0.30	-0.12	0.26	-0.08	0.25	-0.07	0.25	-0.07
7/25	0.33	0.42	-0.09	0.36	-0.03	0.34	-0.01	0.32	0.01
7/26-7/28	0.88	0.97	-0.09	0.85	0.03	0.88	0.00	0.79	0.09
8/1	0.26	0.40	-0.14	0.33	-0.07	0.36	-0.10	0.32	-0.06
8/2-8/4	1.19	1.26	-0.07	1.07	0.12	1.09	0.10	1.01	0.18
8/5	0.36	0.41	-0.05	0.36	0.00	0.36	0.00	0.53	-0.17
8/6	0.35	0.43	-0.08	0.37	-0.02	0.36	-0.01	0.34	0.01
8/7	0.34	0.39	-0.05	0.34	0.00	0.33	0.01	0.31	0.03
8/8	0.42	0.50	-0.10	0.44	-0.02	0.42	0.00	0.41	0.01
8/9-8/11	0.80	1.02	-0.22	0.95	-0.15	0.90	-0.10	0.91	-0.11
8/14	0.27	0.48	-0.21	0.32	-0.05	0.39	-0.12	0.32	-0.05
8/15	0.40	0.60	-0.20	0.44	-0.04	0.51	-0.11	0.42	-0.02
8/16-8/18	0.93	1.06	-0.13	0.96	-0.03	0.91	-0.02	0.89	-0.04
8/19	0.26	0.40	-0.14	0.35	-0.09	0.37	0.11	0.37	-0.11
8/20	0.40	0.48	-0.08	0.40	0.00	0.39	0.01	0.37	0.03
8/21-8/25	1.76	2.08	-0.32	1.77	-0.01	1.83	-0.07	1.78	-0.02
8/26	0.30	0.46	-0.16	0.39	-0.09	0.36	-0.06	0.35	-0.05
8/27	0.30	0.32	-0.02	0.28	-0.02	0.27	0.03	0.26	0.04
Averages	0.32	0.40	0.12	0.34	0.04	0.33	0.05	0.33	0.06

* All units are inches.

Table A-3: Evaporation Rates and Comparison Between Class A and Minipans.*

Date (1987)	4 foot evap.	#1 evap.	diff.	#2 evap.	diff.	#3 evap.	diff.	#4 evap	diff.
6/15	0.37	0.48	-0.11	0.40	-0.04	0.39	-0.02	0.40	-0.03
6/16	0.21	0.29	-0.08	0.24	-0.03	0.29	-0.08	0.22	-0.01
6/19	0.37	0.46	-0.08	0.38	-0.01	0.28	0.10	0.34	0.03
6/22	0.27	0.39	-0.12	0.32	-0.06	0.31	-0.05	0.30	-0.03
6/24	0.23	0.33	-0.10	0.25	-0.02	0.29	-0.06	0.26	-0.03
6/26	0.34	0.49	-0.15	0.40	-0.06	0.41	-0.07	0.39	-0.05
6/27	0.37	0.54	-0.16	0.47	-0.09	0.45	-0.08	0.42	-0.05
6/28	0.38	0.57	-0.20	0.46	-0.09	0.39	-0.01	0.42	-0.05
7/3	0.23	0.31	-0.08	0.25	-0.03	0.23	0.00	0.24	-0.01
7/4	0.22	0.33	-0.12	0.31	-0.09	0.25	-0.04	0.24	-0.03
7/5	0.20	0.28	-0.08	0.23	-0.03	0.24	-0.05	0.20	0.00
7/6	0.28	0.40	-0.11	0.33	-0.04	0.33	-0.04	0.30	-0.02
7/7	0.28	0.40	-0.13	0.34	-0.06	0.31	-0.04	0.30	-0.02
7/8	0.33	0.42	-0.10	0.35	-0.03	0.38	-0.05	0.31	0.02
7/9	0.22	0.36	-0.14	0.28	-0.06	0.25	-0.03	0.27	-0.05
7/10	0.27	0.37	-0.10	0.32	-0.04	0.33	-0.06	0.27	0.01
7/11	0.39	0.49	-0.10	0.51	-0.12	0.35	0.05	0.38	0.02
7/15	0.27	0.38	-0.11	0.32	-0.05	0.31	-0.03	0.28	-0.01
7/16	0.35	0.46	-0.11	0.41	-0.06	0.40	-0.05	0.37	-0.02
7/17	0.30	0.44	-0.14	0.37	-0.07	0.38	-0.08	0.35	-0.05
7/18	0.23	0.32	-0.09	0.29	-0.07	0.26	-0.03	0.23	-0.01
7/19	0.41	0.58	-0.17	0.51	-0.11	0.58	-0.18	0.44	-0.04
7/20	0.42	0.57	-0.16	0.43	-0.02	0.35	0.07	0.44	-0.03
7/21	0.34	0.46	-0.13	0.38	-0.04	0.37	-0.03	0.34	0.00
7/22	0.34	0.52	-0.18	0.43	-0.08	0.45	-0.11	0.39	-0.05
7/23	0.37	0.51	-0.15	0.42	-0.06	0.43	-0.07	0.37	-0.01
7/24	0.49	0.66	-0.18	0.56	-0.07	0.51	-0.03	0.48	0.01
7/25	0.44	0.65	-0.21	0.54	-0.10	0.50	-0.06	0.47	-0.03
7/26	0.28	0.42	-0.14	0.33	-0.06	0.29	-0.01	0.25	0.03
7/27	0.29	0.40	-0.11	0.37	-0.07	0.38	-0.09	0.28	0.01
8/1	0.35	0.21	0.14	0.36	-0.01	0.28	0.07	0.19	0.16
8/2	0.35	0.45	-0.10	0.41	-0.05	0.36	-0.01	0.31	0.04
8/3	0.32	0.44	-0.13	0.39	-0.08	0.38	-0.06	0.31	0.01
8/4	0.31	0.43	-0.13	0.39	-0.08	0.36	-0.06	0.43	-0.13
8/5	0.36	0.44	-0.08	0.42	-0.07	0.37	-0.01	0.32	0.04
8/6	0.34	0.44	-0.11	0.42	-0.08	0.47	-0.14	0.38	-0.04
8/9	0.27	0.30	-0.10	0.32	0.05	0.28	-0.01	0.26	0.01
8/10	0.30	0.37	-0.07	0.37	-0.06	0.47	-0.16	0.32	-0.02
8/11	0.37	0.50	-0.13	0.42	-0.05	0.33	0.04	0.38	-0.01
8/12	0.30	0.38	-0.07	0.30	0.01	0.26	0.04	0.26	0.05
8/13	0.24	0.31	-0.07	0.34	-0.10	0.34	-0.10	0.35	-0.11
8/14	0.21	0.28	-0.07	0.26	-0.05	0.31	-0.10	0.22	-0.01
8/17	0.60	0.69	-0.09	0.66	-0.06	0.67	-0.07	0.60	0.00
8/18	0.44	0.63	-0.18	0.50	-0.06	0.55	-0.11	0.52	-0.08
8/19	0.36	0.49	-0.12	0.42	-0.06	0.38	-0.01	0.29	0.07
Averages	0.32	0.43	0.12	0.37	0.06	0.36	0.06	0.33	0.03

* All units are inches.

Table A-4: Water Level Hook Gage Readings (inches)

Mini Pan #	Average Hook Gage Reading	Standard Deviation	Number of Measurements
1	2.670 2.788	0.035 0.029	9 8*
3	2.715	0.042	50
4	2.765	0.042	16

* Water depth was changed manually to a higher level.

consistent. This is theorized to be due to the relatively constant water level depth.

The two studies on the minipans indicate that the 1 inch insulated pan is a good model of the Class A pan. It is consistent and reliable with an average 3.3 percent difference from the Class A pan.

The automation device was able to keep the water level within an average change of 0.05 inches. The automation system is inexpensive to build and operate. The storage tanks utilized enough water for one weeks' worth of evaporation, so the pans can be operated in remote locations with minimal maintenance requirements.